AD669690

NRL Report 6713

Advances in Fracture Toughness Characterization Procedures and in Quantitative Interpretations to Fracture-Safe Design for Structural Steels

W. S. Pellini

Metallurgy Division

April 3, 1968

NAVAL RESEARCH LABORATORY
Washington, D.C.

94

PREFACE

This report combines features of a status review, synthesis of concepts, and projections of trends in fracture toughness testing and in associated procedures for fracture-safe design. Particular attention is given to explanatory discussions of theoretical aspects which serve the needs of design and materials engineers for a simplified text on Applied Engineering Fracture Mechanics. To accomplish this purpose the presentations are not based solely on mathematical considerations, but are made real by discussions in context of crucial issues involved in general practice.

Because of the wide spectrum of steels, structures, and service conditions that must be considered in general practice, separation is made between appropriate procedures which provide customized treatment for the class of steel and the nature of the application. The various procedures are then integrated into a coherent framework which presents an overall view, and thereby delineates the processes for selection of the appropriate approach. These syntheses are evolved with recognition that the constant allegiance of the engineer is to practicality — consequently, the product of new science will be adopted only when explicit companion procedures are evolved which also represent pragmatic answers to real problems. The first real problem is one of selection of the appropriate approach — if the processes for this selection are not made evident, all else fails.

The extensive coverage which is required was made possible by the basic contributions of many investigators who have enriched the literature in the fracture field. Special recognition should be made of the classical pioneering studies of Professor G. Irwin in the evolution of fracture mechanics to the point that it now provides the general basis for practical quantitative treatment of fracture problems. Other major contributions have been provided by the author's colleagues, including the experimental data, advice, and critique in the evolution of the described concepts. These include Dr. P. Puzak's broad studies of steels and test methods; C. Freed's critical correlations of K_{Ic} and other types of test; E. Lange's and J. Goode's contributions to the development of the DT test to its present form for steels and also nonferrous metals; Dr. F. Loss's expertise in fracture mechanics; and Dr. J. Krafft's basic interpretation of process zone (d_T) factors.

CONTENTS

ABSTRACT

The state of knowledge of fracture-safe design for steels is examined in relation to the requirements for achieving practical solutions to general engineering problems. Analytical procedures evolved from fracture mechanics theory are demonstrated to provide for quantitative interpretations of engineering fracture toughness tests. It is thus possible to couple the procedural simplicity which is inherent to engineering tests with the analytical advantages of fracture mechanics theory. The coupling of these two approaches provides for practical advances in fracture-safe design which cover the totality of general engineering problems and requirements.

The Charpy V test is shown to have applicability for use in the described fashion primarily in relation to the strength transition for high strength steels. Serious limitations exist for reliable quantitative interpretations involving the temperature transition. The Drop Weight Test (DWT) and the related Fracture Analysis Diagram (FAD) are demonstrated to be interpretable in terms of fracture mechanics parameters. Additional applications of the DWT which provide for separate definition of static and dynamic fracture initiation conditions have been evolved for the Nil Ductility Transition (NDT) temperature region. The resulting new reference diagram is defined as the NDT Analysis Diagram (NAD).

Combined coverage of temperature and strength transition aspects are provided by the Dynamic Tear (DT) test. The DT test temperature transition curve provides for indexing to the FAD and NAD interpretive procedures. In addition, the DT shelf energy level is analyzable, in terms of flaw size-stress conditions for fracture, by the K_{Ic} σ_{ys} Ratio Analysis Diagram (RAD). By zoning of the expected position in this diagram for generic classes of steels, coherent matrices are evolved which combine metallurgical and mechanics aspects. The combined diagrams should serve the needs of both the materials and design fields.

PROBLEM STATUS

This is a special interpretive report covering the results of a wide spectrum of investigations within the Metallurgy Division of NRL, aimed at the general problem of metallurgical optimization and fracture-safe design. The major portions of the studies are continuing under established problem and sub-task categories.

AUTHORIZATION

NRL Problem M01-18; Projects RR 007-01-46-5420;
SHIPS SF 020-01-05-0731

NRL Problem M03-01; Projects RR 007-01-46-5414;
SHIPS SF 020-01-01-0850

NRL Problem F01-17; Project DSSP P07-001-11894

Manuscript submitted March 7, 1968.

ADVANCES IN FRACTURE TOUGHNESS CHARACTERIZATION PROCEDURES AND IN QUANTITATIVE INTERPRETATIONS TO FRACTURE-SAFE DESIGN FOR STRUCTURAL STEELS

EVOLUTION OF FRACTURE TESTS

Remarkable progress has been achieved in recent years in the evolution of improved fracture toughness characterization tests and in procedures for quantitative interpretations to fracture-safe design. The advances in this field have derived from emphasis on scientific studies which decreased the need for reliance on experience factors. While service experience always remains the final proof of any test procedure, progress by this route alone is much too slow and cumbersome to satisfy urgent needs. New metals of higher strength and of large section size are rapidly entering service in the form of complex structures for critical applications. For such applications, it is not realistic to depend solely on past experience based on low strength metals; primary reliance for the new problems must be placed on laboratory evolved guidelines.

However, issues of engineering practicality which have decided the acceptability of past developments should be expected to play a continuing role in the present and for the future. Because of the importance of this factor, it is essential to review past experience as prologue for the discussions of this report.

The initial need for the standardization and use of fracture tests evolved from the development of a wide variety of improved steels in the pre-WWII era. The existing Charpy V and Charpy Keyhole notch tests provided qualitative guidance for optimizing strength-toughness relationships, and for quality control in production. Essentially all new classes of steels which emerged during the past two decades were developed or improved on the basis of Charpy V notch data, correlated to experience factors. The Keyhole test has long outlived its usefulness, but it remains as a principal specification reference in general use because of lack of agreement as to test procedures which may replace it.

The 1940's were marked by a dramatic upsurge of activity in studies of the significance of a wide variety of fracture tests, consequent to the catastrophic failures of large welded ships. Large-scale tests of "wide plates," box girders, hatch corners, etc., featuring various types of notches and weld defects, were used as structural prototypes for correlation with these tests. The experience developed from the large-scale tests clearly suggested the development of small laboratory tests which would simulate realistic service notch conditions, such as sharp, natural cracks. The large variety of machined notch tests which were developed during this period were rendered obsolete by the natural-crack tests. The first natural-crack test was the Drop Weight test (DWT), conceived in 1950 for the determination (1) of the Nil Ductility Transition (NDT) temperature.

By the late 1940's the flaw size-stress conditions for the initiation and propagation of fractures in low strength steels began to be understood — at least in rudimentary form. Success in calibrating the Charpy V (C_V) test for ship steels (the 10, 15, and 20 ft-lb temperature criteria for initiation, propagation, and arrest) provided the first definitions urgently required for engineering design purposes. This solution was short lived. Use of the DWT-NDT test by NRL investigators (1953) demonstrated that adjustments of the "critical" C_V fracture energy index values were required for different types of steels (2). While this finding was a major disappointment to what had appeared to be a generalized solution, it marked the start of an era of dominance of the natural-crack tests and the diminution of notched tests to the position of secondary reference. While continued use of the Charpy V test is to be expected, its interpretations must be indexed to the primary reference standards of the natural-crack tests. The NDT indexing of the Charpy V is an example.

Research interest in the specific crack and stress conditions which determine the initiation and propagation of fractures then continued along two apparently separate paths, as follows:

1. Linear elastic fracture mechanics, which is concerned with the mathematical treatment of elastic stress field conditions at crack tips. The stress field expressions relate to plastic work energy requirements for fracture. Experimentally, the natural crack is simulated by the use of a sharp fatigue crack.

2. Dynamic Crack Tests, which involve measurement of strain to fracture, or energy to fracture, of relatively simple specimens. These tests feature the additional service simulation of a dynamic crack initiation in embrittled material. The Robertson Crack Arrest (CAT) test, the Drop Weight NDT (DWT-NDT) test, and the Drop Weight Tear (now called the Dynamic Tear-DT) test, fall in this category.

The case for the applicability of the dynamic crack tests has evolved from correlations with service failures; from tests to destruction of full size flawed structures; and from tests of large, structural elements. The fracture-safe design rationale has a correspondence to fracture mechanics in that test measurements of low plastic work energy are related to fractures which may initiate from small defects and propagate spontaneously through elastic stress field regions. Similarly, test measurements of large plastic work energy are related to fractures which require large flaws and plastic overload for fracture.

It is thus apparent that both fracture mechanics and dynamic crack tests involve simulation of severe natural crack conditions and that the merit indices are similarly relatable to the basic unit processes of plastic work energy in fracture. Engineering assessment would indicate that fracture mechanics theory should provide for analysis of any structural condition, including that of the dynamic crack tests — which represent structures of simple characteristics. Accordingly, there is a rational basis for considering that the dynamic crack test indices of energy absorption should be translatable to the fracture mechanics parameters such as K_{Ic}, K_c, $\mathcal{G}_{Ic}$, and $\mathcal{G}_c$. Once this is accomplished the formal methodology of fracture mechanics becomes available and can be added to the dynamic crack test interpretive procedures.

The benefits of this two-stage "marriage approach" should flow in both directions. While fracture mechanics provides the interpretive base for the dynamic crack tests, these tests in turn serve to promote more extensive use of fracture mechanics theory in engineering practice. On this premise, the totality of the two-stage process, which appears to be the future trend in the evolution of fracture tests, may be characterized as applied-engineering fracture mechanics. The case for this approach and the promise of practicality which these trends offer is the basic theme of this paper.

REAL STRUCTURES, REAL DEFECTS, AND REAL MATERIALS

Design practices and notations tend to idealize structures and stress conditions. Similarly, fracture specimens and notations tend to idealize the spectrum of flaws and applicable stress levels. Additionally, there is the idealization of the metal as an isotropic, homogeneous entity, subject to highly accurate specific indexing of fracture toughness. A general appreciation of the limits of what "can be real" is the essence of any practical process of fracture-safe design.

From design considerations, the nominal stresses calculated for "stress analyzable" geometries provide only partial information required in fracture-safe design. For efficient transfer of loads between members, the structure must yield at points of connection. These represent the most critical regions for fracture initiation.

The relative complexity of structures may be defined in relation to the degree of concentration of strain at points of connection. Gentle, faired connections relate to structures of simple geometry. However, even such connections generally require strain-gage analysis if the exact level of stresses is to be established. The term "experimental stress analysis" refers to this most advanced procedure for determination of stresses which cannot be calculated directly. Even computer-program analyses do not void the fact that real structures are not fabricated with the exact contours of the drawings. The most complex structures represent designs which tend to have only approximate relationships between the drawing and the actual connection or joint. In practice, a large percentage of such structures feature connections which are "designed in the shop" by the welder who makes the joint, by the nature of the machine fit up, etc. All we know about these locations is that a severe degree of plastic flow must develop if the members are efficiently proportioned to transfer loads equitably.

It is concluded that most structures must be assumed to contain regions of yield level stress, irrespective of the low nominal elastic stresses quoted for the stress analyzable portions of simple geometry. Thus, for calculations of critical flaw sizes, regions of change of geometry or of complex connection must be assumed to involve plastic load stresses of varied intensities. Such regions pose problems for accurate use of fracture mechanics because of its analytical limitations of elastic level stress fields.

Real structures involve the presence of a spectrum of flaws. Even assuming the sharpest possible variety, say a fatigue crack, is inadequate insofar as covering the worst case. Metal damage can be present at the crack tip due to strain aging, due to fatigue processes, due to weld zones, due to brittle metallurgical inhomogeneities, etc. Additionally, rapid loading such as a hydraulic pulse, impact, etc., causes the crack tip to become unstable at stresses below those for a static load. A long crack is more severe than a short stubby crack of the same depth. Calculations of critical flaw sizes must therefore include engineering deductions of flaw severity conditions with respect to crack tip and crack geometry aspects.

The fracture toughness of metals is isotropic only for the highly brittle state. Otherwise, real metals display marked directional fracture toughness properties. The "weak" direction of lowest resistance to fracture is generally associated with the direction of primary rolling or forging, i.e., with the "flow lines." For exact definition of fracture toughness, it is necessary to consider all three possible orientations — longitudinal (direction of primary flow), transverse, and through-thickness. Such complete surveys are not ordinarily feasible, and standardized practices based on evaluation for a specific direction are generally followed.

For metals of high intrinsic fracture toughness, the directional differences are not important for most engineering assessments. Metals of intermediate fracture toughness require more careful examination of directional aspects with relation to the geometry of the structure. For intercomparison of metals (predesign evaluation), it is essential that the fracture test direction and the relative degree of forging or cross rolling of the material be specified. If this is not done the significance of the fracture toughness value may be in serious doubt for the user of the information.

These various considerations highlight the fact that fracture toughness characterizations of real metals are not provided with the precise definition required for exact analytical treatment. Claims for exactness of flaw size calculations for various locations in a real structure, based on fracture toughness values of unrelated or undefined orientation leave most metallurgists singularly unimpressed. Similar restrictions on the real accuracy of critical flaw size calculations emerge for reasons of definability of stress levels, crack tip conditions, flaw size, and geometry. These limitations do not imply impracticality for the use of fracture mechanics analytical procedures. However, it is clearly evident that high exactness of definition of critical flaw size-stress conditions is not possible for complex structures, constructed of nonhomogeneous materials, containing a spectrum of flaws which must be found and defined by presently limited nondestructive flaw detection methods. Moreover, it is not reasonable to design to the "failure edge;" a reserve for deviation from idealized conditions must be allowed for. Fracture-safe design is aimed at assuring a "nonevent," rather than the prediction of exact conditions for the event of fracture.

These reflections on the real engineering world serve as a prelude to the discussions of this report. The basic philosophy is that much may be gained by modification of analytical procedures which presently emphasize unattainable exactness. Since practical engineering solutions to fracture-safe design represent approximations, it is realistic to accept matching analytical procedures which are simplified to provide "on the safe side" assessments. With this philosophy, much that is overly complex may be reduced to practical procedures.

MECHANICAL SEVERITY CONSIDERATIONS

The appearance of fracture surfaces is often used to define the processes of metal separation. It is conventional to describe these processes for a flat plate configuration. The terminology which applies to the fracture surface features also relates to the plasticity events at the crack tip for initiation and for propagation of the fracture. Figure 1 (top) illustrates the spectrum of possible fracture modes, which range from a brittle, flat fracture to a ductile, full slant (shear) fracture. Conditions which involve a flat appearance at the center and slant appearance at the surfaces are known as mixed-mode fractures. The slant fracture regions at the surface may be recognized as the familiar shear lips.

Fracture mechanics terminology evolves from a definition of the nature of stress fields associated with the crack tip plastic zones which are illustrated schematically at the bottom of Fig. 1 in relation to the fracture modes shown above. The flat fracture is usually defined as plane strain because it represents a fracture process controlled by stress fields which restrict the volume of plastic strain to a narrow plane. The full-slant fracture is defined as plane stress because it is associated with "relaxed" stress

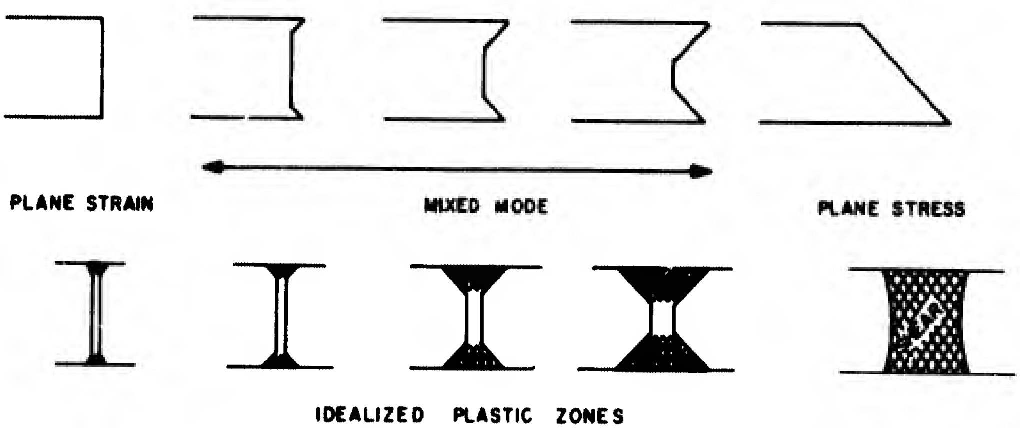

Fig. 1 - Schematic illustrations of fracture modes and related plastic zones

fields which allow extensive shearing on 45-degree planes in advance of the crack tip. Mixed-mode fractures represent stress conditions of plane strain in the center region and plane stress at the surfaces. The plane strain and plane stress terminologies also serve to describe the effective mechanical severity imposed by the crack tips, i.e., the relative effect that a specific crack has on restricting plastic flow.

All natural crack, flaw-simulation tests have one feature in common — a very sharp crack is introduced to limit plastic flow to the minimum narrow zone or band. In the absence of a crack or in the presence of a machined notch, fracture may be preceded by gross plastic instability over the entire section, which requires a large energy input. Sharp cracks concentrate the zone of plastic work and minimize the work energy requirement for fracture. The term "fracture toughness" relates to the plastic work energy required for fracture and was evolved as a short form notation of this aspect.

The effectiveness of a crack in promoting fracture initiation with a minimum of plastic work energy is directly related to the severity of the mechanical conditions at the crack tip. There are three aspects to be considered: (a) the acuity of the flaw, (b) the presence of embrittled material at the crack tip which results in enhancement of mechanical severity by a dynamic popin, and (c) the lateral dimensions of the crack tip.

Figure 2 (top) illustrates the spectrum of specific crack tip conditions which may be expected in service. The limit crack tip acuity is represented by the increase in notch sharpness to a fatigue crack tip condition. However, this is not the limit severity condition for crack tips insofar as initiation of fracture with minimum energy is concerned. Increasing severity is obtained by metallurgical damage at the crack tip, such as may be produced by aging embrittlement of the fatigue crack tip zone. The maximum-severity condition is represented by the presence of a brittle zone (due to metallurgical inhomogeneity, etc.) at the crack tip. Such a brittle zone may result in a popin, and the virgin metal is then tested in a dynamic mode even though the loading rates are slow (static).

The significance of the embrittled crack tip popin relates to the fact that some metals are highly sensitive to rate of loading. For such metals the instability plastic zone sizes (energy index) for fast loading are much smaller than for slow loading. If the tests are to be used "across the board" for all metals, it is important to decide if the loading-rate effect is to be included or not. There are two ways to obtain a rate effect — by fast loading of a virgin crack tip or by popin produced by a brittle element at the notch tip. In service it is possible for either condition to develop and subject the virgin metal to dynamic situations.

Figure 2 (bottom) illustrates specific crack-severity aspects that relate to geometry, by reference to surface cracks. Two geometries are represented by a crack featuring a width approximately twice the size of the depth, which is defined as a "stubby" or "penny shaped" crack, and a crack featuring a very long width in relation to the depth, which is defined as a "semi-infinite" crack. These relate respectively to the low- and high-limit severity, surface crack geometries to be expected in service.

The figure illustrates schematically that the long crack features high restraint to plastic flow of metal along the border of the crack tip. Plastic flow in the crack opening direction requires lateral flow of metal in order to maintain a constant volume, because there is no net loss of metal possible. Thus, a mechanical condition which limits lateral flow also limits plastic flow in the opening direction, and smaller plastic zone sizes result. Fracture instability then develops with a smaller critical plastic zone, and the plastic work energy (fracture toughness) is decreased.

This process may also be visualized for cracks which are placed through the thickness of a plate, as would be the case for a plate-edge crack or a through-thickness crack. For any given crack acuity and depth, the thickness of the plate affects the

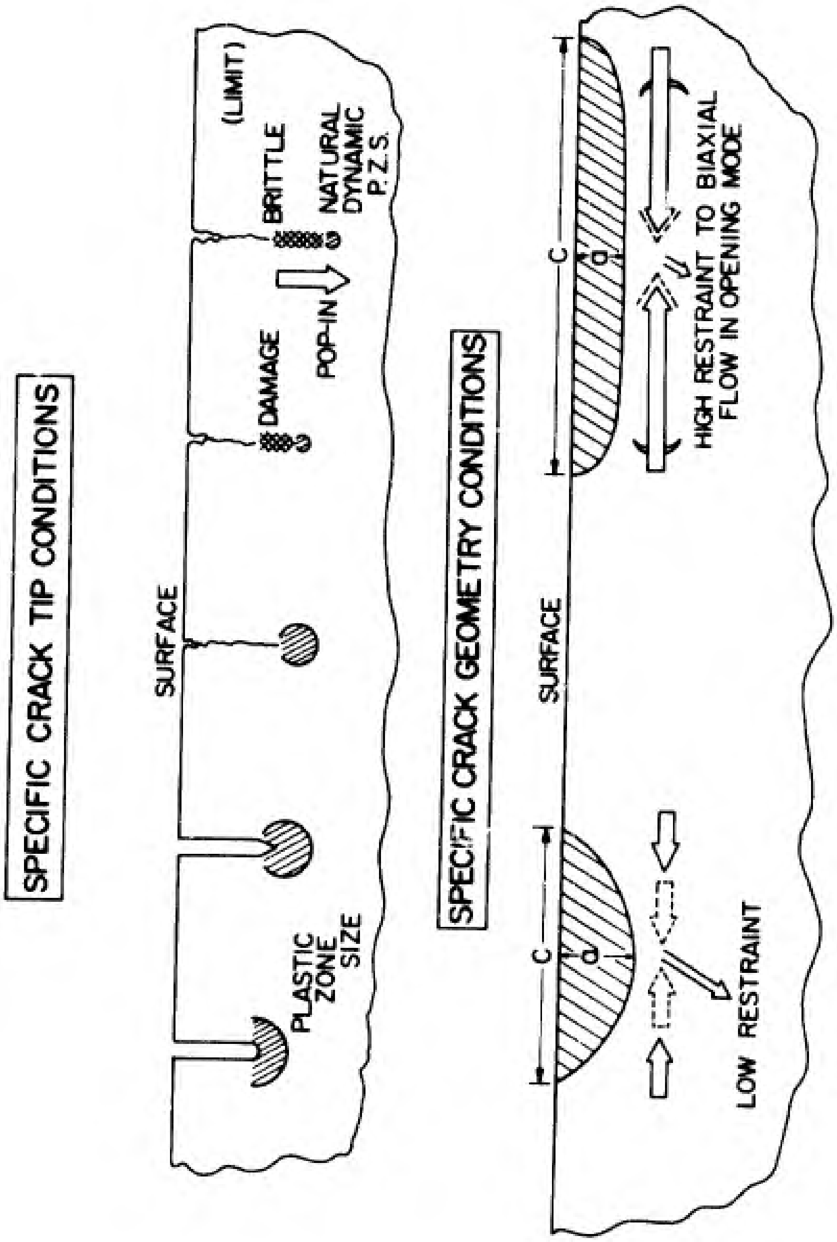

Fig. 2 - Spectrum of specific crack tip and crack geometry conditions

mechanical constraint of the crack tip for initiation and also for propagation. Increasing the plate thickness increases the crack tip lateral restraint. As the result, the critical size of the plastic zone for the onset or propagation of fracture is decreased.

It is important to recognize that by increasing plate thickness a point of maximum constraint is attained beyond which there is no effective increase in total constraint. At this point no additional decrease in the plastic work energy for fracture is obtained. The required plate thickness for maximum constraint is a function of the inherent (metallurgical) fracture toughness.

These various considerations dictate the design and interpretation of fracture tests. The fracture mechanics requirement for rigorous mathematical definition of elastic stress fields in advance of the plastic zone leads to the use of highly controlled notch tip conditions. For this reason it is necessary to use a sharp fatigue crack, produced carefully at low load stresses to eliminate fatigue damage. Also, as the inherent metal toughness increases, it becomes necessary to increase section size to develop the required maximum lateral constraint and thus assure onset of fracture with the minimum plastic zone size that can be imposed on the metal, i.e., plane strain conditions. If this is not done, mixed-mode fractures result which are difficult to analyze mathematically. In principle, all metals can be made to fracture in plane strain if sufficient thickness is used for test. In practice the metal thickness is finite, hence mixed-mode or plane stress fractures are natural events as increased toughness is attained.

The basic concept of dynamic crack tests derives from the need for simulating limit-severity conditions associated with brittle crack tips or with dynamic loading, as representative of the worst case in service. These tests are also involved with section size effects. The implications of the fracture transition from plane strain to mixed mode or plane stress are analyzed in terms of increase in total energy absorption for fracture. For tests of specimens which approximate the actual service section size, the energy increase attendant to the fracture-mode transition is taken directly as an index of assurance for fracture-safe design. If the level of fracture toughness for plane stress fracture is very high, it is then concluded that sub-size specimens would properly represent sections of considerably greater thickness. If the plane stress fracture toughness is low, the projection to greater thickness requires interpretations to be described.

FRACTURE MECHANICS TESTS

Significance of K Parameters

Fracture mechanics tests define fracture resistance in terms of the elastic stress field intensity attained in the region in advance of the crack tip plastic zone. The stress field intensity parameter is defined as K for conditions below the level required for crack tip instability (crack extension). The critical value of K at which crack extension initiates is defined as "K critical," i.e., K_{Ic}. The subscript I denotes that the applied stress causes the crack to "open" (crack-opening mode). The formal definition of the stress intensity K at various points in the elastic stress field, and similar definition of the strain level ϵ in the plastic zone, are explained in Fig. 3. The figure provides a schematic illustration of relationships between the stress-strain fields and metal separation processes. The level of stress intensification is illustrated to increase as the load stress (σ_N) is increased. The notch tip responds to the increasing stress field by yielding, to form and enlarge a crack tip plastic zone. The figure illustrates the extension of the yield boundary due to this increase.

The plastic zone size is a function of the stress field intensity and the yield strength of the metal. To attain the same size of plastic zone, a larger amount of work must be performed for a metal of high yield strength as compared with one of lower yield strength.

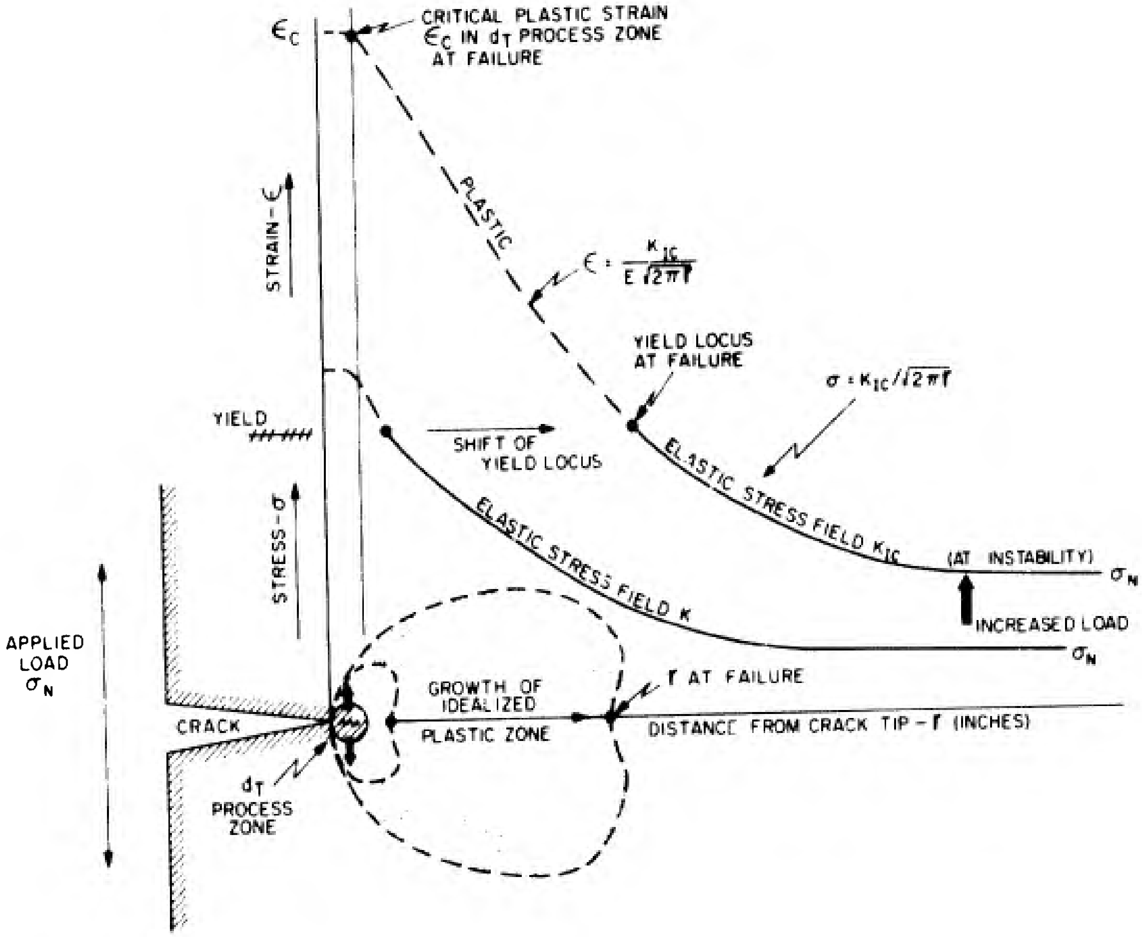

Fig. 3 - Intensification of elastic and plastic stress-strain fields in advance of crack tips subjected to rising load. Conditions at the point of crack tip instability are defined by subscript "c", i.e., critical for metal failure.

Since the work performed is a product of force times distance, it follows that plastic strain to a specified distance from the crack tip requires more force for a metal of higher yield strength. Thus, more energy is required for the extension of the plastic zone with increasing yield strength.

At some point in the growth of a crack tip plastic zone, the level of strain developed in the most highly strained portion of the plastic zone (defined as the process zone or "d_T") becomes sufficiently high to cause physical separation between or through the grains. The fracture process is initiated at this point. The critical strain for separation in the d_T process zone is defined as ϵ_c and represents the inherent ductility of the metal. In effect, the limit ductility of the metal in the d_T region is the factor which "cuts off" the rise in the K stress field. The critical K value of the stress field at the point of strain instability in the plastic zone is known as K_{Ic}, for conditions involving plane strain.

Figure 3 illustrates extrapolation of the specific elastic singularity form of the K stress field to the plastic region. The plastic strain extrapolation is defined by the relationship $\epsilon = K/E\sqrt{2\pi r}$. Crack extension occurs when the critical strain $\epsilon_c = K_{Ic}/E\sqrt{2\pi d_T}$. The stress field condition for instability may be expressed as $K_{Ic} = \epsilon_c E\sqrt{2\pi d_T}$. This mathematical relationship to d_T is of major metallurgical interest, because d_T is a "metals quality" parameter related to microstructural and inclusion conditions. The behavior of the d_T ligament may be idealized as a small tensile specimen, for which the elongation limit at failure is controlled by metal ductility.

Values of K_{Ic} are calculated from experimental determinations of crack-tip opening displacements. A clip gage is inserted at the crack surface to determine the point of instability at the crack tip. The nominal stress is calculated from an applicable beam or tension formula (see Appendix). Calculation of the instability stress intensity K_{Ic} is then made from crack depth and the nominal stress. Crack extension occurs at a unique value of K_{Ic}; however, this value may be attained by different combinations of flaw depths and nominal stresses.

There is a wide variety of fracture mechanics tests. Two simple types are illustrated in Fig. 4. Specific limitations on dimensions are imposed to assure that valid K_{Ic} values are obtained. These relate to width, length, crack depth, and ligament aspects. It is important to note that the minimum value of the thickness B is defined in terms of the K_{Ic} to yield strength ratio, as follows:

$$B \geq 2.5 \left(\frac{K_{Ic}}{\sigma_{ys}}\right)^2 .$$

The minimum-thickness limit has been established as general guidance by the ASTM-E24 Committee. Deviations from the rule require experimental proof that the minimum value of K_{Ic} (maximum restraint) has been attained.

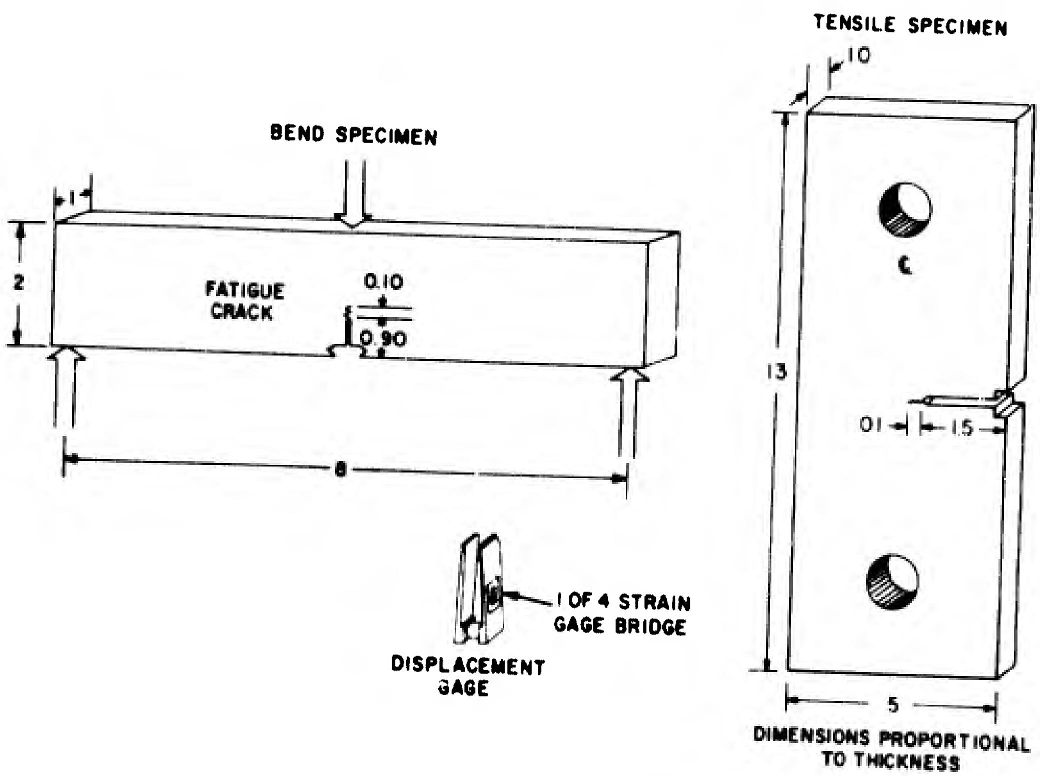

Fig. 4 - Examples of tension and bend type, fracture mechanics K_{Ic} test specimens

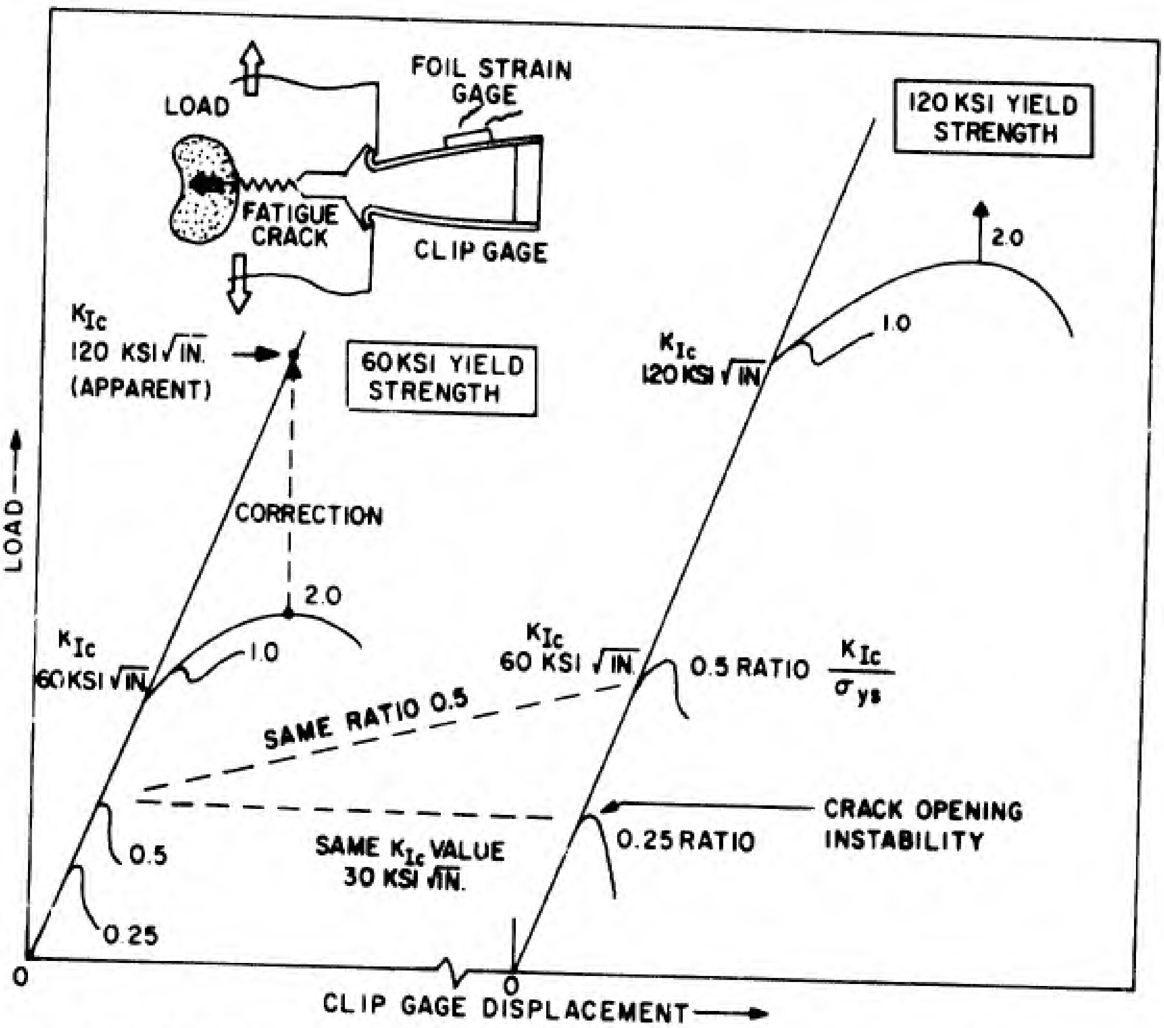

Fig. 5 - Schematic examples of K_{Ic} test, load-clip gage displacement plots. The drop of load points indicates crack tip opening instabilities at various levels of elastic and plastic loads. The significance of K_{Ic} values and of K_{Ic}/σ_{ys} ratios is illustrated.

The instability conditions that may be detected by the nominal-load clip gage displacement plots are illustrated in Fig. 5. Sharp popin instabilities with consequent falling load usually occur at low levels of stress in the elastic region. Other types include indistinct instabilities which develop at loads above the nominal yield stress and are followed by rising load. These generally represent a "tearing" action at the crack tip. Finally, when no distinct popin occurs there is the practice (not generally accepted) of simply taking maximum load as an approximation of the point at which a tearing movement of the crack has developed. This method is referred to as "roundhouse curve" determination.

It is important to note that high K_{Ic} numbers can be obtained only by moving to high levels of nominal elastic stress. Thus, high strength steels may give high K_{Ic} values if sufficient fracture toughness permits the climb to high positions in the elastic-clip gage-displacement curve. Low strength steels are restricted to low K_{Ic} values. The K_{Ic} value does not provide an index of fracture toughness per se. It is necessary to define the position of the K_{Ic} instability in relation to the subject curve by mathematical expressions which involve the ratio of K_{Ic}/σ_{ys}.* It should be recalled that earlier discussions define K_{Ic} as the stress-field intensity. Fracture toughness is an energy index (force times extension). The plastic zone size is the ductility index of how much extension was developed; the relationship of the point of instability to the clip-gage displacement axis relates to this factor. As an example, Fig. 5 illustrates that a K_{Ic} value of 60 ksi $\sqrt{\text{in.}}$, relating to a steel of 60 ksi yield strength, defines a relatively high fracture toughness condition of ratio 1.0. The nominal stress will be close to yield at instability. The same 60 ksi $\sqrt{\text{in.}}$ value for a 120 ksi yield strength steel defines to a brittle condition of 0.5 ratio. The instability is then developed at comparatively low elastic load levels. Figure 5 illustrates other aspects of K_{Ic} and K_{Ic}/σ_{ys} ratios in relation to the load-displacement curves; these are self-evident.

If the minimum B thickness requirement of the above formula is met, maximum lateral restraint is imposed. This level of restraint provides for measurement of the lowest value of fracture toughness, i.e., K_{Ic}. If the section is less than the previously defined B thickness, the lateral restraint may be less than maximum, and a K_c, geometry-dependent, instability value will be determined. The K_c definition signifies that the crack-opening displacement will be controlled by a total triaxial constraint to plastic flow which is less than the maximum which can be imposed on the metal.

Graphical Definition of Critical Flaw Conditions

Assuming that a valid plane strain K_{Ic} fracture toughness has been measured by the test, it is then possible to utilize equations derived by linear elastic fracture mechanics analyses to calculate critical flaw size-stress relationships for surface, edge, or internal cracks of various geometries. The implications are that instability will develop as the K value in advance of any crack tip plastic zone reaches the specified critical intensity of K_{Ic}.

Simplified graphical definitions of critical surface-flaw depths related to specific K_{Ic}/σ_{ys} ratios are presented in Fig. 6. The two diagrams relate to stubby (a/2c = 0.5) and long (a/2c $\leq$ 0.1) flaw geometries; i.e., 1:2 and 1:10 flaws which relate respectively to the least and most severe features of mechanical constraint. For each diagram, there are four curves related to nominal load stresses which range from yield to one quarter of yield. All other notations except the B scale should be disregarded at this point, since these will be discussed in the section to follow. The B scale relates to the minimum section thickness required for determining a valid K_{Ic} value, according to the recommendations of the ASTM E24 Committee. The relationship of the K_{Ic}/σ_{ys} ratio to the B thickness (inches) is indexed to one of the curves for convenience. The curve which should be used for this purpose is denoted by the bold arrow pointing to the B scale and also to the K_{Ic}/σ_{ys} ratio axis.

We shall now illustrate the use of the diagram to determine the B thickness requirement for any defined K_{Ic}/σ_{ys} ratio. For example, if we assume a steel of 50 ksi yield strength, it follows that increases in K_{Ic} values from 25 to 50 and then to 100 ksi $\sqrt{\text{in.}}$ results in ratios of 0.5, 1.0, and 2.0 respectively. The minimum section thicknesses for K_{Ic} determinations are then deduced (use curve with bold arrow) to be approximately 1.0, 2.5, and 10 in., respectively.

We shall now illustrate the use of the relative stress curves for the definition of critical flaw depths. As an example, assuming K_{Ic}/σ_{ys} ratios of 0.5 and 1.0, and levels

*For purposes of simplification of charts and discussions in this report, the simple ratio K_{Ic}/σ_{ys} will be used; this will be defined as the "engineering ratio." Formal relationships ordinarily involve the square of this ratio.

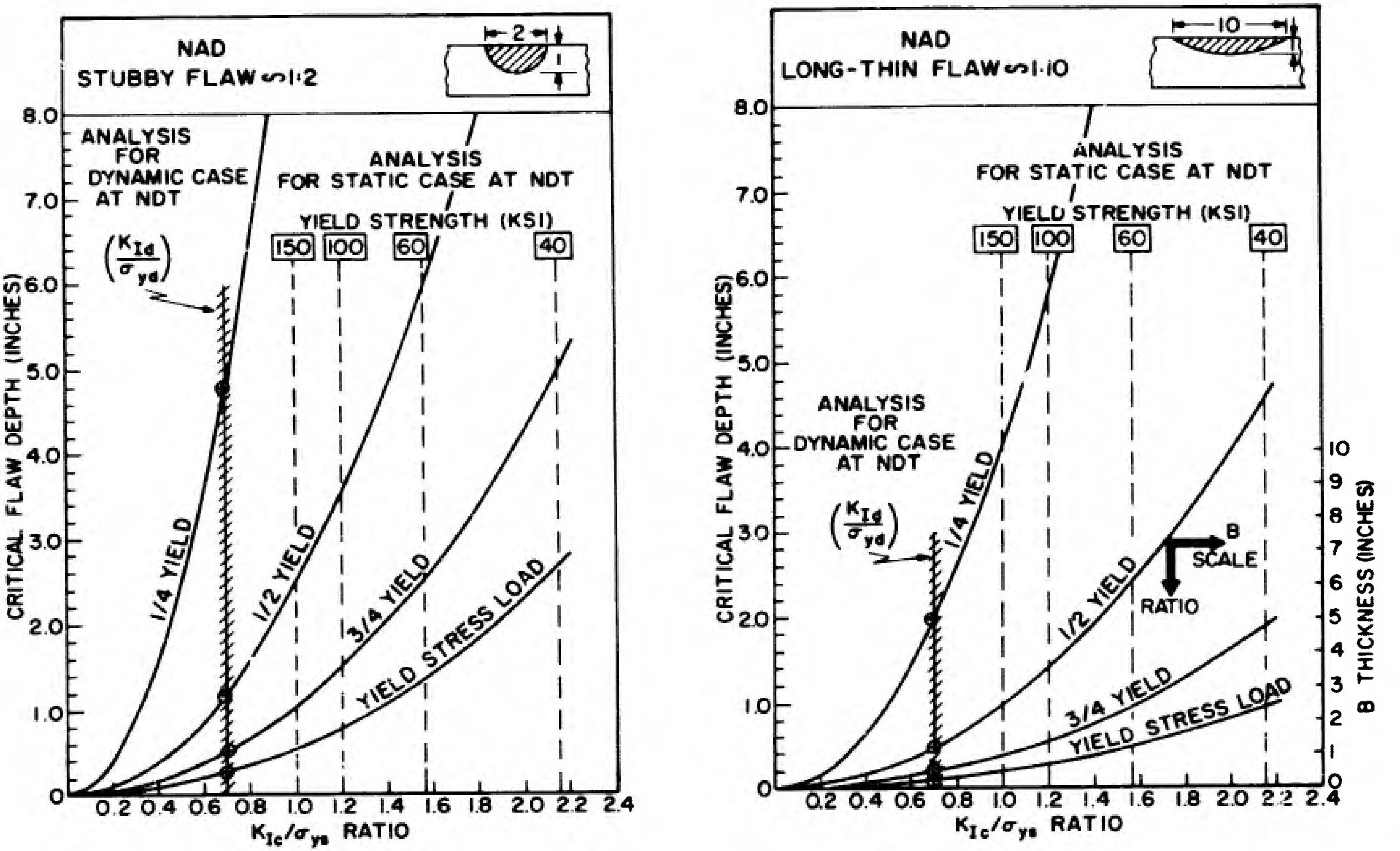

Fig. 6 - Generalized plots of critical flaw depth-stress relationships. The plots are defined as the NDT Analysis Diagram (NAD) for interpretations which are specifically related to the NDT temperature region.

of relative stress of yield and one-half of yield, the following critical flaw depths are indicated for the stubby (1:2) flaw:

K_{Ic}/σ_{ys} Ratio	Critical Flaw Depths for Relative Stresses of	
	Yield	One-Half of Yield
0.5	0.2 in.	0.5 in.
1.0	0.5 in.	2.5 in.

It may be observed that all flaw sizes (depth and width) are small for low K_{Ic}/σ_{ys} ratios for both flaw geometries. With increasing ratios above 0.5, a wide range of flaw sizes is defined in relation to relative stress and respective flaw geometries. Relative stress is a useful index because the stress levels in structures relate to one-half yield or less in regions of simple geometry, and to yield stress levels for regions of complex connection or load transfer.

The applicable formula for critical surface flaw-plane strain calculations is:

$$K_{Ic} = \frac{1.1\sigma}{\sqrt{Q}} \sqrt{\pi a}$$

where

K_{Ic} = ksi $\sqrt{\text{in.}}$

σ = nominal load stress (ksi)

$1.1/\sqrt{Q}$ = geometry factor (see text)

a = critical crack depth (in.)

Since $(K_{Ic}/\sigma)^2 = 1.21\pi a/Q$ it follows that the calculated critical flaw depths are in direct proportion to the ratio of $(K_{Ic}/\sigma)^2$. The geometry factor, Q, is 2.15 to 2.4 for a stubby flaw and 1.0 to 0.8 for a semi-infinite flaw. Thus, for a given $(K_{Ic}/\sigma_{ys})^2$ ratio the calculations for these two types define critical flaws which are 2.5 times deeper for the stubby flaw as compared to the semi-infinite flaw.

It is emphasized that these calculations are for plane-strain conditions and therefore require that the plastic zone size associated with the crack border is the minimum attainable for the level of fracture toughness. In effect, the same conditions that apply for determining the minimum value of K_c, i.e., K_{Ic}, must be satisfied. As a first approximation, this requirement would dictate that the flaw must reside in a section of thickness equal to or greater than the B value required for valid K_{Ic} measurement. This value may be noted from the B scale for the specific K_{Ic}/σ_{ys} ratio of interest. For a given K_{Ic}/σ_{ys} ratio there are specific conditions of flaw depth and geometry that would permit initial localized instability, which is then followed by an arrest, because the thickness requirement for plane strain propagation is not satisfied. From an engineering point of view, the concern is with instabilities that are not arrested. Therefore, the only reasonable guide that could be provided for a finite thickness of interest is that indicated by the B value. If plane strain conditions are not satisfied, it may be assumed that K_c conditions control the safety of the structure. Such conditions translate to a requirement for flaw sizes in excess of those defined by the curves of Fig. 6.

Another limitation inherent in the above surface-flaw formula relates to the nature of the elastic stress field analyses on which it is based. As derived by Irwin, the analyses are limited to flaw depths of half the plate thickness or less. Other formulas have been derived which provide for calculations of surface-flaw depths extending to 0.75 thickness. These aspects are beyond the introductory scope of this report.

Flaw-normalization procedures described by the Q factor in the above formula provide only approximate definitions of instability conditions. Because of uncertainties associated with the Q factor, surface-flaw tests are not recommended for K_{Ic} determinations by the ASTM E-24 Committee. The reason is that invariant K_{Ic} values are not obtained for different surface flaw geometries. The premise of exact analytical calculations for surface cracks must be recognized to have inherent limitations at the present state of development.

Unless otherwise stated, K_{Ic} values refer to static (slow load) measurements. If a dynamic load is applied, or if brittle material is located at the crack tip, a dynamic value of K_{Ic} (defined as K_{Id}) should be used (discussions relating to the dynamic case are presented in the section to follow). The dynamic case requires a determination of the dynamic yield strength, and Fig. 6 then must be interpreted in terms of dynamic K_{Ic} to dynamic yield strength ratios. The calculated flaw sizes then relate to the dynamic condition. The practical problem is that conducting dynamic K_{Ic} tests poses experimental difficulties, such as determining the dynamic response of the specimen for calculation of the instability load stress. At the present state of development, dynamic K_{Ic} testing is not practical.

It is not implied that all materials are rate sensitive to an appreciable degree. For the low-strength mild steels in the cleavage fracture range (toe of transition) the dynamic K_{Ic} value may be one-half or less of the static K_{Ic} value at a specified temperature. High strength steels may show very low rate sensitivity – in the order of 10 percent decrease or less, compared to the static K_{Ic}.

Fracture mechanics $\mathcal{G}_c$ and $\mathcal{G}_{Ic}$ notations relate to K_c and K_{Ic} conditions expressed in energy terms (see Appendix, items 1 to 4). The term "$\mathcal{G}_c$ testing" refers to fracture mechanics tests based on measurement of the crack-extension force at the onset of rapid propagation. Such tests require wide specimens and long flaw sizes, which become of unrealistic dimensions as fracture toughness increases. For this reason, the original fracture mechanics developments based on $\mathcal{G}_c$ testing were shifted to K testing. For K testing, which is based on a sensitive measurement of the "first event" signs of crack-opening displacement at crack tips, specimens of more reasonable dimensions emerge. However, as indicated by the B scale of Fig. 6, K testing also involves requirements for relatively large specimens as fracture toughness increases. The required sizes above 1 or 2 in thickness are obviously beyond practical limits for general engineering usage.

RELATIONSHIPS BETWEEN FRACTURE MECHANICS, ROBERTSON AND DROP WEIGHT TESTS

Drop Weight Test Definition of K_{Ic} and K_{Id} Values

The level of plane strain fracture toughness increases with temperature due to effects of decreasing yield strength and increases in the critical strain (ϵ_c) in the d_T process zone. Fracture mechanics theory in these respects is not well defined, and the interplay of these two factors is subject to controversy. According to one theory, due to Irwin (3), the increase in K_{Ic} with temperature is essentially linear, while other theories predict an increase in the slope of the K_{Ic}-temperature relationship. Experimental data generally indicate an increase of slope.

Crack Arrest Temperature (CAT) curves of the Robertson test for 1, 2, or 3 in. plates indicate a rapid increase in fracture toughness above the NDT temperature. This increase is due to the change from a dynamic K_{Ic} (K_{Id}) fracture toughness below the NDT temperature, to K_c mixed-mode fracture toughness at NDT + 30° to +60°F and finally to K_c plane stress fractures at NDT + 120°F or higher (4).

The concept of linear slope increase of K_{Ic} with temperature suggests that with a sufficient increase in plate thickness, the Robertson test CAT curve should show a fairly straight-line rise, of low slope. This concept does not suggest that a Robertson test CAT curve for a 2 in. plate is invalid, but that it is valid only for a plate of this general thickness. How thick a steel must be to "flatten out" the CAT curve to high temperatures above the NDT is a matter of mathematical conjecture – estimates for mild steel are in the order of 10 in. or more. The increasing-slope theory would suggest a shift of the CAT curve rise to moderately higher temperatures rather than a "flattening out." The relative validity of either of these opposing concepts requires experimental verification using very thick specimens.

The fracture appearance of the Drop Weight Test (DWT) at the NDT temperature is flat and devoid of visible shear lips. This appearance is in exact correspondence with the CAT test fracture at the NDT temperature. Above the NDT temperature the DWT specimen does not fracture, while the Robertson test plate fractures show shear lips. Obviously, the event which terminates the fracture of the DWT test at the NDT is the development of K_c mixed-mode transition, which involves high energy absorption at the shear lip surface regions. Thus, the NDT may be considered as the temperature of initial transition from plane strain to mixed-mode fracture; i.e., K_c conditions begin to influence the dynamic fracture propagation processes.

Fracture mechanics calculations of dynamic K_{Ic} (K_{Id}) values for the NDT temperature may be made from considerations of the flaw size-stress conditions of the DWT. The flaw depth and geometry features are represented by the brittle weld bead popin of approximate dimensions a = 0.2 in. and $2c$ = 0.8 in. (ratio of 1:4). The geometry factor for this flaw corresponds to Q = 1.22 at yield stress loading. The DWT loading conditions require that the dynamic yield stress (σ_{yd}) be considered as the applied load stress. Calculation of the dynamic K_{Ic} (K_{Id}) at NDT can then be made for the subject flaw size and for an approximated dynamic yield stress equal to the static stress plus 30 ksi, as suggested by Irwin (3). The generalized calculation for dynamic K_{Ic} (K_{Id}) is as follows:

$$K_{Id} = 1.1\,\sigma_{yd}\left(\frac{\pi a}{Q}\right)^{1/2}$$

$$= 1.1\,\sigma_{yd}\left(\frac{\pi(0.2)}{1.22}\right)^{1/2}$$

$$= 0.70\,\sigma_{yd}\ \mathrm{ksi}\sqrt{\mathrm{in.}}$$

For a steel of 70 ksi yield strength (say A533), the dynamic yield stress is taken as 100 ksi; thus

$$K_{Id} = 0.70(100) = 70\ \mathrm{ksi}\sqrt{\mathrm{in.}}$$

The exactness of the calculated K_{Id} value is probably well within useful limits required for engineering usage. Correlation evidence presented by Irwin (3) indicates very good correspondence of K_{Id} values determined by this procedure with K_{Ic} values obtained directly by other fracture mechanics tests. Because of the difficulties of conducting dynamic fracture mechanics tests, the DWT offers a practical method for K_{Ic} determinations related to the NDT temperature region. If the relationships of K_{Ic} to K_c and the temperature slope effects are clarified, the DWT would then provide a practical approach for extrapolation of applicable K_{Ic} or K_{Id} values to include the transition temperature range.

In the absence of fracture mechanics procedures for analytical definitions of these factors, recourse may be taken to approximations which provide useful interim engineering guidance. As a first step, we shall consider the limits of flaw geometries of conventional DWT brittle weld beads. These range between $a/2c$ ratios of 1:3 to 1:4. The calculated K_{Id} values then range between $K_{Id} = 0.7\,\sigma_{yd}$ ksi $\sqrt{\text{in.}}$ and $0.8\,\sigma_{yd}$ ksi $\sqrt{\text{in.}}$ For the 70 ksi yield strength A533 steel described previously (σ_{yd} = 100 ksi), the K_{Id} value will fall in the range of 70 to 80 ksi $\sqrt{\text{in.}}$ This range is fairly narrow even by conventional standards of fracture mechanics test definitions of K_{Ic} values. We propose to use the lower end of the range to provide a conservative value for engineering purposes. It should be noted that the K_{Id}/σ_{yd} ratio is then defined as 0.7 at the NDT temperature.

The ratio definition provides for entry of the Fig. 6 flaw size definition diagram for interpretations of dynamic instability conditions (use ratio 0.7 for the K_{Ic}/σ_{yd} scale as relating to K_{Id}/σ_{yd}). The required B value for plane strain condition for a 0.7 ratio is indicated to be approximately 1.5 in. This minimum section thickness requirement does not correspond to service experience and is obviously not correct for the dynamic case. This fact is noted to emphasize that the noted B scale should not be used in relation to dynamic fracture conditions. The B relationships were evolved from static K_{Ic} test experience and have not been proposed for use under dynamic conditions.

It is well established by DWT and service experience that 0.5 in. or possibly 0.3 in. thickness is adequate to provide for dynamic plane strain conditions at NDT or lower temperatures. Thus, there is no need to use the B scale for thickness interpretations. All thicknesses in excess of the quoted 0.3 to 0.5 in. range will provide adequate thickness restraint for dynamic fracture propagation.

Extension of these engineering procedures to cover the case of static K_{Ic} condition at NDT requires introductory discussion. We should first recognize that the above interpretations support the established concept that the NDT represents the temperature at which very small flaws suffice for dynamic fracture initiation. Moreover, these do not invalidate the fact that steels of 1, 2, or 3 in. thickness should show a rapid rise in critical flaw sizes above the NDT. The fracture mechanics analysis simply states that this increase results from a change of dynamic plane strain K_{Id} conditions at the NDT temperature to higher fracture toughness values related to K_c mixed-mode conditions, at temperatures above the NDT. Increase in section size to say 10 in. does not change the fracture mechanics calculation of the K_{Id} level at NDT, assuming that metallurgical effects are not involved to raise the NDT temperature.

Figure 7 provides a schematic illustration of relationships between K_{Ic}, K_{Id}, K_c, Robertson CAT, and DWT determinations. The curves are representative of low strength mild steels of approximately 1 in. thickness. The gradual rise in slope of the static K_{Ic} curve with temperature terminates with a rapid rise to K_c values (dashed part of curve), considerably below the NDT temperature. A similar rise of the K_{Id} curve with temperature terminates in the same manner to K_c values as the NDT temperature is exceeded. Extrapolations of the static or dynamic K_{Ic} curves to higher temperatures for increased thickness are subject to the same questions as were discussed in relation to the CAT curve. To avoid questions which cannot be answered at this time, we shall restrict all further discussions to the 1 to 3 in. thickness range, for which there is ample experimental evidence of K_{Id} transition to K_c conditions with increasing temperature above the NDT.

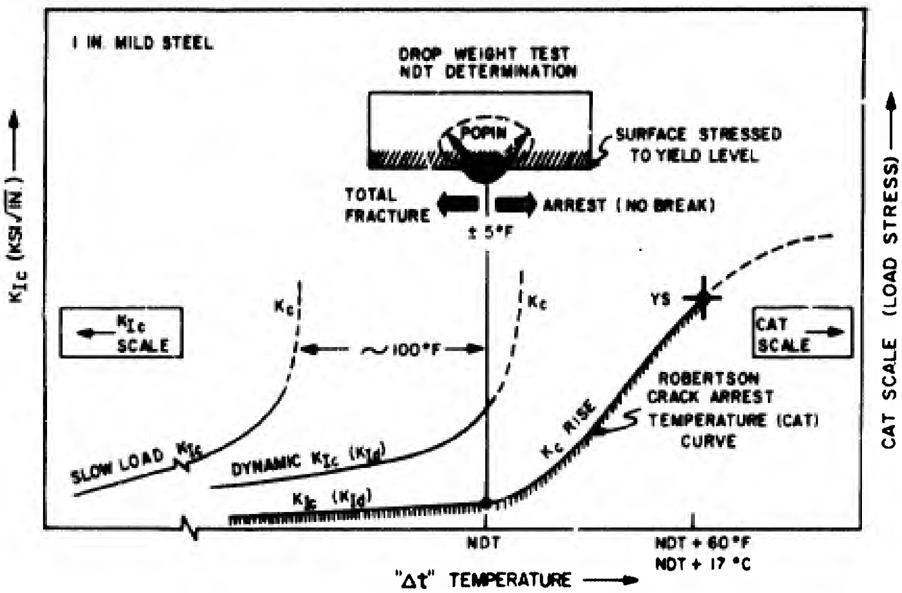

Fig. 7 - Generalized temperature scale relationships of static K_{Ic} and dynamic K_{Ic} (K_{Id}) measurements for mild steels of approximately 1 in. thickness. The graph illustrates transition to K_c conditions and correspondence to the NDT temperature and to the Robertson CAT curve.

NDT Analysis Diagram (NAD)

According to best available estimates, the static K_{Ic} value at NDT may be approximated by multiplying the K_{Id} value by the ratio of σ_{yd} to σ_{ys}. Estimations of the K_{Ic} value at NDT for steels of various yield strengths can then be made by calculating the K_{Id} value (as described previously) and then defining the K_{Ic} value by the σ_{yd}/σ_{ys} ratio approximation. The calculated K_{Ic} value then provides for definition of the K_{Ic}/σ_{ys} ratio at NDT. These calculations for steels of 40, 60, 100, and 150 ksi yield strength result in K_{Ic}/σ_{ys} ratios of 2.15, 1.55, 1.2, and 1.0 respectively. The vertical lines in Fig. 6, which are indexed to yield strength levels, are placed at these respective ratio values. Interpolations may be made for steels of intermediate strength levels by noting the trends of the applicable ratios, with changes in yield strength. These combined procedures provide for NDT indexing of Fig. 6 flaw size definitions to dynamic conditions (use 0.7 ratio for all yield strength levels) and for static conditions relating to ratios which are specific to the yield strength level. In order to define clearly the use of Fig. 6 in relation to the NDT temperature region, the full diagram (complete with the vertical ratio lines) will be defined as the NDT Analysis Diagram (NAD).

Figure 6 may be used in four ways, as follows:

1. General — entry at the applicable ratio point, derived from direct experimental determination of K_{Ic} or K_{Id} values.

2. Dynamic at NDT — entry by use of the 0.7 ratio line for all strength levels relating to strain rate sensitive steels (NAD).

3. Static at NDT — entry by use of the ratios defined for specific strength levels (NAD).

4. Static General — for determination of B thickness values relating to any specified ratio.

The NAD procedure provides useful guidelines for the engineer without the requirement for understanding all the ramifications and limitations of fracture mechanics. The DWT (also the DT test, as will be described) serves to define the temperature for which these analyses apply. For general engineering use, the applicable range may be taken as NDT + 20°F to NDT - 50°F. Restrictions to a narrower range are not justified because the effects of temperature over this range should not be expected to influence the critical flaw sizes in excess of the accuracy of the calculation methods. As will be demonstrated in the next section, these definitions are in line with those of the FAD for the NDT temperature range. The NAD amplifies the definitions provided by the FAD, but at the expense of requiring more detailed analysis of flaw size, geometry, and stress conditions.

The NAD refinements provide for direct interpretations of decreased mechanical constraint effects due to limited section size. Thus, conditions which relate to K_c fracture toughness control may be separated from those that imply K_{Ic} control. Considerable advantage may be realized if plane strain K_{Ic} conditions do not apply due to section size limitations, because larger flaw sizes will be tolerable. Such direct analyses represent the most detailed and exact procedure for utilizing the NAD. In many cases such detailed definitions may not be required. For use in such cases, we shall describe an intermediate type of NAD interpretation which approaches the simplicity of the FAD.

The proposed procedure is based on providing engineering guidelines for the use of the NAD which do not require analyses of the section-size problem. These guidelines will be based on the consideration that a very large fraction of problem cases to be analyzed will fall in the range of less than 4 in. thickness and less than 120 ksi yield strength. If the thickness clearly exceeds this range, say 6 in. or more, it is suggested that the more detailed use of Fig. 6 be made according to previously described procedures.

The proposed simplified use of the NAD follows established fracture mechanics simplification practices of defining safe or conservative "upper bound" flaw sizes which should be of concern for possible failure. The flaw size limits are placed sufficiently high to exclude uncertainties — in effect, these procedures define the "worry limit" at which the flaw sizes become too large for comfort. The NAD provides for this approach by use of the 1.2 ratio line, which is selected to define flaw sizes which clearly should be larger than those which could cause failures for steels of less than 120 ksi yield strength and not greater than 4 in. thickness. The 1.2 ratio relates to the calculated K_{Ic}/σ_{ys} value for steels in the range of 100 to 120 ksi yield strength, higher ratios apply to steels of lower yield strength. The B scale indicates that the 1.2 ratio requires a minimum section size of 4 in. to provide for plane strain conditions. Therefore, any combination of less than 120 ksi yield strength or less than 4 in. thickness will relate to fracture conditions involving deviations from plane strain. In effect, the flaw sizes deduced by use of the 1.2 ratio are conservative, and "worry" should begin if the flaws of interest approach the defined values or are significantly larger. Obviously, flaw geometry and relative stress must be considered for specific engineering interpretations.

This description serves another purpose; if understood as to derivation, the reader may proceed to establish similar upper-bound limits specialized to his interests. While additional discussions could be made, there is no substitute for detailed study of Fig. 6 and reflections as to its significance. The capsule treatments of flaw-size definitions that are provided have a wide variety of practical engineering ramifications.

FRACTURE MECHANICS INTERPRETATION OF FRACTURE ANALYSIS DIAGRAM (FAD)

The NDT indexed Fracture Analysis Diagram (FAD) was evolved from service experience. Its verification far exceeds that of any other procedure (4,5). After over six years of active use there has been no evidence of unfavorable experience; to the contrary, there has been considerable confirmation by users. Questions of the validity of the FAD which are based on theoretical considerations must likewise involve questions of the associated service-failure correlations.

One of the two main arguments against the generalized use of the FAD is based on considerations that static K_{Ic} conditions may govern below the NDT in some cases, and for these the FAD is considered pessimistic. The other principal argument relates to thickness effects and the postulated "depressing" of the CAT curve. From these considerations, the validity of the FAD for thick steels (considerably over 3 in.) is questioned for temperatures above the NDT.

Predictions of plane strain conditions considerably above the NDT due to thickness effects are not corroborated by service experience. There is no recorded evidence of plane strain fractures for very thick steels at temperatures of 100 F or more above the NDT. The theoretical, K_{Ic} extrapolations for low strength steels of 6 to 10 in. thickness indicate that such failures could develop as much as 400 F above the NDT. This prediction follows because the assumed K_{Ic} slope above the NDT is relatively flat. It may be calculated to increase approximately 15 ksi $\sqrt{\text{in.}}$ per 100°F rise above the NDT for the described A533 steel. The increase for a steel of 40 ksi yield strength would be less, and in the order of 10 to 12 ksi $\sqrt{\text{in.}}$ for 100° F rise. If this is the fact, there is reason indeed for pessimism and alarm.

In these respects, it should be noted that the theoretical extrapolations do not consider the effects of increased temperature on the basic micromodes of fracture which involve "transition" from cleavage to ductile rupture. These effects should influence the separation processes in the σ_T process zone and thereby defeat the increased application of added mechanical restraint due to thickness, as the transition range is entered. This concept may be defined as a "metallurgical barrier," specific to an intrinsic temperature range for a specified steel. This concept does not suggest that the CAT curves may not be shifted to moderately higher temperatures with increased thickness. However, it does suggest that this process will be effective only within modest limits, after which the increasing ductility of the metal defeats the mechanically enforced crack tip, plane strain condition. This concept is not contradicted by the wide variations in transition temperature that can be obtained by changes in notch sharpness, loading rate, etc. All of these effects relate to changes in the degree of mechanical severity at temperatures below the limiting metallurgical barrier.

To our knowledge, there has been no detailed check of the FAD flaw size predictions based on fracture mechanics calculations for flaw sizes. We may now consider whether the calculations check the failure experience defined by the FAD. If this is the case it would be comforting for both the theory and engineering practice. For proper analysis, we shall consider only steels of 1 to 3 in. thickness and thus avoid questions relating to very thick steels, for which no one presently has answers except negatively as to failures. The procedures for calculating critical flaw conditions for the dynamic K_{Ic} (K_{Id}) and static K_{Ic} conditions were explained in the previous section. For the dynamic case, the conservative K_{Id}/σ_{yd} ratio of 0.7 will be applied. For the static case, the conservative lower-limit definition provided by the K_{Ic}/σ_{ys} ratio of 1.2 will be used, with the additional related restriction that the analyses apply to steels of less than 120 ksi yield strength. Most of the service failure cases on which the FAD was derived relate to steels below this strength level.

Additionally, we shall consider dynamic initiation conditions as being fully satisfied for this thickness range, for reasons cited. For the static case it is necessary to consider the B limitation associated with the 1.2 ratio index. The calculations will be made on the basis that the B limitation is satisfied; however, a notation of $>>K_c$ will be used to indicate that the instability conditions may be expected actually to involve larger flaws, because of the expected K_c control for initiation relating to sections of 1 to 3 in. thickness.

The flaw lengths will be deduced by the use of the Fig. 6 curves relating to the stubby flaw of 1:2 geometry, which gives the most conservative length value. For flaws of 1:10 ratio, the length values will be greater. The reason for this choice is that the FAD flaw lengths are often considered "unrealistically" long. Thus, we choose a condition which is the most severe test of the FAD definitions, which have been based on flaws of a variety of geometries.

The flaw size predictions derived from Fig. 6 are presented in Fig. 8 (left side). The upper left chart illustrates the dynamic K_{Ic} (K_{Id}) predictions of a (depth) and $2c$ (width) in relation to the FAD. The lower left chart illustrates the static K_{Ic} predictions in relation to the FAD. The curves above the NDT temperature are considered to be K_c controlled with respect to temperature. This follows because the CAT curve passes from K_{Id} to K_c control in this region, as described previously. In effect, the flaw sizes defined below NDT require increased stress for instability above the NDT temperature.

The diagram on the right side of Fig. 8 presents a summary of these two analyses in terms of flaw lengths for comparison with the flaw length definitions of the FAD. It is noted that the FAD definition of under 1 in. for yield stress loading is close to the value defined for the static case and in concurrence with 0.4 in. size defined for the dynamic case. The FAD definition of under 1 in. provides adequate generalized warning for both cases.

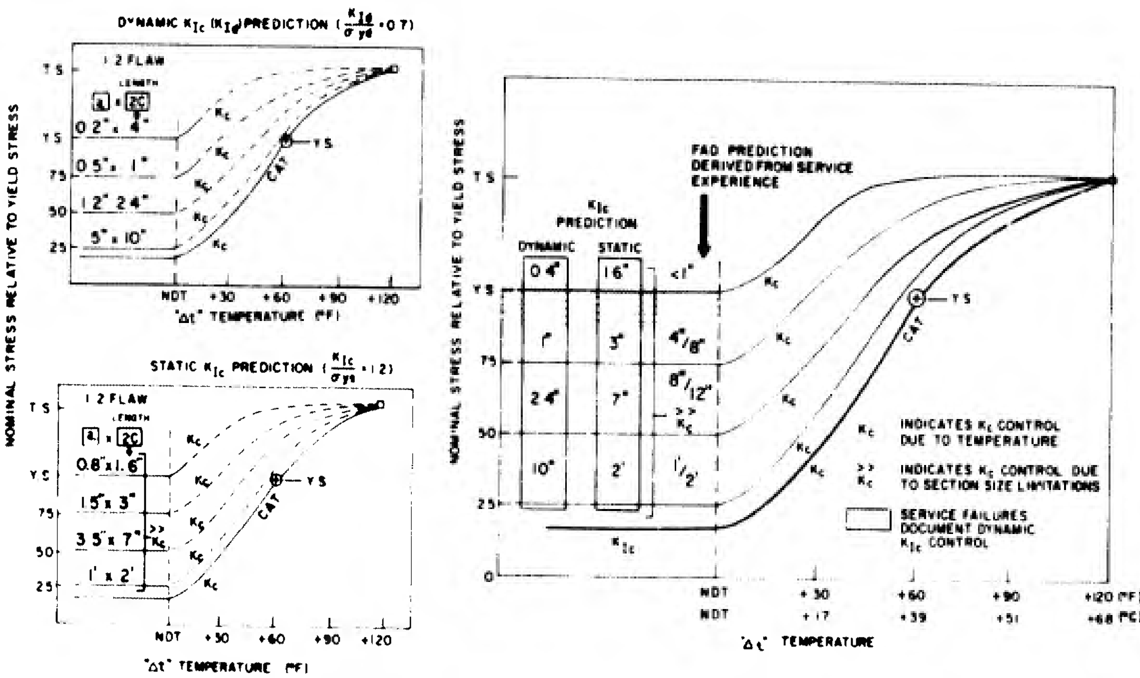

Fig. 8 - Fracture mechanics interpretations of Fracture Analysis Diagram (FAD). The calculated flaw sizes correspond to the FAD predictions derived from service experience.

The large, FAD flaw sizes for levels of stress less than approximately 0.8-yield stress indicate that K_c initiation conditions have governed the service failures. The low end of the FAD prediction range generally matches the K_{Ic} prediction.

FAD service experience does not validate the predictions of dynamic K_{Ic} (K_{Id}) failures for 1 in. flaws at 0.75-yield stress and for 2.4 in. flaws at 0.5-yield stress. Apparently flaws of this size and related stress levels cannot generally be "contained" within embrittled regions of sufficient size to provide for a catastrophic propagation of popin instabilities. The very small flaws of 0.4 in. or less, defined for yield stress levels, are easily contained in such regions; moreover, these tend to be associated naturally with weld zone residual stress fields of yield stress magnitude. At this point we should remember that it was the tiny flaws that caused WWII ship failures. At the time there was much confusion over the fact that longer flaws lay dormant. The answer apparently is in the very large size required for fracture initiation in regions of low nominal stress. Only the very small flaws were located appropriately in embrittled, highly stressed regions. These in effect served as a "fuse" which initiated the dynamic fracture propagation process.

The NDT indexed FAD in its original form may now be interpreted with greater clarity, as follows:

1. The NDT temperature indexes the CAT curve rise properly (confirmation related to previous discussions).

2. The NDT temperature indexes the critical flaw size at yield stress level as being generally less than 1 in. (confirmation). A separate definition of about 0.4 in. for the dynamic case (known previously) and approximately 1.6 in. for the static case (improved definition) emerges. However, the limiting condition remains the dynamic case.

3. The flaw size spectrum for stresses significantly below the yield level relates primarily to K_c controlled initiation conditions for steels of 1 to 3 in. thickness (new definition). Propagation under K_c control due to temperature is involved above the NDT (known).

These analyses should serve to explain the basic significance of the FAD and at the same time provide a tribute to analytical capabilities of fracture mechanics theory. Questions of thickness effects, when resolved, may be incorporated in the FAD. The system is sufficiently flexible to provide graphical representations of improvements in fracture mechanics theory. As for other graphical interpretations of similar type to be presented, it is suggested that these procedures be considered as the practical process by which fracture mechanics is extended to generalized use by the engineering field.

DYNAMIC TEAR TEST (DT)

The Dynamic Tear (DT) test was evolved at NRL in 1960 and until recently was known as the Drop Weight Tear Test (DWTT). One of the original purposes was to determine the temperature region of plane strain to mixed-mode transition for thin steels of less than the 5/8 in. limit set for the DWT-NDT test. In effect, the purpose was to define the CAT curve "rise."

This concept was suggested (6) to the Battelle Memorial Institute (BMI) and the Bethlehem Steel Corporation Research Laboratory in 1962, for purposes of defining the temperature of expected "arrest" for steels used in gas transmission pipelines. Battelle Memorial Institute used a pressed-knife-edge notch applied directly to the tension surface (now known as BDWTT), and the K_c rise was observed visually as a change from flat fracture to slant, plane stress fracture. The Bethlehem Laboratory utilized the brittle crack design for early studies. Both types were validated by extensive pipeline burst tests. The burst-test fractures were initiated in a brittle section and propagated into the test section material at controlled temperatures. Fracture arrests in these full scale tests were obtained at the temperatures of rapid K_c rise indicated by the DT type tests. The sharp, K_c-rise features of the test provided a reliable index of arrests within narrow temperature limits. As the result, the test is now being considered industrially for routine application to steel specifications for pipelines.

From 1960 to 1967, the NRL interests in the use of the DT test were directed primarily to problems of fracture toughness definitions for high strength steels and for nonferrous metals, such as titanium and aluminum alloys (7,8). There was evident need for a limit-severity crack test based on the embrittled notch tip concept that could be applied uniformly to all types of metals, in the temperature transition range or on the shelf, i.e., at full ductility.

Fracture toughness questions for steels are involved with both *temperature* and *strength transitions*. We introduce the term "strength transition" because with increased yield strength, the fracture toughness level of steels "on the shelf," i.e., above the transition, decreases rapidly. The mechanical aspects that have been discussed for the temperature transition apply similarly to the strength transition. At a very high strength level, the best of steels are highly brittle, as at the "toe" of the temperature transition. The K_{Ic} tests for this level of fracture toughness may be made with specimen thickness of 1 in. or less. With decreasing strength, the attainable intrinsic (metallurgical) fracture toughness increases greatly. Hence, the section thickness required to develop plane strain conditions required for K_{Ic} testing must increase to the same very large sections (10 in. or more) described for the temperature transition, otherwise a change from plane strain to plane stress conditions results due to inadequate thickness.

The size effect implications of fracture mechanics theory thus raise questions of major import to the use of thick steels, for both the temperature and the strength transitions. Distressingly, the rate of accumulation of fracture mechanics data for sufficiently thick steels, or even experimental verification of the "sufficient" thicknesses for valid K_{Ic} measurements, will be slow to evolve. We can envision a decade of slow progress, particularly for the steels of intermediate and high fracture toughness.

In order to evolve sufficient information in a reasonable time frame, it appears necessary to use a simple limit-severity crack test, such as the DT type, which has flexibility for the evaluation of section size effects. From a practical point of view, the deviations from K_{Ic} plane strain to K_c mixed-mode or plane stress fracture conditions, with increasing temperature or decreasing strength, are exactly the information the engineer requires.

The DT test was formerly known as the DWTT because of the drop weight method of loading used initially for all specimen sizes. Starting in 1963, Charpy type pendulum machines were evolved which cover the range of 5/8 in. to 2 in. thickness specimens. Figure 9 illustrates two machines of this type, the smaller of which features a double pendulum for "shockless" testing. For specimens of larger thickness, simple drop weight machines are used. The largest of these presently has a 160,000 ft-lb capacity. Figure 10 illustrates this machine and also one of intermediate capacity.

Figure 11 illustrates the features of the 1 in. thick, standardized DT specimen and the appearance of typical fractures. The notch element consists of a brittle electron-beam weld. The embrittlement is obtained by the use of a small titanium wire which is melted by the electron beam to produce a weld of highly brittle, iron-5% titanium alloy. The early form of the test utilized a brittle steel bar welded to the tension side of the test specimen (7). Table 1 gives the dimensions and weights of the various specimens used for steels of increasing thickness. The table also includes the 5/8 in. thick,

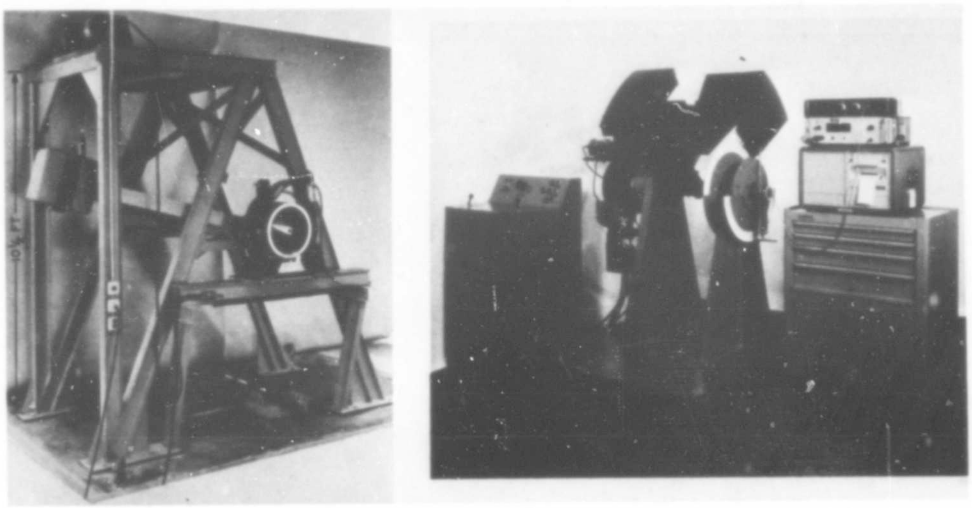

Fig. 9 - Dynamic Tear (DT) test pendulum machines, illustrating single pendulum type (5000 and 10,000 ft-lb capacity) on the left. The instrumented, double pendulum type (right) provides for shockless testing of 5/8 in. DT specimens (2000 ft-lb capacity).

Table 1
Dimensions and Weights of Various Steel Specimens Used in the DT Test

Specimen Designation	Dimensions (in.)				Weight of Steel Specimen (lb)
	B	W	S	a	
5/8 in. DT	5/8	1-5/8	6-1/2	1/2	2
5/8 in. DPN*	5/8	1-5/8	6-1/2	1/2*	2
1 in.	1	4-3/4	16	1-3/4	24
2 in.	2	8	26	3	127
3 in.	3	8	26	3	190
6 in.	6	12	60	3	1220
12 in. (in test)	12	15	84	3	4580
15 in. (proposed)	15	18	84	3	6880

S = Span between supports B = Thickness
W = Depth a = Brittle weld length

*Deep pressed notch — bottom of machined notch sharpened by pressed knife edge.

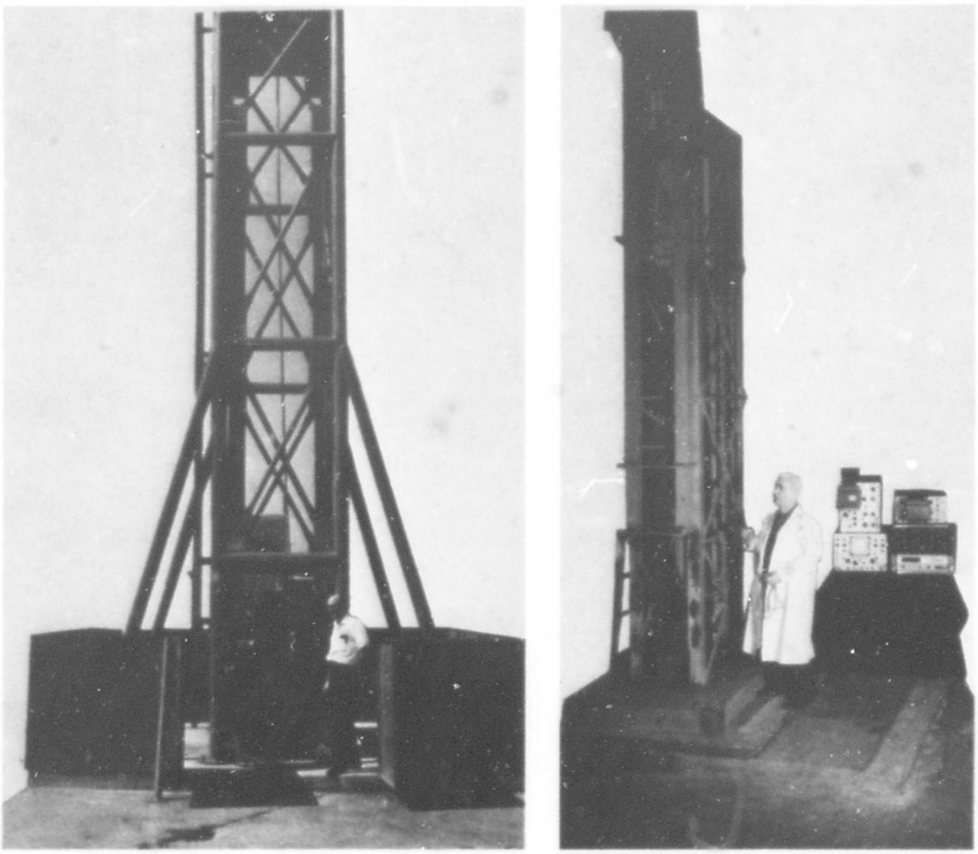

Fig. 10 - Range of present, large drop weight type DT test machines; 160,000 ft-lb capacity (left) and 20,000 ft-lb capacity (right). Conventional DWT-NDT machines may be used also by changing to a modified anvil.

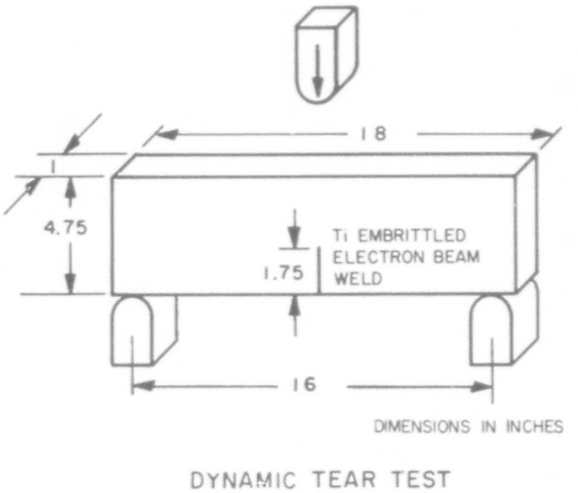

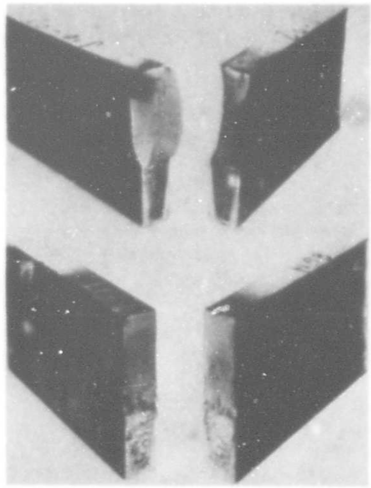

Fig. 11 - Features of 1 in. DT specimens. The broken halves illustrate fractures of low (bottom) and high (top) energy absorption. The flat regions at the bottom indicate the brittle weld; the "U"-shaped saw cut configuration provides for easy fracture initiation.

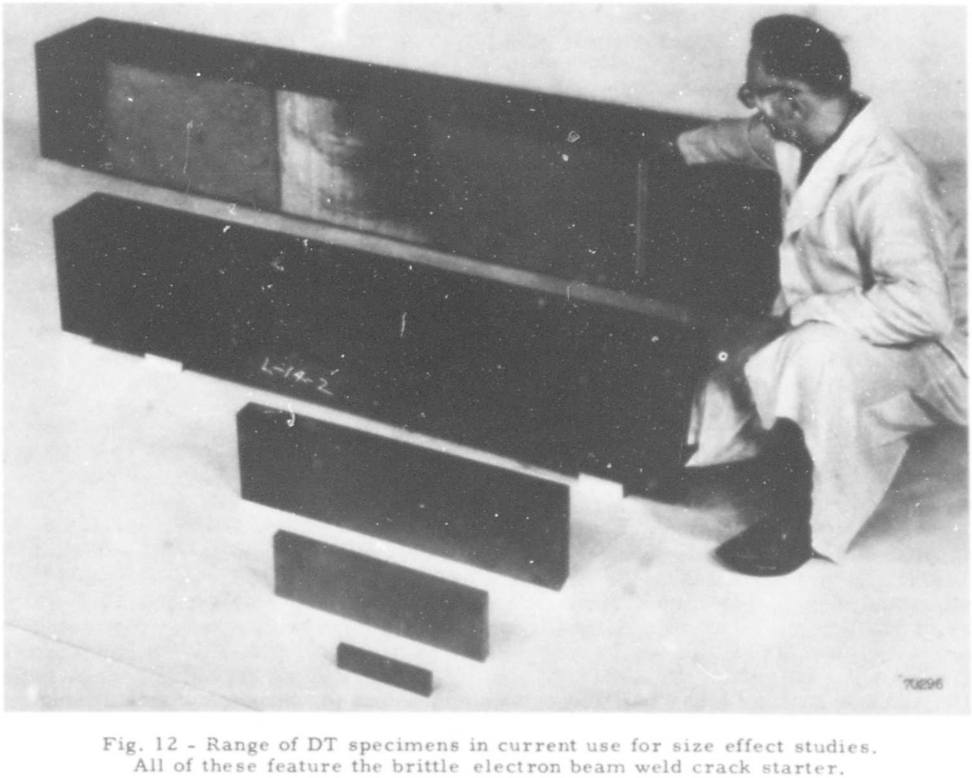

Fig. 12 - Range of DT specimens in current use for size effect studies. All of these feature the brittle electron beam weld crack starter.

deep-pressed notch (DPN-DT) type under investigation for special applications to be described. Figure 12 illustrates the range of section sizes which can be investigated on a common basis of an electron-beam weld, brittle crack tip conditions.

The brittle crack element of the test serves the purpose of generating a dynamically propagating instability, or popin. This feature emphasizes that the purpose of the test is to provide limit-severity test conditions for metals which are rate sensitive. For metals which are not rate sensitive, the brittle crack becomes the equivalent of a deep fatigue crack obtained inexpensively. Rate sensitivity effects are thus disclosed, if present, and the minimum plastic work energy characteristics for fracture of the metal are defined consistently. Alternatively, tests would have to be conducted to determine if rate sensitivity was involved. This is one of the problems of conventional static testing.

The DT test value is based on measurement of the energy for fracture of a specified area of metal. For the small specimens, the pendulum machines measure the energy absorption in a Charpy machine mode. For large specimens, requiring the use of the drop weight machines, energy values are calculated from an oscilloscope trace derived from force-time instrumentation of the loading tup. As a check, use is also made of lead compression bars which provide a measure of the residual energy of the weight following fracture, by calibration of the degree of compression.

A previous report (7) documented that the rise of the DT energy curve is relatable to the NDT temperature and to the Robertson CAT curve. Figure 13 illustrates the Fracture Analysis Diagram (FAD) for a 2 in. thick A201B steel, as indexed by the NDT temperature. The rise of the DT energy curve based on a 5/8 in. DT specimen (brittle weld tip) is seen to follow the course of the CAT curve portion of the FAD. As discussed previously, this effect is predictable from fracture mechanics theory and represents a change from dynamic K_{Ic} plane strain conditions to K_c mixed-mode conditions.

Figure 14 illustrates the course of the standard 1 in. DT specimen transition temperature energy curves for various steels. The indicated NDT temperatures were established directly by the use of the DWT. These curves define the rise in fracture toughness with temperature in relation to the most severe crack initiation condition which can be imposed on the metal. Accordingly, the applicable description is that of limit-severity curves. The NDT temperatures are always located on the toe region of DT energy transition curves. At the present state of experience, it appears that the NDT temperature can be inferred indirectly from the DT curves within a 30°F (i.e., ±15°F) temperature range. The usual decrease in shelf level fracture toughness, as the result of increase in strength level, is clearly apparent from examination of the curves for sections of a HY-80 steel plate heat treated to three strength levels. While the shelf level for a specific strength level is a function of metal quality factors, this case involving a single steel provides a clear example of strength effects.

FRACTURE TOUGHNESS OF HIGH STRENGTH STEELS

Strength Transition Aspects - OMTL Diagram

The discussions to follow relate to the effects of increasing yield strength on the level of fracture toughness that is attained at full ductility, i.e., on the upper shelf of the transition range if shelf conditions are attained. As explained previously, the temperature transition feature is essentially eliminated at very high strength levels. For such steels the room temperature value may be taken as the index. Plates of 1 in. thickness were used for the bulk of the studies for reasons of availability and cost. Plates of 2 and 3 in. thickness were cut to 1 in. DT specimen dimensions for purposes of establishing the metallurgical quality on a common index of section size.

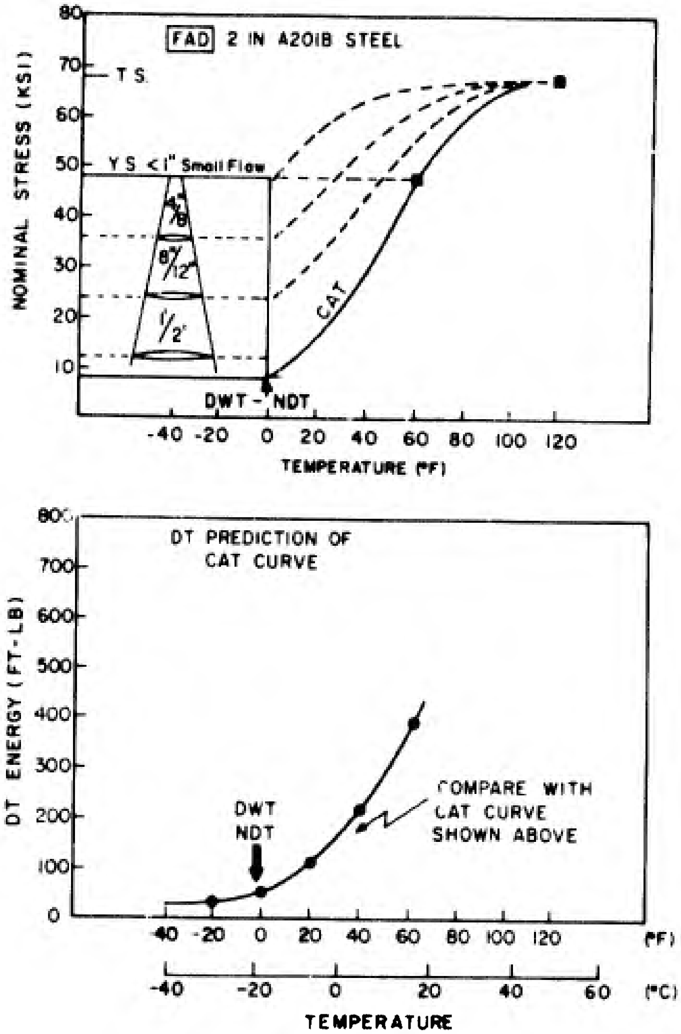

Fig. 13 - Illustration showing that the temperature rise of the DT energy curves corresponds to the CAT curve defined by the FAD. The temperature position of the FAD was established by DWT-NDT determination.

It should be noted that practically all engineering data for 1 in. or thicker steels, of intermediate and high strength, have been based on C_V values. The fracture significance of the C_V values was not known prior to these studies. Fracture mechanics data for steels of plate thickness have become available only recently; moreover, these are related in large measure to the ultrahigh strength range.

The first aims of the study during the early 1960's was to evolve an integrated reference index of the relative fracture toughness properties of different types of steels and methods of production. This objective required the accumulation of sufficient data relating to traditional steels, new steels that were being evolved by industry, and the procurement of selected grades produced by special, high-quality melt practice, and various degrees of cross-rolling. Fracture toughness evaluations were made in the "weak" (WR) and "strong" (RW) directions, i.e., along and across the direction of primary rolling respectively. The beneficial effects of 1:1 cross-rolling, which results in optimum properties, with elimination of a major loss of fracture toughness in the weak direction, were documented.

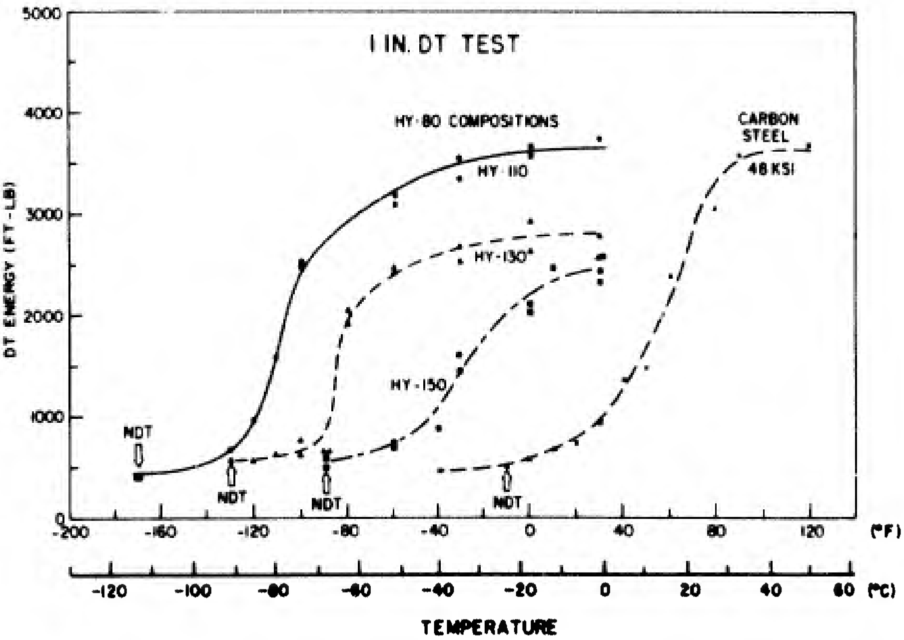

Fig. 14 - Representative DT energy transition curves. The NDT temperatures determined by DWT are always located at the toe region of the respective DT curves. HY designation relates to yield strength level (ksi).

Determination of the best attainable level of fracture toughness as a function of strength level would be hopelessly confused if a mixture of strong direction and weak direction data are used for intercomparison. Because the utilization of steels generally involves either biaxial or random orientation with respect to possible fracture paths, all data to be reported represent tests in the "weak" (WR) direction if such exists. Obviously, this limitation places a premium on uniform cross-rolling for the attainment of the best fracture toughness values for the strength level.

The evolution of this large body of data were based on two tests: (a) the C_v test, because this was and remains the standard term of reference in the steel industry and in engineering circles, and (b) the DT test, for reasons of limit-severity crack features described previously, and because it provides direct evidence of the fracture mode involved. Both tests were practical for the survey (and for subsequent use for routine engineering indexing of quality) because of reasonable preparation cost and simplicity of testing. Selected steels were also tested using fracture mechanics procedures to determine K_{Ic} values. These were limited to establishing trends and correlations with the Charpy-V and DT tests, because of high cost.

The early survey involved steels produced by conventional melting, deoxidation, and rolling practices. For intermediate and high strength levels the combination of metalloid impurities, low cleanliness with respect to nonmetallic phases, and 2:1 or higher rolling ratios resulted in relatively inferior "weak" direction fracture toughness properties. Exploratory investigations of higher purity steels produced by improved melting and deoxidation practices, combined with 1:1 cross rolling, produced directionally uniform properties of much higher fracture toughness value. The efforts of the metallurgical industry in the past five years were directed to such improvements. As the result, a wide variety of improved steels were surveyed and indexed in a master chart which has become known as the Optimum Material Trend Line (OMTL) diagram (7).

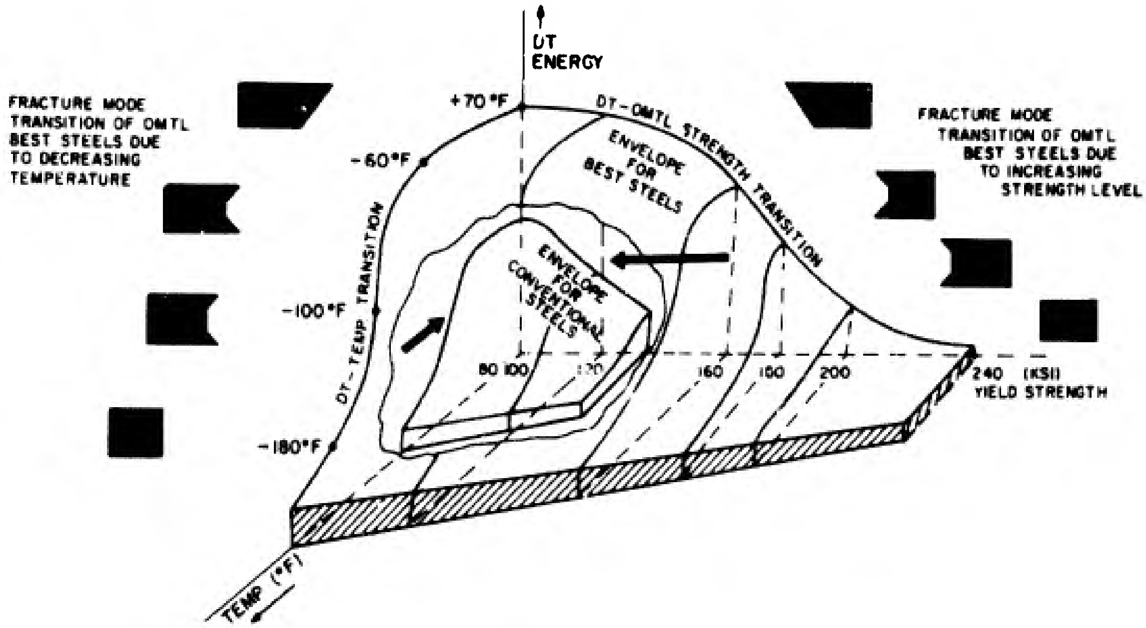

Fig. 15 - Three-dimensional representation of temperature and strength transitions for OMTL quality steels. The surface envelope defines the "fall back" of the DT energy-temperature transition toward room temperature, and the decrease in shelf level energy with increased strength. Common fracture modes for the two transitions are illustrated. The inner envelope relates to commercial, conventionally processed Q&T steels.

Figure 15 describes the general aspects of the OMTL strength transition in comparison to temperature transitions. These aspects are illustrated schematically by a three-dimensional diagram. It is important to appreciate these aspects in a general sense, before proceeding with detailed discussion of specific data.

The general form of the temperature transition DT curves may be recognized as relating to Fig. 14 data. The form of OMTL strength transition curve (Fig. 19 data) is remarkably similar to the temperature transition curves. The three-dimensional diagram describes two "surface envelopes" of DT energy values related to strength and temperature transitions for the best (OMTL) and for the previously described conventionally processed steels. It is illustrated that the surface envelope for the conventional steels lies below that of the OMTL quality steels for both the strength and temperature transitions.

Other features of interest are illustrated by the change in fracture appearance of the DT test consequent to the temperature and strength transitions. The sketches are typical of DT test fractures relating to OMTL quality steels. These illustrate common transition from plane stress to mixed-mode and finally to plane strain fracture. Figure 16 presents photographs of DT specimens which illustrate the common features of fracture-mode transition relating to temperature and strength aspects of these steels.

The engineering significance of the DT strength transition was investigated (7) in 1962-1964 by means of the Explosion Tear Test (ETT). This structural prototype test featured a 2 in. long, through-thickness, brittle weld similar to the DT test weld. The

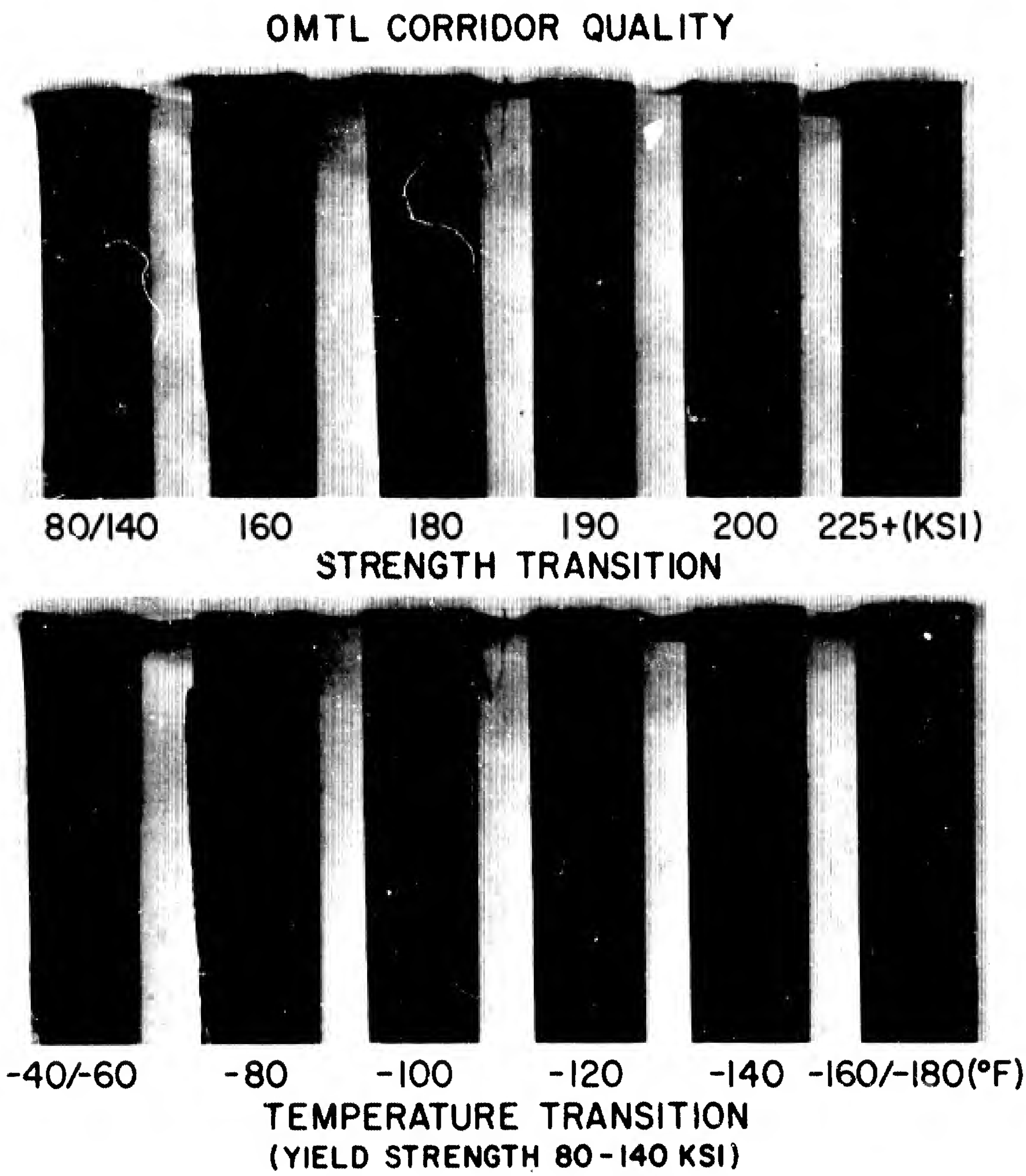

Fig. 16 - Common features of the fracture mode transitions. The top row relates to the strength transition for OMTL quality steels. The bottom row relates to the temperature transition for OMTL quality steels of 80 to 140 ksi yield strength. Ink lines have been added to denote clearly the demarcation between flat fracture central regions and slant (shear) fracture regions.

brittle weld is placed centrally in a plate of 1 x 22 x 25 in. dimensions. The test plate is bulged to cylindrical configuration on explosion loading. The brittle weld serves to introduce a 2 in. crack. The test may be recognized as indexing the level of stress required for propagation of fracture in the presence of a large crack. The general behavior of the ETT test in relation to the temperature or strength transitions is illustrated in Fig. 17. The dramatic decrease in fracture toughness consequent to the transitions is obvious from this figure.

Extensive ETT surveys documented that the fracture modes for the large ETT plate were exactly reproduced by the DT test. The flat break conditions for the ETT served to index DT values for which propagation at elastic stresses was possible. With rise in the OMTL strength transition curve, a sharp change occurred to fractures requiring gross plastic overload. The level of plastic strain required to propagate "tearing," plane stress fractures increased in proportion to the DT energy level.

It was determined that the OMTL diagrams presented in terms of DT energy or C_V shelf energy were strikingly similar. This observation led to an additional finding of major significance in 1963-1964. This finding was the correlation of DT and C_V shelf values shown in Fig. 18. At this point a single OMTL diagram could be presented with

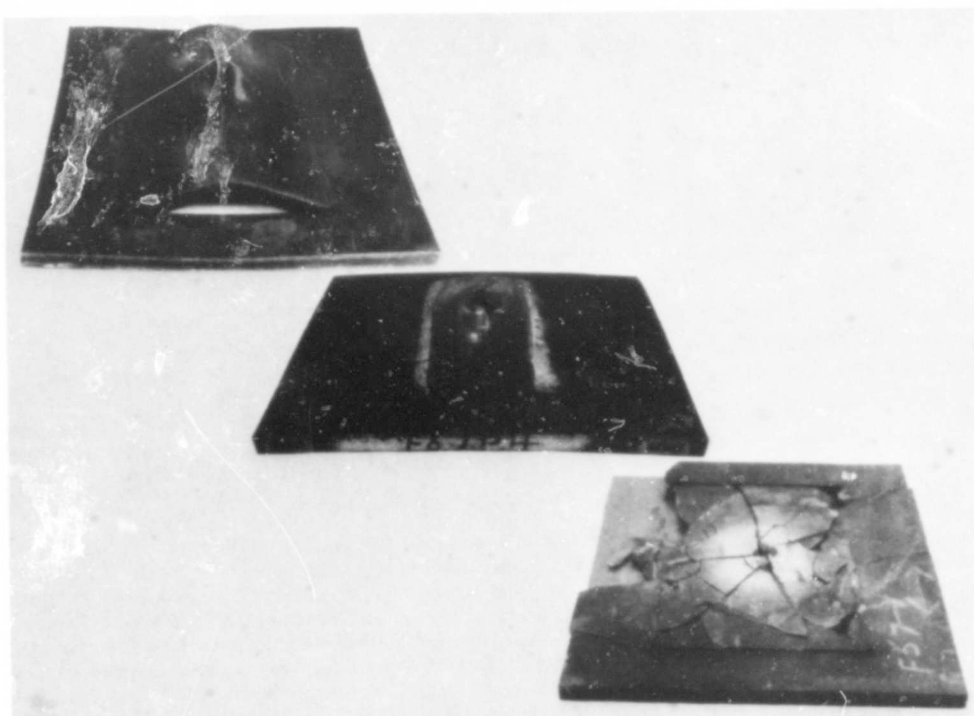

Fig. 17 - Explosion tear tests (1 x 22 x 25 in.) featuring a centrally located 2 in. brittle weld crack-starter element. The series (top to bottom) illustrates the decrease in fracture toughness following the OMTL strength transition. A similar decrease in fracture toughness develops for the temperature transition of OMTL quality steels of 80 to 140 ksi yield strength level. The fractures exactly duplicate those of corresponding DT tests.

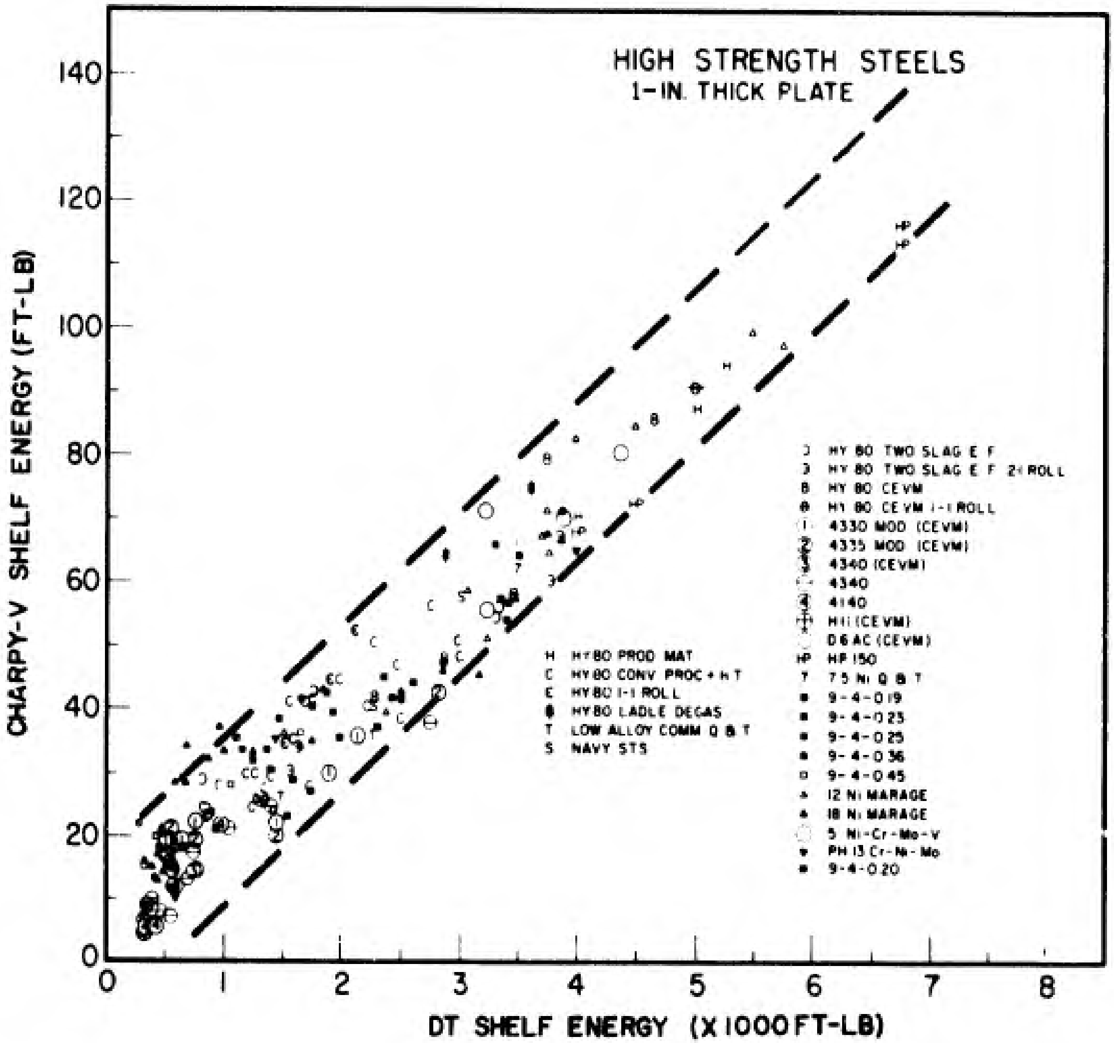

Fig. 18 - Correlation of C_v shelf energy with DT shelf energy

reference to both C_v and DT energy scales. It was cautioned that the C_v correlation does not hold in the C_v transition range and should be used only for "on the shelf," or equivalent, C_v values.

The K_{Ic} correlation approach was then pursued for both the DT and C_v specimens. Correlations between K_{Ic} and C_v tests also were evolved independently by the U.S. Steel Research Laboratory. The successful establishment of these correlations now provides for common indexing of the OMTL diagram in terms of DT, C_v and K_{Ic} scales. Figure 19 presents the combined index diagram. The bold arrow emphasizes the remarkable increase in fracture toughness obtained by metallurgical improvement with respect to purity, cleanliness, cross-rolling, and the use of new steel hardening mechanisms. This achievement is a tribute to the steel industry — the OMTL quality steels did not exist prior to five years ago.

Correlations of K_{Ic}, DT, and C_v Data

The development of correlation-indexing procedures for various types of fracture tests is of major importance to engineering applications of fracture mechanics. The

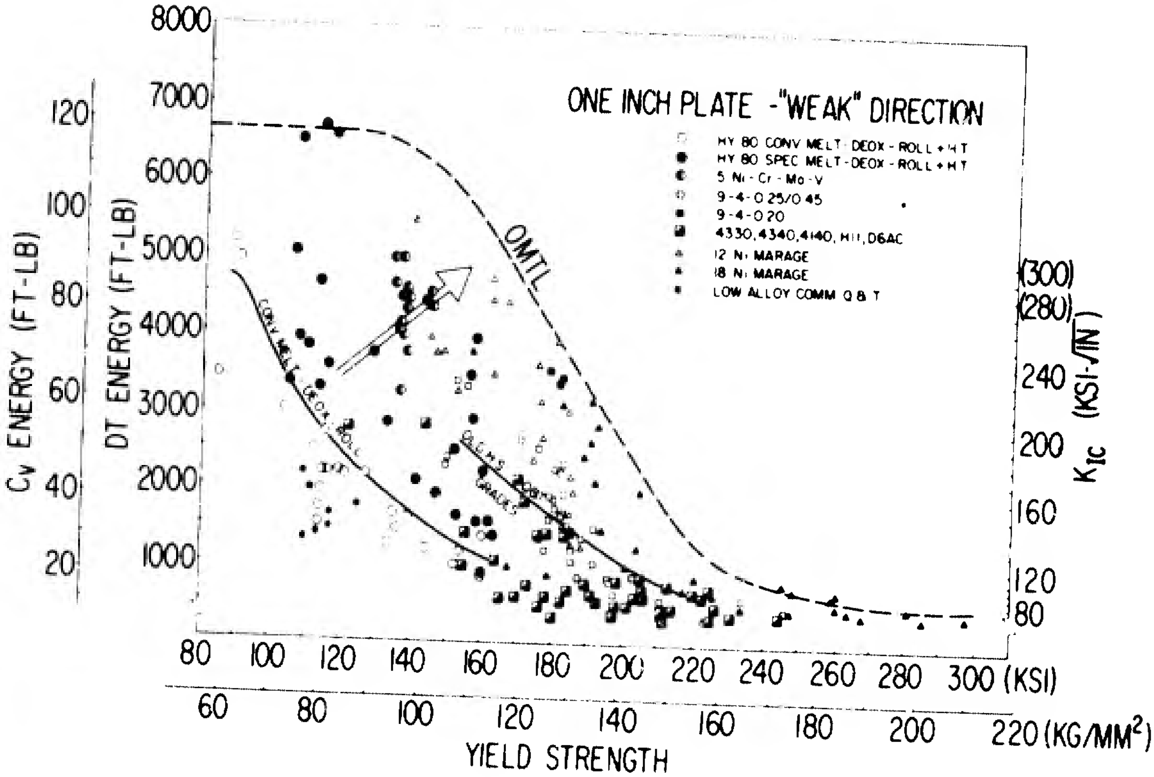

Fig. 19 - Updated version of OMTL diagram. Data points relate to 1 in. DT test values; the other scales are indexed by correlation.

correlation that has been developed between the two fracture toughness parameters, K_{Ic} and DT, is based on a significantly wide variety of steels. The investigations (8,9) included 12% and 18%Ni maraging steels, and quenched-and-tempered 5Ni-Cr-Mo-V, 9-4-0.25 (Ni-Co-C), 4140, and D6-AC steels.

The single-edge-notched tensile specimen (SEN) was used to determine K_{Ic} values. The specimen is illustrated in Fig. 4. In both the DT and the K_{Ic} investigations, the specimens were approximately one inch thick; this usually represented the full plate thickness, although in several cases the specimens were cut from a two inch thick plate. Many of the K_{Ic} specimens were side-grooved to a depth of five percent of the thickness on each side. This technique is ordinarily used to increase the detectability of the point at which crack tip instability occurs. A fatigue crack of 0.10 in. was formed at the tip of the edge notch in accordance with best practices.

Load-displacement clip gage outputs for the K_{Ic} specimen were drawn by an X-Y recorder. When initial deviation from linearity occurred at or very near maximum load (a popin), this value was used to calculate K_{Ic}; otherwise, the load at the lowest, distinct indication of instability was chosen for the calculation. A plastic zone correction (one iteration) was included in the calculation of K_{Ic}.

In Fig. 20, K_{Ic} is plotted against yield strength. The graph indicates that an inverse relationship exists between K_{Ic} fracture toughness and yield strength, similar to that of the OMTL curve. The K_{Ic}-OMTL curve results from a selection from the best of available steels which defined the DT-OMTL curve.

The plot of K_{Ic} versus DT energy is presented in Fig. 21. It is evident that a direct correlation exists; increases in K_{Ic} values correspond to increases in DT energy. The

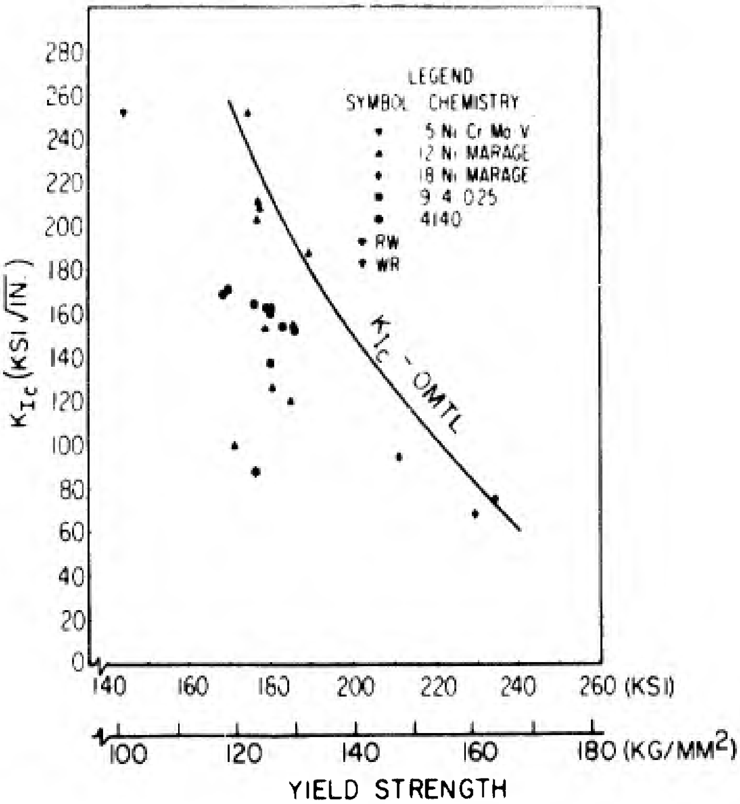

Fig. 20 - Relationships of K_{Ic} values to yield strength. The K_{Ic}-OMTL emerges by proportionate selection of DT-defined, OMTL quality steels.

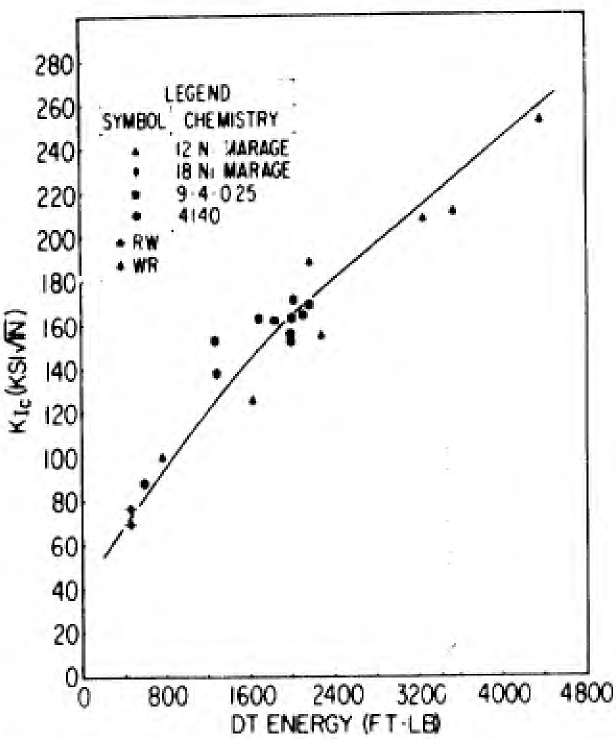

Fig. 21 - Correlation of DT and K_{Ic} test values

vertical line drawn at 3500 ft-lb on the DT energy scale represents the approximate value at which the fracture surface of the DT specimen attains full slant fracture. The line serves a second purpose, in that at this point the σ_N/σ_{ys} ratio in the K_{Ic} test approaches 1.0. Beyond this value, the development of initial instability requires increasing load involving gross yielding.

There are several factors which might be considered to affect the accuracy of the correlations. Since K_{Ic} may be a function of loading rate, the high rate of loading and brittle crack popin for the DT test may be suspected of causing the specimen to fracture with a lower toughness indication. However, as the steels involved in the correlation (on the shelf for the low strength range and for any type of fracture for the high strength range) are relatively insensitive to notch-tip strain-rate effects, this factor is not significant.

The change in slope of the K_{Ic}-DT correlation with increasing fracture toughness provides possible clues as to the physical events which are involved. These may be interpreted in terms of the state of stress fields and also in terms of the contributions of the d_T process zone.

The following viewpoint emerges from consideration of states of stress fields. For brittle materials, plane strain conditions are dominant in both the K_{Ic} and the DT tests. This dominance is indicated by a commonality of flat fracture surfaces. As toughness increases, plane strain conditions may still exist at the notch tip in the K_{Ic} test as indicated by the flat triangular area of the "first event" fracture surface, which then may be followed by mixed-mode or plane stress fracture. The crack in the DT specimen shows similar first and second events; however, the energy index is derived primarily from the nature of the total fracture process.

It might be expected that the slope of the relationship between K_{Ic} and DT values for brittle materials will differ from the slope relating to tougher materials. Figure 21 indicates that this is the case. For brittle metals involving low K_{Ic} and DT values, the correlation curve has a steeper slope than for the tough metals. This slope difference suggests that for the tougher metals the DT energy is increasing considerably faster, due to increasing dominance of mixed-mode and plane stress state of stress, than is the case for the first event fracture initiation assessment provided by the K_{Ic} test. This has the effect of decreasing the slope of the correlation curve.

The d_T, process zone analysis suggests that the size of the zone and its limit ductility (ϵ_c) governs both the K_{Ic} and the K_c plane stress fracture toughness levels. For a specific metal, K_{Ic} increases must therefore relate to K_c plane stress increases. It evolves that the correlation data have a rational significance, as analyzed from both stress field and d_T process zone theory.

The DT energy is plotted against K_{Ic}/σ_{ys} in Fig. 22. In both tests the resistance of the metal to crack propagation is a function of the plastic zone size, and K_{Ic}/σ_{ys} is an indication of this factor for the K_{Ic} investigation. The normalization of K_{Ic} by the yield stress improves the correlation. This improvement further indicates that the correlation has a fundamental validity.

In Fig. 23, the strain energy release rate, G_{Ic}, is compared to the DT value divided by the nominal fracture area (excluding the brittle weld). This plot was drawn in order to compare similar quantities on each axis (in.-lb/in.^{2}). The least amount of scatter in any of the figures is indicated in this graph. Mutual comparison on an energy basis indicates that the two tests are measuring the same natural event of energy absorption for fracture.

Correlations of DT energy with C_V shelf values were presented previously in Fig. 18. The correlations of C_V and K_{Ic} values are shown in Fig. 24. The scatter of this

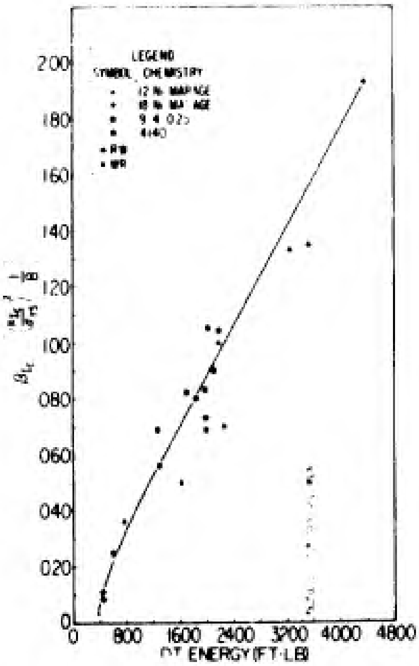

Fig. 22 - Yield strength normalization of Fig. 21 data by calculation of β_{Ic} parameter

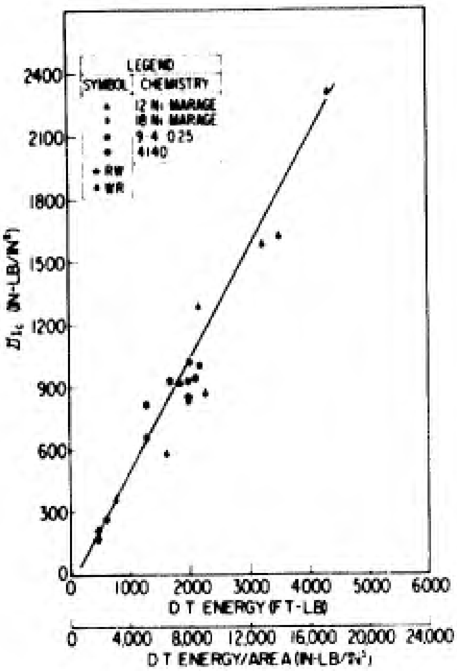

Fig. 23 - Correlation of $\mathcal{G}_{Ic}$ and DT fracture energies per unit area. $\mathcal{G}_{Ic}$ is mathematically related to K_{Ic} and is an expression in terms of energy.

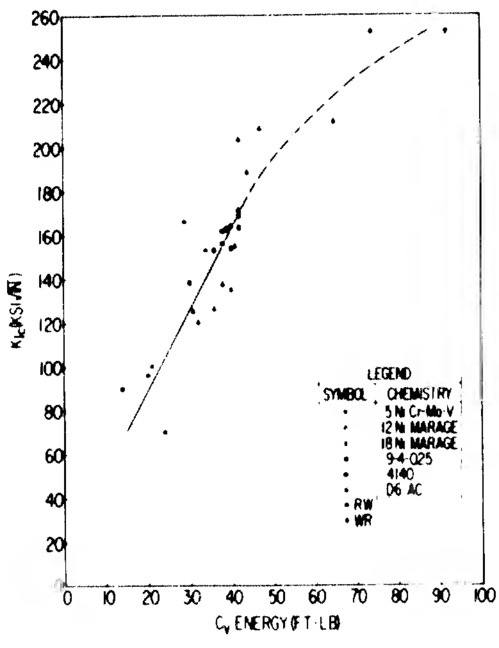

Fig. 24 - Correlation of K_{Ic} values and C_V shelf energy values for the same steels used for the K_{Ic} and DT correlation

correlation is reduced considerably by normalization procedures which include the yield strength, as evolved at the U.S. Steel Research Laboratory. The NRL data based on this normalization procedure are shown in Fig. 25. Checks were made with correlations obtained by U.S. Steel investigators, and these were found to fall closely to the curve of this figure. A rigorous explanation for the excellence of the C_v correlation is not currently available. It is emphasized that the correlations cannot be applied to the C_v transition temperature range.

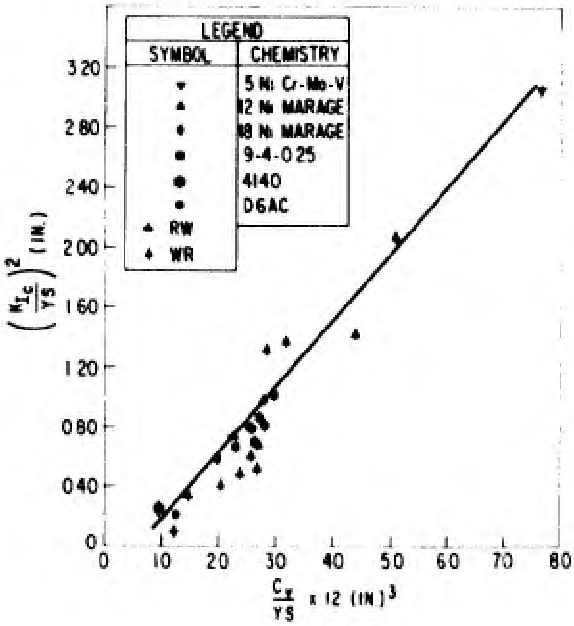

Fig. 25 - Yield strength normalization of K_{Ic} and C_v relationships evolved from Fig. 24 data

OMTL Corridor and Zonal Charts

The strength transition for steels of 1 in. thickness is illustrated by the corridor zone between the two OMTL curves shown in Fig. 26. The higher curve relates to the best material (OMTL) for the strength level, as defined by all data available to date. The lower curve is defined as the "normal expectancy" OMTL and relates to fracture toughness levels which may be expected with high confidence in procurement of the best material. In addition to the OMTL corridor, the figure also indicates the zonal location of data points for steels of primary interest. The chemical composition and yield strength characteristics of these steels are listed in Table 2.

Figure 27 reproduces the plate material OMTL corridor and additionally indexes the DT data zonal locations for weld metal (developed for use with the zoned metals) as deposited by various techniques. The hatched trend lines for the various weld deposition practices and associated welding wire quality aspects were derived from additional DT and C_v data not zoned in the diagram. The importance of changing from stick-metal-arc (SMA), to gas-metal-arc (GMA), and then to gas-tungsten-arc (GTA) welding deposition procedures with increased strength level is readily apparent. In order to obtain a fracture toughness match with the OMTL corridor quality, plate material (which requires special melt practices resulting in higher purity with respect to O_2, N_2, S, P, etc.),

Table 2
Characteristics of Steels Referenced in Report

Steel Type	Range of Nominal Yield Strength (ksi)	Minimum/Maximum Range of Chemical Composition (percent)														
		C	Mn	P	S	Si	Ni	Cr	Mo	Co	V	Ti	Al	Cu	B	Zr
High Alloy Grades (Q&T)																
HY-80 (3Ni-Cr-Mo)	80-95	— 0.18	0.10 0.40	— 0.025	— 0.025	0.15 0.35	2.00 3.25	1.00 1.80	0.20 0.60	— —	— 0.03	— 0.02	— —	— 0.25	— —	— —
HY-100 (3Ni-Cr-Mo)	100-115	— 0.20	0.10 0.40	— 0.025	— 0.025	0.15 0.35	2.25 3.50	1.00 1.80	0.20 0.60	— —	— 0.03	— 0.02	— —	— 0.25	— —	— —
HY-130(T) (5Ni-Cr-Mo-V)	130-145	— 0.12	0.60 0.90	— 0.010	— 0.010	0.20 0.35	4.75 5.25	0.40 0.70	0.30 0.65	— —	0.05 0.10	— 0.02	— —	— 0.15	— —	— —
9-4-0.25 (8Ni-4Co-.25C)	175-200	0.24 0.30	0.10 0.35	— 0.010	— 0.010	— 0.10	7.00 9.00	0.25 0.60	0.35 0.60	3.50 4.50	0.06 0.12	— —	— —	— —	— —	— —
9-4-0.20 (9Ni-4Co-.20C)	175-200	0.17 0.23	0.20 0.40	— 0.010	— 0.010	— 0.10	8.50 9.50	0.65 0.85	0.90 1.10	4.25 4.75	0.06 0.10	— —	— —	— —	— —	— —
Marage																
12Ni-5Cr-2Mo	160-190	— 0.03	— 0.10	— 0.010	— 0.010	— 0.12	11.50 12.50	4.75 5.25	2.75 3.25	— —	— —	0.10 0.35	0.20 0.50	— —	— —	— —
18Ni-8Co-4Mo	200-235	— 0.03	— 0.10	— 0.010	— 0.010	— 0.10	17.00 19.00	— —	4.00 4.50	7.00 8.50	— —	0.10 0.25	0.05 0.15	— —	— —	— —
18Ni-8Co-5Mo	230-260	— 0.03	— 0.10	— 0.010	— 0.010	— 0.10	17.00 19.00	— —	4.60 5.10	7.00 8.50	— —	0.30 0.50	0.05 0.15	— —	— —	— —
18Ni-9Co-5Mo	260-300	— 0.03	— 0.10	— 0.010	— 0.010	— 0.10	18.00 19.00	— —	4.60 5.20	8.00 9.50	— —	0.55 0.80	0.05 0.15	— —	— —	— —

Table 2 (Continued)

Steel Type	Range of Nominal Yield Strength (ksi)	Minimum/Maximum Range of Chemical Composition (percent)														
		C	Mn	P	S	Si	Ni	Cr	Mo	Co	V	Ti	Al	Cu	B	Zr
Commercial Low Alloy (Q&T)																
Ni-Cr-Mo-Cu-V-B	100-125	0.10 0.20	0.60 1.00	— 0.040	— 0.040	0.15 0.35	0.70 1.00	0.40 0.65	0.40 0.60	— —	0.03 0.08	— —	— —	0.15 0.50	0.002 0.006	— —
Cr-Mo-Ti-V-B	100-125	0.12 0.21	0.70 1.00	— 0.040	— 0.040	0.20 0.35	— —	0.40 0.65	0.15 0.25	— —	0.03 0.08	0.01 0.03	— —	— —	0.0005 0.0050	— —
Cr-Mo-Ti-Cu-B	100-125	0.12 0.20	0.40 0.70	— 0.040	— 0.040	0.20 0.35	— —	1.40 2.00	0.20 0.40	— —	— —	0.04 0.10	— —	0.20 0.40	0.0015 0.0050	— —
Mn-Mo-B	100-125	0.10 0.20	1.10 1.50	— 0.040	— 0.040	0.15 0.30	— —	— —	0.20 0.30	— —	— —	— —	— —	— —	0.001 0.005	— —
Cr-Mo-B-Zr	100-125	0.10 0.21	0.60 1.10	— 0.040	— 0.040	0.40 0.80	— —	0.40 0.80	0.18 0.28	— —	— —	— —	— —	— —	0.0025 —	0.05 0.15

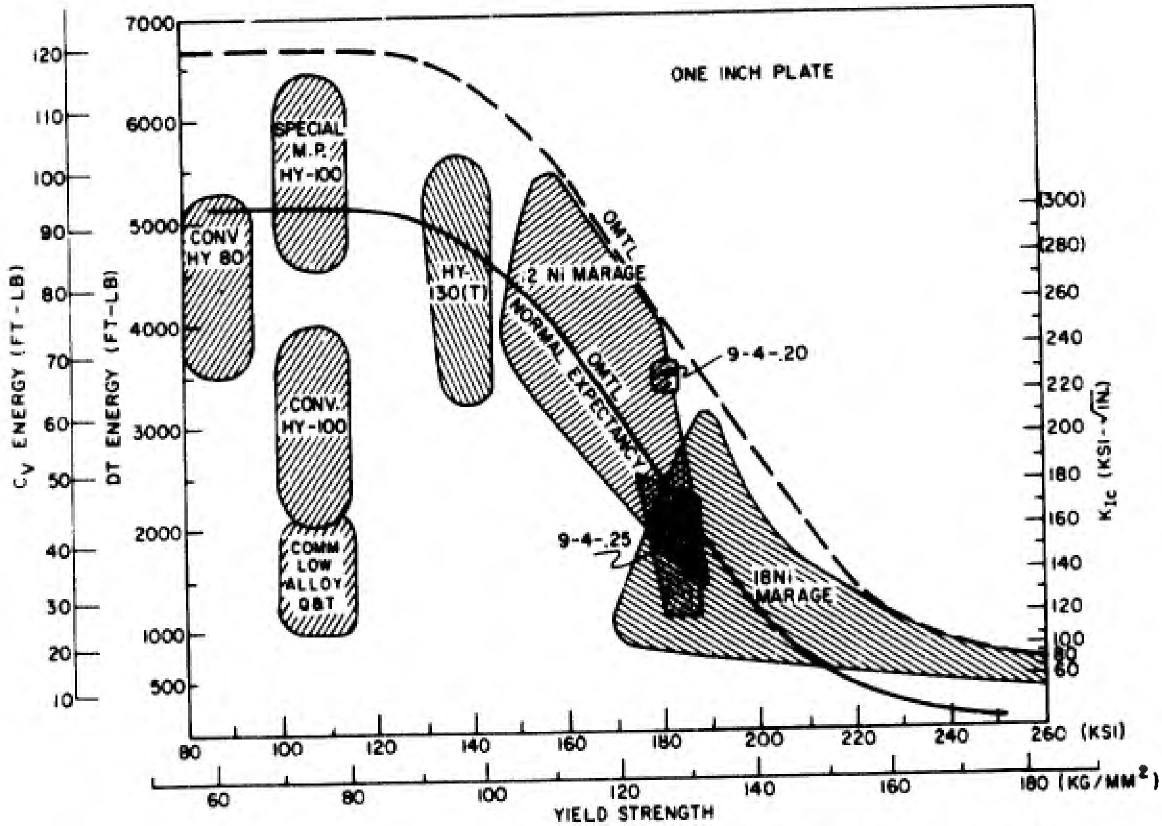

Fig. 26 - OMTL corridor and zonal locations for steels of special interest

it is necessary to utilize welding techniques and wire which provide similar quality aspects. It should be noted that the deposition technique can only serve to retain such quality as is inherent to the wire. For example, a poor quality wire will not result in high quality GTA weld deposits.

The OMTL corridor, and the plate material zonal reference areas, will be used as reference in flaw size analysis diagrams to be presented. The critical flaw sizes, calculated by use of the K_{Ic} scale, will be overlayed on the OMTL diagrams so as to develop engineering interpretations which reduce a large body of data and calculations to simple form.

Development of Flaw Size Analysis Diagrams

The K_{Ic} scale of the OMTL diagrams relates to the level of fracture toughness that would be measured for a plate of adequate thickness to ensure plane strain conditions. There are presently at least three schools of opinion regarding the minimum thickness requirements for measurements of K_{Ic} values. The most restrictive is represented by the ASTM-E24 Committee definition of $B \geq 2.5(K_{Ic}/\sigma_{ys})^2$. On this basis, only values of less than 120 ksi $\sqrt{\text{in.}}$ would be considered valid for plates of 1 in. thickness in the ultra-high strength range of the corridor region. Less restrictive practices are being used, based on the assumption that the factor in the stated formula may be taken as 1.5 or 1. Finally, there is the engineering point of view that apparent K_{Ic} values obtained for less than adequate thickness may be adjusted by calculation to provide approximate K_{Ic} values. Previous discussions have emphasized that for metals of high toughness, the

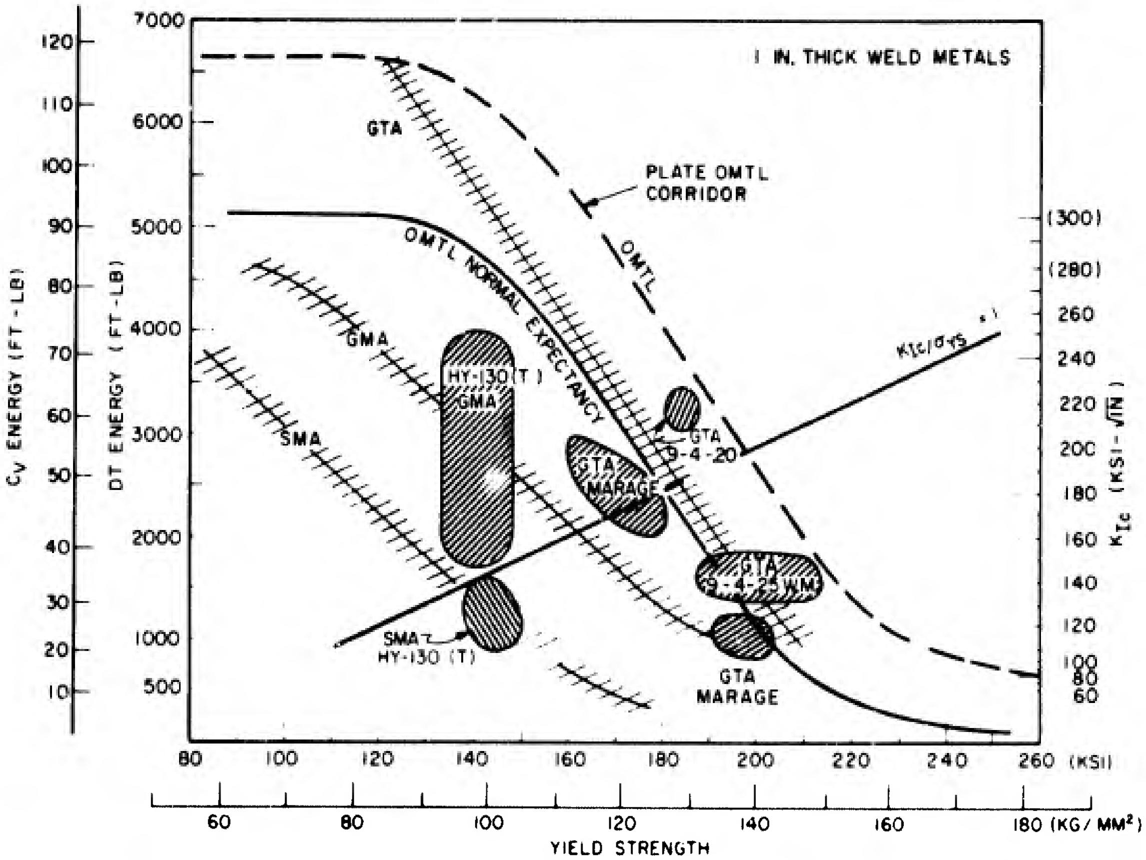

Fig. 27 - Zonal location of DT test data for weld metals developed specifically for joining various steels of primary interest. The trend lines relate to the various weld deposit techniques and associated weld wire quality aspects.

adjusted value is adequate for most engineering purposes. The "one-iteration" statement in the section on K_{Ic}-DT correlation relates to such adjustments. It means a "one-calculation" adjustment. In some cases a series of calculations is made with the intent of obtaining a refined definition of the approximate K_{Ic} value. The process involves calculation of the plastic zone size and addition of the radius (r_y) to the physical crack depth (a_0). A second calculation of K_{Ic} is then made on the basis of an assumed crack of $a_0 + r_y$ depth.

All contentions considered, it is a fact that K_{Ic} values quoted in the literature are obtained by all of these various procedures. Because of these complications, the ASTM-E24 Committee has recommended that the method used be cited. The use of correction procedures for calculating K_{Ic} values is not a reflection simply of dedication to K_{Ic} testing, but results from the fact that alternate K_c (or related $\mathcal{G}_c$) testing procedures have not been evolved to a point of acceptance for use in experimental fracture mechanics.

The K_{Ic} values derived for the correlations represent acceptance of usual practices in K_{Ic} measurements, including the adjustment technique. The problem that has arisen in the use of corrected K_{Ic} values for calculations of critical flaw sizes, is the complications of "correcting back" to a calculated K_c value for plates of less than adequate thickness. This procedure is often ignored, or not appreciated, by engineers who attempt to use fracture mechanics calculations for metals of relatively high fracture toughness.

The iso-flaw depth lines (for 1:10 flaw and load equal to yield stress) presented on the left side of Fig. 28 were calculated on the assumptions that plane strain conditions governed for all levels of the indicated K_{Ic} scale. These definitions are representative of the described incorrect procedures, if the specific thickness under consideration does not provide for K_{Ic} plane strain conditions. For example, the 1 in. iso-flaw depth line (top line) was derived on the assumption that a plate of 10 in. thickness was involved. For sections of significantly smaller thickness, the subject calculation is invalid even on theoretical bases.

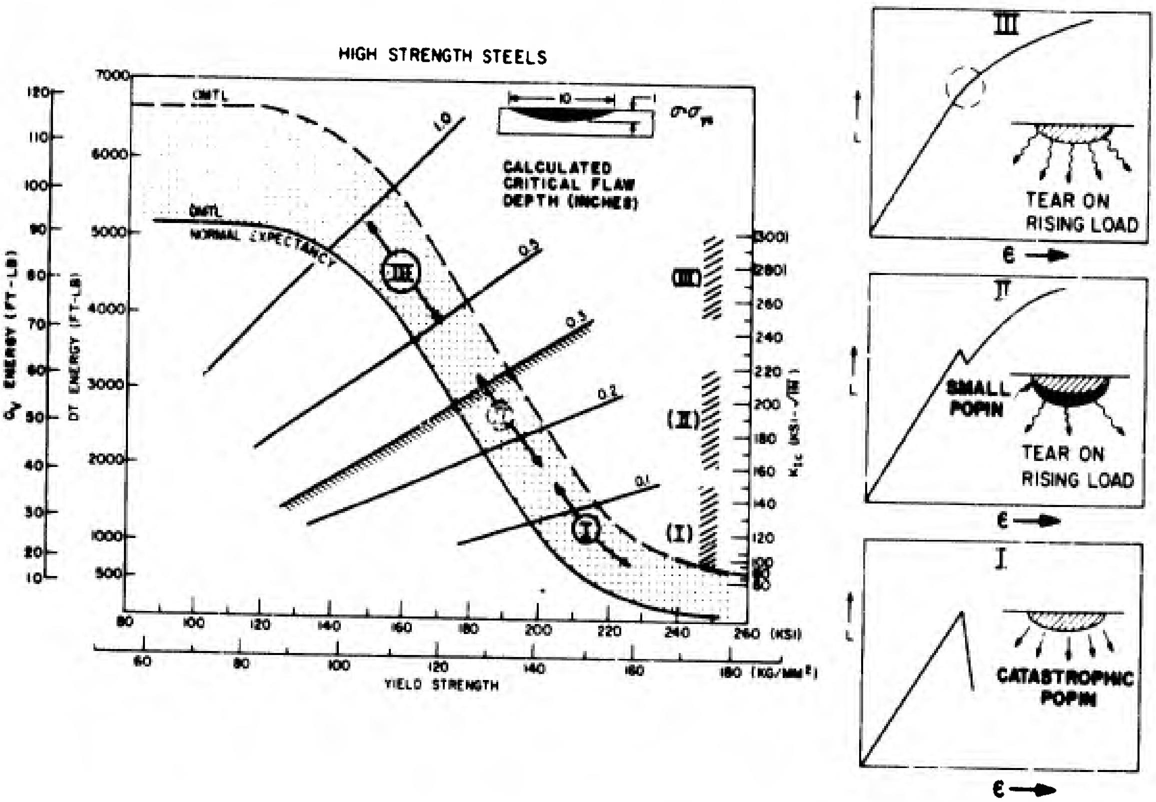

Fig. 28 - Physical interpretations (right) of crack tip instability events for K_{Ic} values (I, II, III) relating to K_{Ic}/σ_{ys} ratios which follow the course of the OMTL corridor. The iso-flaw depth lines are calculated on the assumption that plane strain conditions govern at all levels of fracture toughness.

Figure 28 illustrates another aspect of significance to interpretations of K_{Ic} values for steels of different yield strength. The K_{Ic} to yield strength ratio (K_{Ic}/σ_{ys}) is the parameter of fracture toughness level which normalizes the effects of yield strength and relates to the plastic zone size (work energy). Actually, the formal relationship to plastic zone size involves the square of this ratio; however, for simplicity of discussion the simple engineering ratio value will serve the purposes of this report.

The physical events associated with crack tip instabilities related to increasing K_{Ic}/σ_{ys} ratio values are illustrated schematically in Fig. 28 (right). The relationships of these physical events to the OMTL corridor K_{Ic}/σ_{ys} ratio values (deduced by consideration of the K_{Ic} and corresponding yield strength values) are noted by the I, II, and III notations. The range of K_{Ic} values which apply to the various corridor positions are indicated by the dashed bands which are identified by the same I, II, and III notations.

The load-displacement curves illustrated (right side) relate to nominal load and to the crack tip opening as measured by the clip gage. The curves denote that a catastrophic popin which is not arrested (fast fracture) is developed only for low K_{Ic}/σ_{ys} ratios. For intermediate ratios, a small instability is developed which arrests, and further slow propagation requires rising load stress. For high ratios, only a slight deviation from linearity is involved, and the instability starts with a tearing process which requires rising load for slow propagation.

These are the various behavior patterns of the 1 in. thick specimens from which the K_{Ic} correlations were made. The crucial question is whether the type III behavior would in fact be replaced by a type I behavior with large increase in thickness. Theory predicts that the initial instability would occur at the highly restrained crack tip, but there is no experimental evidence that fracture propagation would occur at the instability load. For steels of high K_{Ic}/σ_{ys} ratios the initial instability causes blunting of the crack tip; consequently higher K values for further extension of the crack would be required, i.e., rising load. For such conditions the event of initial instability may not be of engineering significance.

The intriguing question of the minimum thickness that would be required for measurement of valid K_{Ic} values (or for valid calculations of critical flaw sizes), with rise along the OMTL corridor, is answered in Fig. 29 (left). The formally required thicknesses, by the ASTM E-24 Committee definition, range from 1 in. or less at the low end, to 10 in. or more at the high end of the corridor. The origins of the 1, 4, and 10 in. requirements are evident from the plots on the right-hand side of the figure. These represent thicknesses above which geometry-dependent K_c values reach a constant minimum, i.e., K_{Ic}. There is a rapid rise of K_c values above the K_{Ic} line as thickness becomes less than the required minimum — these are indicated schematically by the dashed portions of the curves.

In the development of Flaw Size Analysis Diagrams to be presented, flaw depth calculations for steels of adequate thickness were made directly from the K_{Ic} scale value. For thicknesses less than the adequate value, the appropriate K_c value was calculated. The K_c value relates specifically to the finite thickness of plate being considered. The calculations are approximate at best, and probably underestimate the K_c values. There is little formal fracture mechanics information on procedures for calculating K_c conditions. Details of the processes used are beyond the scope of this report; a brief description is provided in the Appendix.

Flaw size calculations were made for 1 in. and 3 in. plates based on the K_{Ic} scale value and with consideration of thickness constraint adjustments (K_c) in accordance with the procedures described above. The Flaw Size Analysis Diagrams are presented in Figs. 30 and 31. The diagrams feature critical iso-flaw depth lines with separate notations indicating the calculated flaw depths for 1 in. and 3 in. plates. Both diagrams relate to the most severe flaw geometry, i.e., the 1:10 flaw (semi-infinite). The charts represent conditions for yield stress loading (Fig. 30) and for one-half of yield stress loading (Fig. 31). Critical flaw depths which relate to stubby flaws (1:2) may be deduced by multiplication of the flaw depths noted for the 1:10 flaw by a factor of 2 to 3. Formally, the conversion factor is in the order of 2.5 for plane strain conditions. The diagrams are zoned by K_{Ic}/σ_{ys} ratio lines of 0.5, 1.0, and 1.5. These define four zones of rapidly increasing fracture toughness and critical flaw sizes. The slopes of the iso-flaw depth lines follow those of the K_{Ic}/σ_{ys} lines because the basic element in the flaw size calculations is this ratio, as discussed previously.

A simplified analysis of the iso-flaw depth diagrams is presented in Fig. 32. The increase in fracture toughness following the course of the OMTL corridor is analyzed in this figure in relation to the K_{Ic}/σ_{ys} ratio locus of 0.5, 1.0, and 1.5, as follows:

1. Above the 1.5 ratio line, stresses in excess of yield and through-thickness flaws in excess of 12 in. length are required for fracture propagation for a 3 in. plate, in the expected plane stress mode.

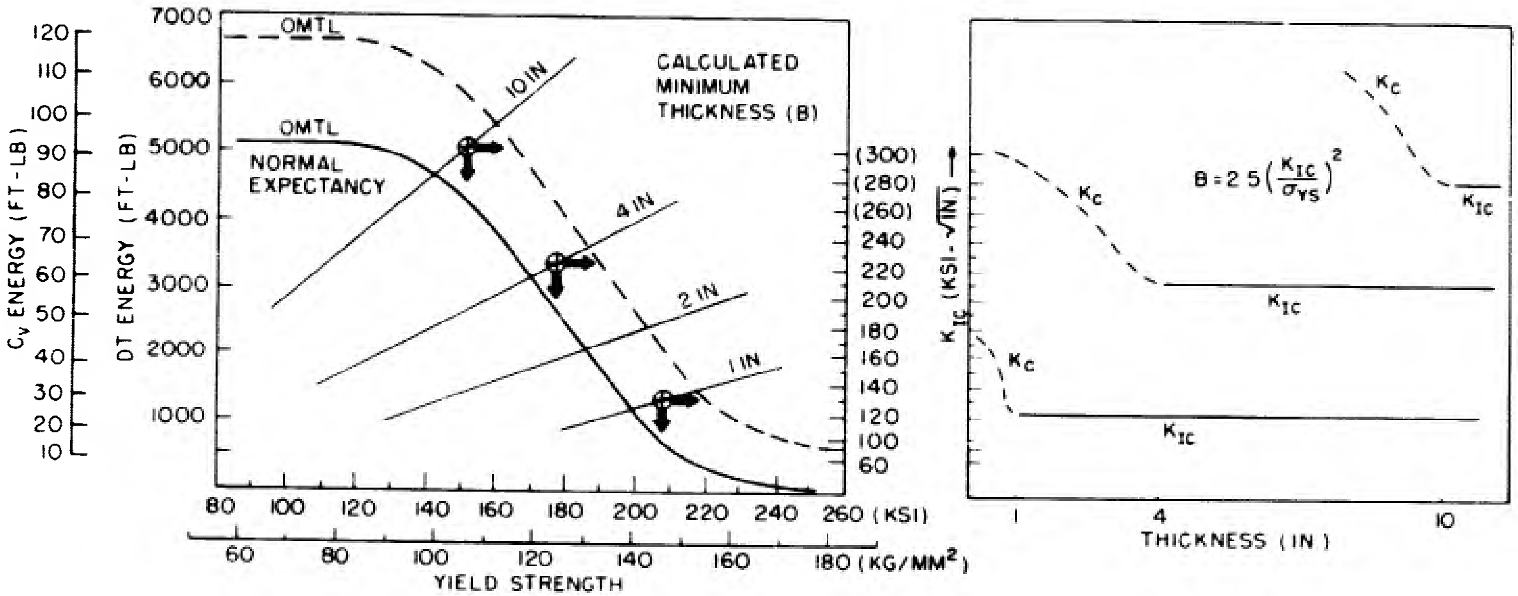

Fig. 29 - Significance of the "adequate thickness" requirement for K_{Ic} testing. The indicated minimum thickness requirements are indexed to the three circled points in the OMTL corridor. The individual iso-thickness lines are determined by calculations of B for various K_{Ic}/σ_{ys} ratios of the diagram. The slopes of the lines indicate the locus of fixed ratios.

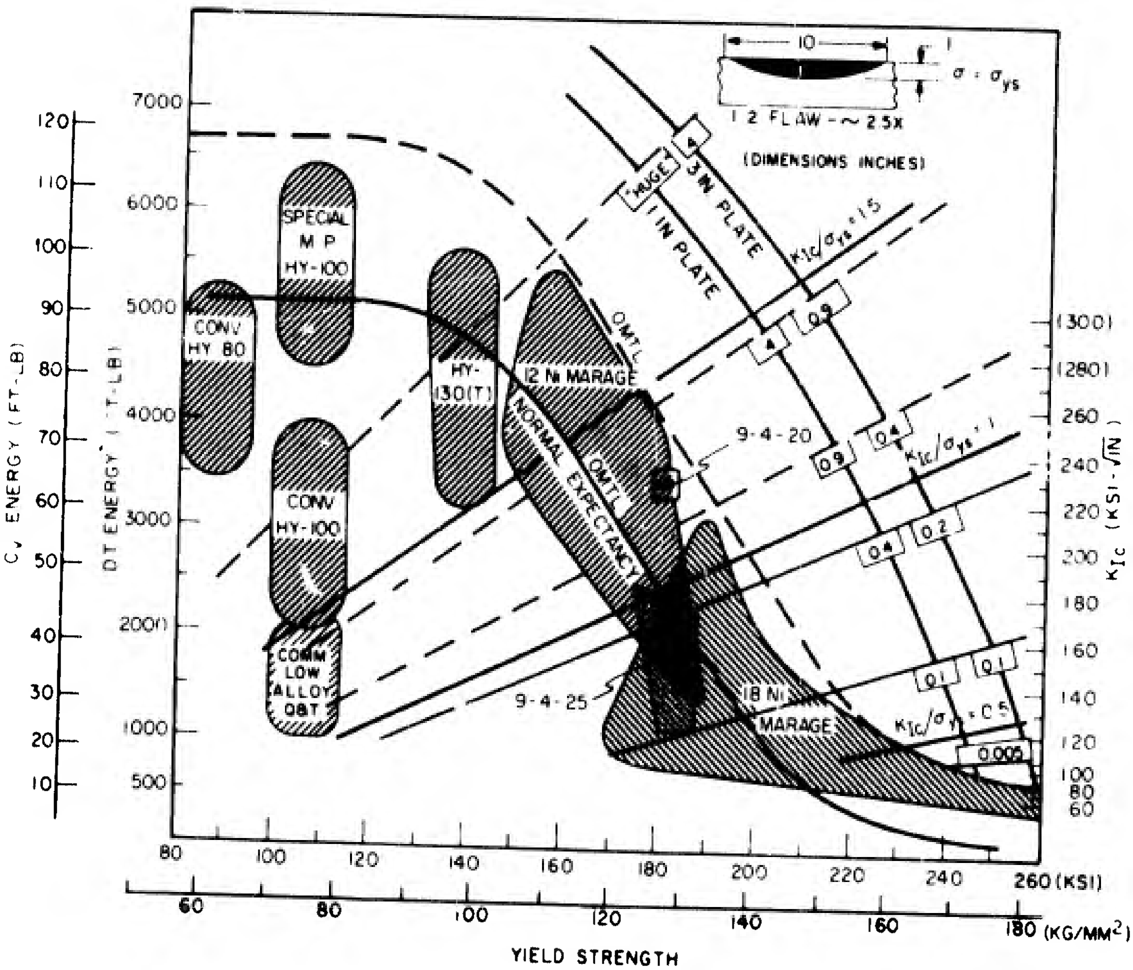

Fig. 30 - Iso-flaw depth lines for surface cracks of 1:10 geometry and for yield stress loading. The overlay on the OMTL corridor and the zonal designations provide ready reference for engineering purposes. The calculations apply to 1 and 3 in. thick steels, as noted. For the case of a 1:2 geometry flaw, multiply the noted crack depth values by 2.5.

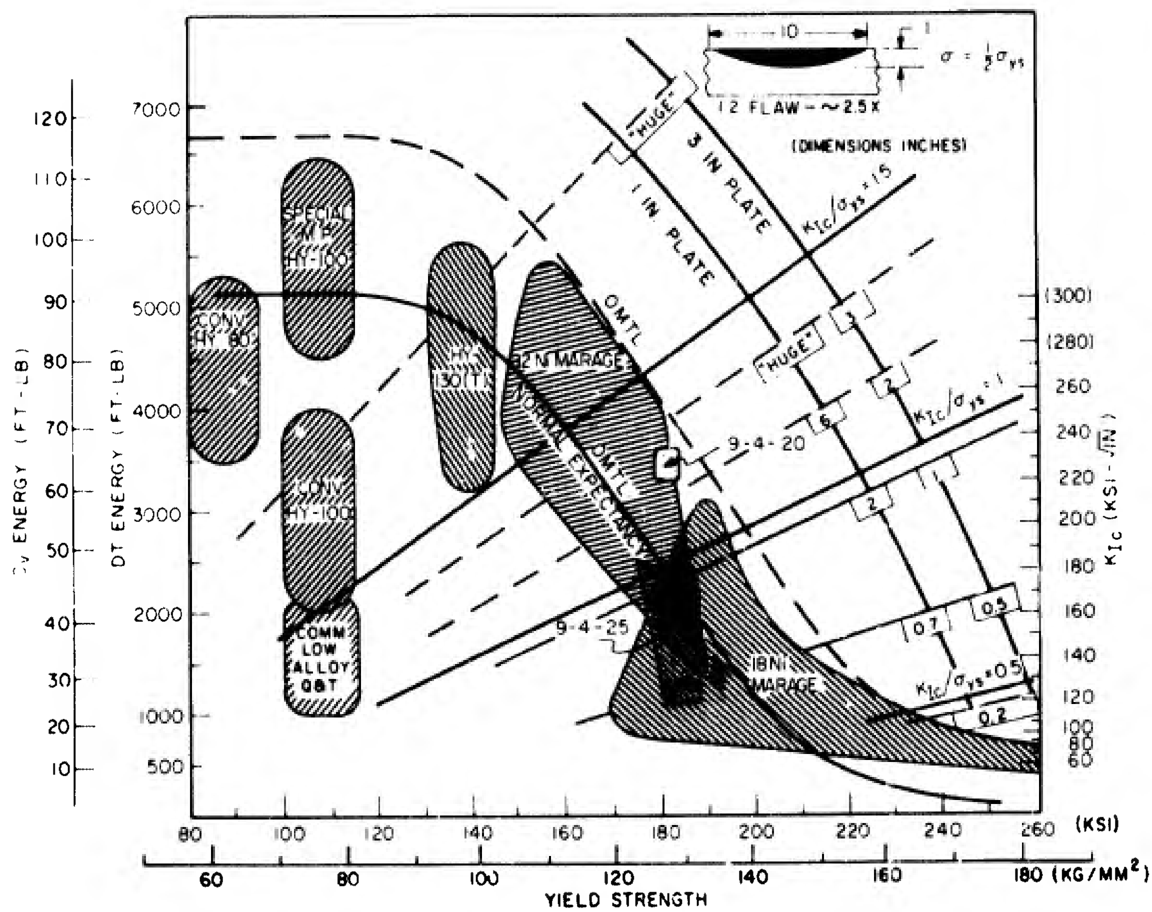

Fig. 31 - Iso-flaw depth lines for surface cracks of 1:10 geometry and for load stresses of one half of yield level; comments of Fig. 30 apply

2. Above the 1.0 ratio line, stresses in excess of yield and through-thickness flaws in excess of 6 in. length are required for fracture propagation for a 1 in. plate, in the expected plane stress mode.

3. In the general location of the 0.5 ratio line, plane strain fractures may be initiated and propagated from relatively minute defects (0.1 in. or less) for both 1 in. and 3 in. plates. Relatively high elastic stresses are required above the 0.5 ratio line, and relatively low elastic stresses are sufficient for the region below this line.

The bold arrow which points above the 1.0 ratio line emphasizes a large increase in fracture toughness and critical flaw sizes for 1 and 3 in. plates. In the high range of the OMTL corridor, "huge" flaw sizes and gross plastic overload are required for highly ductile, plane stress fracture of 1 and 3 in. plates.

The bold arrow which points downward from the 1.0 ratio line indicates a dramatic decrease in fracture toughness consequent to change from mixed-mode to plane strain fractures as the 0.5 ratio line is approached. The specific flaw sizes in this region vary over a wide range, depending on level of stress, flaw geometry, and thickness constraint.

The toe region of the corridor represents relatively brittle material. The critical flaw sizes are minute and for many cases beyond the limits of detectability by nondestructive testing.

The bold vertical band at approximately the 180 ksi yield strength level serves to highlight other interesting facts. At this point the fracture toughness of 1 to 3 in. thick steels spans the range from the 1.5 ratio (at the OMTL line), to the 1.0 ratio (at the lower bound of the corridor), and to below the 0.5 ratio for low quality steels. Thus, the best steels feature relatively high fracture toughness, i.e., plane stress fracture for 1 in. thickness and mixed-mode fracture toughness for 3 in. thickness. The lowest quality steels of this strength level are highly brittle. By an increase in yield strength from 180 ksi to 210 ksi, the best quality steels become brittle. By a decrease in yield strength to 150 ksi, extremely high fracture toughness is attained for OMTL corridor steels of 1 to 3 in. thickness. The dramatic effects of yield strength changes of ±30 ksi from the 180 ksi base point are made evident by these analyses. The OMTL corridor fracture toughness transition is very sharp in the midpoint region and has the same features as increasing or decreasing temperature at the midpoint of the transition temperature range.

ANALYTICAL PROCEDURES FOR STRENGTH TRANSITION

Ratio Analysis Diagram (RAD)

The OMTL corridor transition features are a consequence of the decreasing ratios of K_{Ic}/σ_{ys}. The ratio values provide yield strength normalization indices of fracture toughness. The formal relationship to the plastic zone size involves the square of the ratio; however, for most practical purposes, the simple ratio serves as an engineering index. The significance of the ratios in relation to other parameters is defined in Table 3.

The calculations relating to plane stress conditions represent approximations. While exactness is not possible at the present state of development of fracture mechanics for mixed-mode or plane stress conditions, the order-of-magnitude changes involved clearly indicate that it is not necessary to wait for exact solutions, if feasible. The

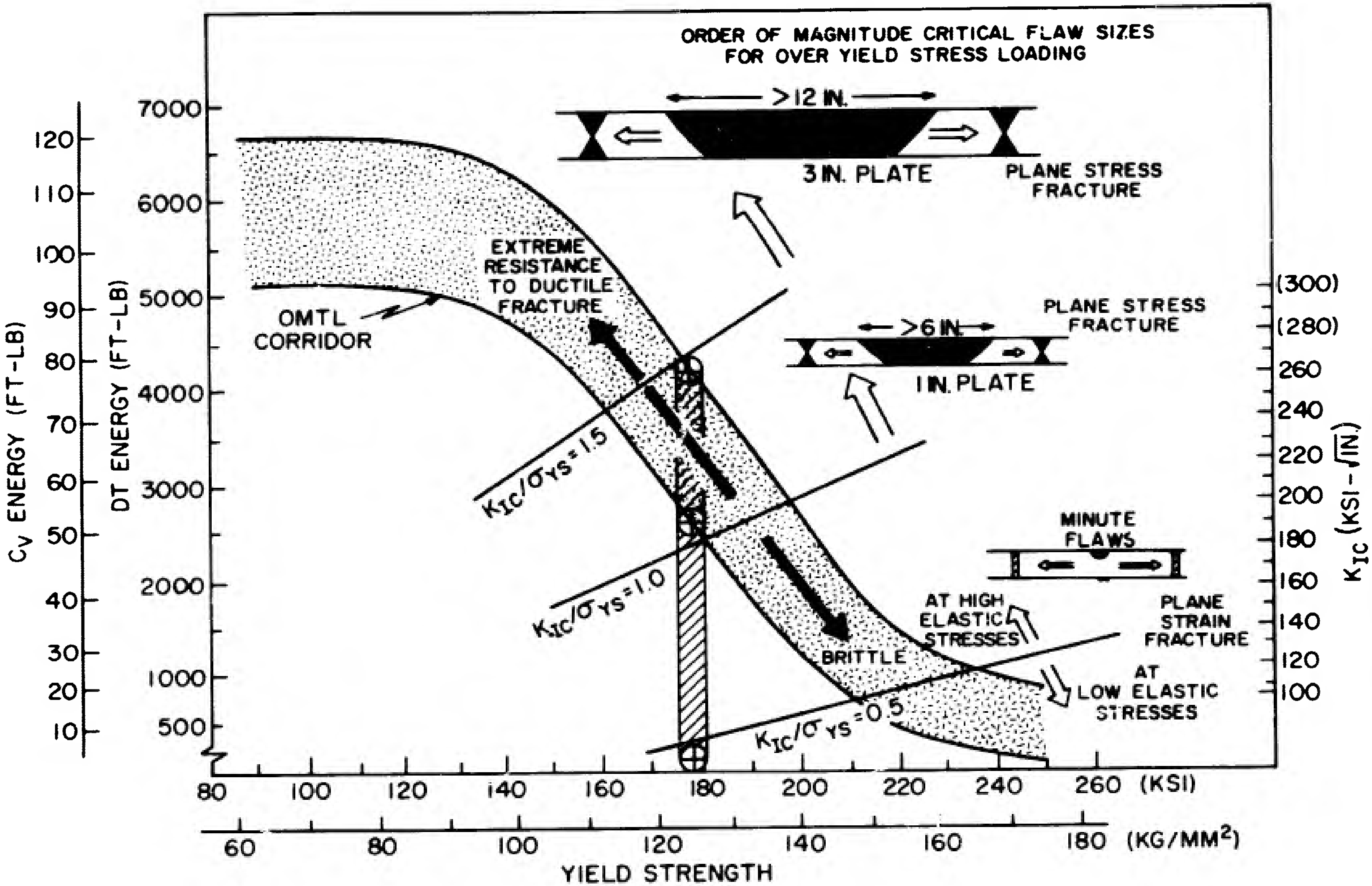

Fig. 32 - Simplified analyses of the dramatic transition in fracture toughness represented by the K_{Ic}/σ_{ys} ratio line intercepts with the OMTL corridor. Note critical "midpoint" features at approximately 180 ksi yield strength; also note the wide range of fracture toughness at this strength level.

Table 3
Significance of K_{Ic}/σ_{ys} Ratios in Relation to Other Parameters

Engineering Index Ratio (K_{Ic}/σ_{ys})	Relative Plastic Zone Size (Plane Strain) $(K_{Ic}/\sigma_{ys})^2$	Relative Fracture Toughness Parameter		Relative Fracture Toughness Parameter	
		Plane Strain	Plane Stress	1 in. Thickness	3 in. Thickness
0.5	0.25	1	3	1*	1*
1.0	1.0	4	12	4* (12)†	4*
1.5	2.25	9	27	27†	9* (27)†
2.0	4.0	16	48	48†	48†
3.0	9.0	36	108	108†	108†

*Plane strain.
†Plane stress.

increase in relative fracture toughness consequent to increase of the ratio values is dramatic by any procedure of examination, graphical or numerical.

These definitions of the engineering significance of the K_{Ic}/σ_{ys} ratios provide for the evolution of a Ratio Analysis Diagram (RAD), presented in Fig. 33. The diagram evolves by extrapolation of the K_{Ic}/σ_{ys} ratio lines to low strength levels. The previous flaw-size-analysis plots are modified by the use of a linear scale below the K_{Ic} value of 100 ksi $\sqrt{\text{in.}}$, to provide for this extrapolation. The changes in fracture modes and critical flaw sizes described in relation to Figs. 30 and 31 apply across the entire diagram, because these are basically related to the ratio lines at all strength levels.

The C_v scale relating to the K_{Ic}-C_v correlation is presented on the right-hand side of the diagram, and the C_v scale relating to the DT-C_v correlation is presented on the left. The resulting C_v scales are in almost exact correspondence at C_v values of less than approximately 50 ft-lb. For higher C_v values, the C_v scale derived from K_{Ic}-C_v relationship is compressed in comparison to the DT derived scale. This compression results from the experimental difficulties of determining K_{Ic} values in excess of 200 ksi $\sqrt{\text{in.}}$ These values relate to high K_{Ic}/σ_{ys} ratios and should be considered as approximate K_{Ic} values for reasons cited previously.

The complications of approximate K_{Ic} values apply to some degree to the 1.5 ratio line and certainly to the 2.0 and 3.0 ratio lines. Obtaining valid K_{Ic} values in excess of 120 ksi $\sqrt{\text{in.}}$ for 80 ksi yield strength steel involves the same problem as obtaining valid values in excess of 210 ksi $\sqrt{\text{in.}}$ for a 140 ksi yield strength steel. Whenever the ratio increases to 1.5 or higher values, it signifies that the K_{Ic} value is determined for stress conditions above yield. For such conditions the "iteration" calculation corrections must be made.

These aspects do not complicate the interpretations of the RAD because the high ratio lines are used to signify very high fracture toughness relating to plane stress ductile fracture. For these conditions it is not necessary to be concerned with small differences in flaw sizes — all flaw sizes will be "huge," and the propagation stress required will be of plastic-load intensity.

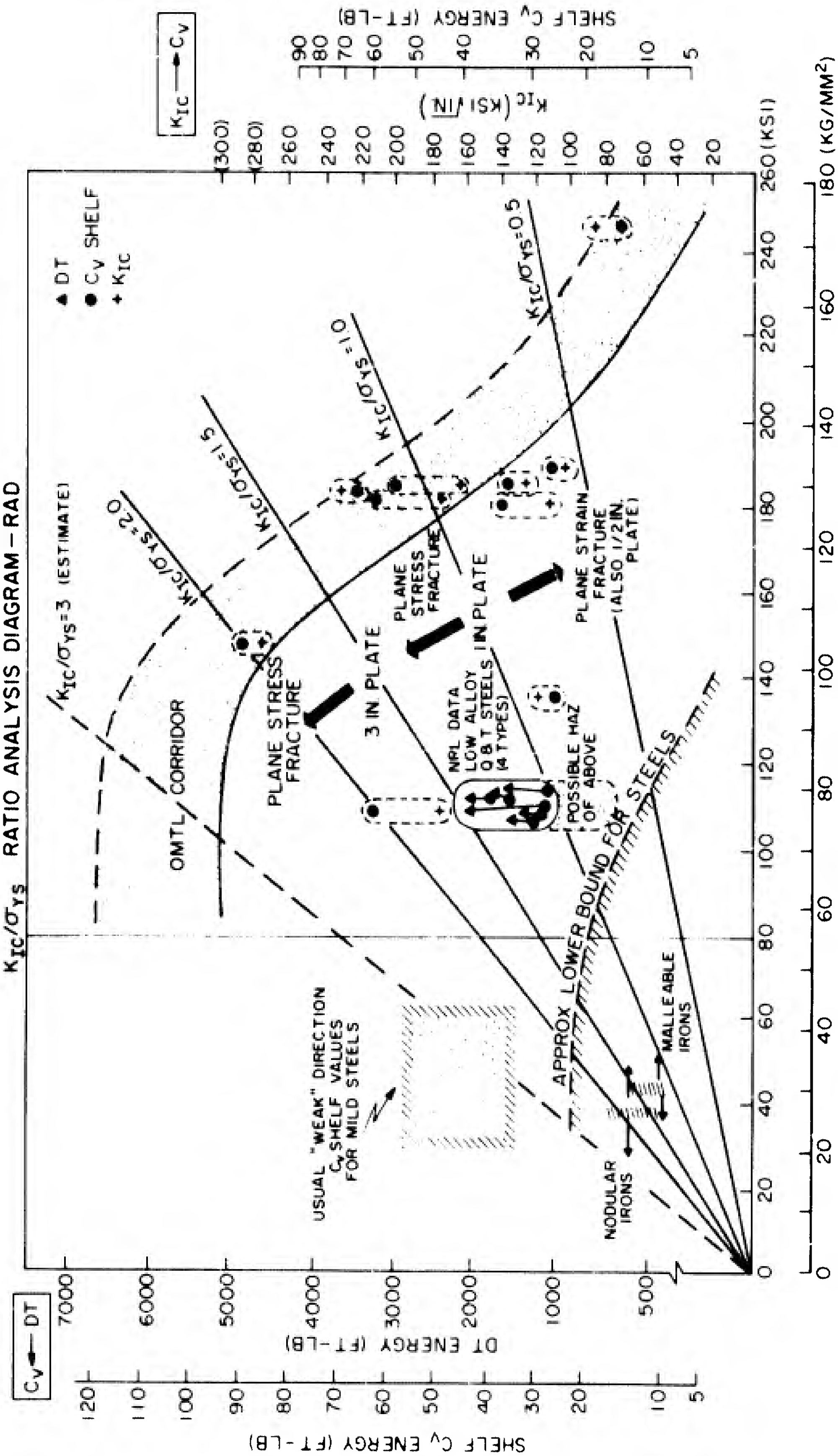

Fig. 33 - K_{Ic}/σ_{ys} Ratio Analysis Diagram (RAD). See text for details.

Practical use is made of the RAD by simple entry based on either C_V shelf energy values or DT energy values, as represented by the left-hand scales. Obviously, the yield strength must be known to plot the point in the diagram. If the K_{Ic} value is available, entry is made from this scale. The bold arrows pointing upward in the diagram serve as a reminder of the transitions to plane stress for 1 in. and 3 in. thickness. The bold arrow pointing downward signifies transition to brittle plane strain conditions, which would also include 0.5 in. plates at and below the 0.5 ratio line. The Flaw Size Analysis Diagrams (Figs. 30, 31) interpretations may be used for determining critical flaw sizes in the regions between the 1.5 and 0.5 ratio lines, if desired. Above the 1.5 ratio line there is no need to calculate flaw sizes (huge). Below the 0.5 ratio line the calculated flaw sizes are ordinarily below the detectability limits of nondestructive testing for most purposes.

Checks of the validity of the diagram in the higher strength range were made from data for seven steels presented in the ASTM-STP 410 publication (10) plus three additional steels, involving data provided by U.S. Steel Research Laboratory and Westinghouse Research Laboratories investigators. The points enclosed in the "dashed" envelopes represent C_V shelf values and related K_{Ic} values for the ten steels, which are described in Table 4. It is apparent that the DT indexed C_V scale remarkably locates all of the points in correspondence to the K_{Ic} scale. This correspondence indicates that C_V shelf values may be used within reasonable limits to index the K_{Ic} value, and thus serve to characterize the K_{Ic}/σ_{ys} ratio for steels of known yield strength.

The group of points at approximately the 110 ksi yield strength level represents widely used low alloy, commercial Q&T steels of the different types noted in Table 2. These were obtained as 1 in. plates and were tested by the 1 in. DT test, and also by the C_V test to define "weak" direction shelf values. It is noted that these lie in the region above the 1.0 ratio line (by both C_V or DT indexing) and thus should represent material

Table 4
Data from ASTM-STP 410* (1 and 2 in. Plates)

Steel	σ_{ys} (ksi)	C_V at 80°F (ft·lb)	K_{Ic} (ksi $\sqrt{\text{in.}}$)	K_{Ic}/σ_{ys} Ratio
18Ni (250) A-538 Grade B	246	16	87	0.35
18Ni (200)	192	25	107	0.56
18Ni (190)	187	58	167	0.89
12Ni-5Cr-3Mo	186	65	233	1.25
5Ni-Cr-Mo-V	149	89	279	1.87
4147 A-372 Class V - Type E	137	26	121	0.88
T-1 A-517 Grade F	110	62	177	1.61
18Ni 190-VIM (Long.)†	186	61	168	0.91
18Ni 190-VIM (Trans.)†	187	35	123	0.66
HP-9-4-.25‡	180	40	110	0.61

*U.S. Steel Applied Research Laboratory.
†Additional data; courtesy of S. Rolfe, U.S. Steel Applied Research Laboratory.
‡Additional data; courtesy of E. Wessel, Westinghouse Research Laboratories.

which fractures in a plane stress mode at DT shelf temperatures. The DT fractures confirmed the prediction of the diagram. However, it must be noted that these are not the equivalent of the dramatic slant fractures obtained for the high shelf energy OMTL steels.

Explosion Tear Tests (ETT) of these materials at ambient temperatures (above 0°F) have indicated plane stress fracture features similar to the DT specimen fracture at the same temperatures. However, the "resistance" to plane stress fracture propagation is considerably less than that of OMTL quality steels of the same strength level, which develop much higher C_v shelf and DT energies. The ETT confirms this by evidence of much lower levels of plastic bulging for fracture propagation for these steels compared to the OMTL quality steels. The need for such high levels of plane stress fracture toughness, and corresponding increased resistance to propagation of ductile fractures, is a matter of engineering decision related to unusual service conditions, to be discussed.

The as-rolled or normalized structural steels of 30 to 60 ksi yield strength have a wide range of DT and C_v shelf energy values. In general the "weak" direction values may be expected to lie in the zonal locations indicated by the diagram.* These steels may have relatively high plane stress fracture toughness, but not as high as is developed by the OMTL Q&T steels of the 80 to 140 ksi yield strength range. The engineering problem in the use of the 30 to 60 ksi yield strength steels is that the transition temperature may fall in or above the ambient range.

Steels with C_v shelf values in the order of 10 to 20 ft-lb, for strength levels in the order of 30 to 50 ksi yield strength, are not ordinarily articles of commerce. This exclusion from the diagram is indicated by the "lower bound" curve for commercial steels, covering the range of 30 to 140 ksi yield strength. To attain C_v shelf values below this curve would require very peculiar metallurgical conditions. However, such values may be found in the nodular irons and malleable irons of 30 to 50 ksi yield strength. The locus of the 0.5, 1.0, and 1.5 ratio lines at this level of yield strength suggest that such materials would fracture in plane stress mode for shelf levels in the range of 10 to 20 ft-lb. Previous NRL investigations in 1952 and 1953 disclosed that such was the case. Figure 34 presents data for a 38 ksi yield strength nodular iron featuring a 16 ft-lb C_v shelf value (11). As illustrated by photographs of 1 in. thick plate, Crack Starter Explosion Tests (using the DWT brittle weld), shattering type brittle fractures associated with the transition temperature region of the C_v curve are replaced by plane stress, plastic-overload fractures at C_v shelf temperatures. The same relationships between the explosion tests and C_v curves were demonstrated for 1 in. thick plates of malleable irons which feature a C_v temperature transition to approximately 12 ft-lb shelf values (12).

The subject references to the nodular and malleable iron investigations provided extensive experimental documentation that the rudimentary plane stress fractures, related to such low C_v shelf values (or low DT values implied by the RAD), provide poor resistance to propagation of ductile fracture. Extensive "easy" tearing was obtained with the application of very low levels of plastic bulge strain in the Crack Starter Explosion Tests. In the 1952 nomenclature, the results were described as representing "low energy shear," which represented the first use of this term. In comparison, mild steels of similar strength levels, but of C_v shelf values in the order of 40 to 60 ft-lb, responded to Crack-Starter Explosion-Test deformation by developing full spherical bulges, with very limited

*Usual practices for C_v testing result in values related to fracture in the strong direction. The RAD provides for proper interpretations of these values. The reasons for uniform reference to "weak" direction properties in this report were explained in the introductory section to high strength steels.

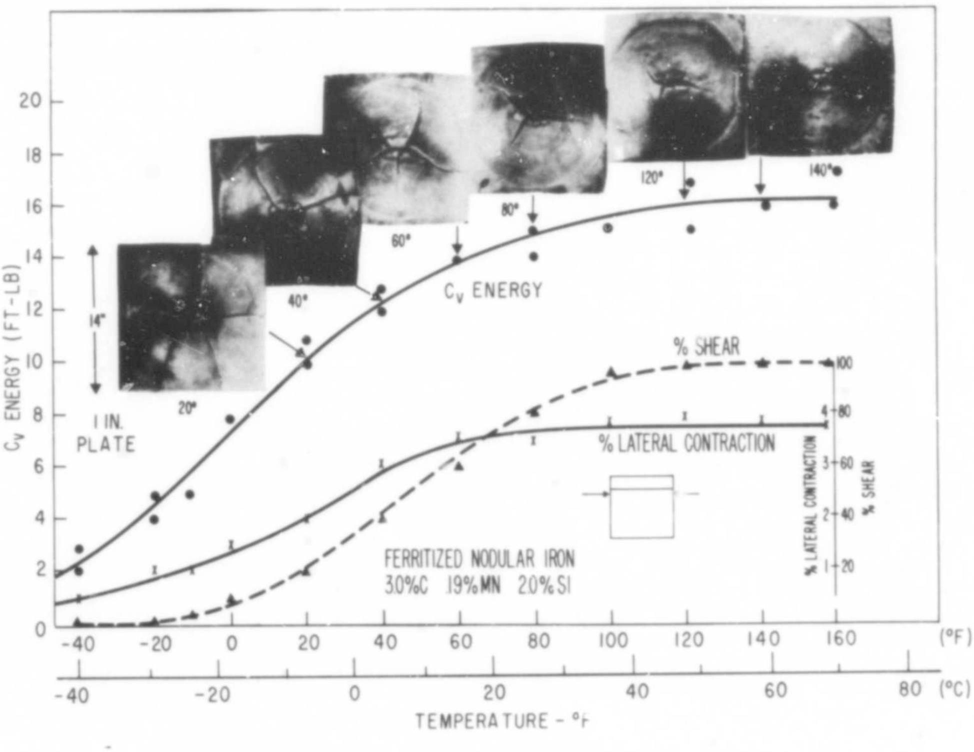

Fig. 34 - Explosion Crack Starter Tests for nodular iron. Transition from plane strain (shatter) fractures to arrests of plane stress (tearing) fractures is related to C_v transition to 16 ft-lb shelf value.

tearing at temperatures of plane stress fracture. These were described as representing "high energy shear." At this early date it became apparent that the C_V shelf value was an index of relative resistance to propagation of ductile fracture and was so reported.

The described data for the irons, mild steels, low alloy Q&T steels, and the 180 ksi steels uniformly demonstrate that plane stress fracture conditions for 1 in. plates are attained at C_V shelf values which lie above the 1.0 ratio line or higher positions in the RAD. The 1 in. DT test also uniformly demonstrates plane stress fracture conditions for steels above the 1.0 ratio line for the entire range of 35 to 180 ksi yield strength. Over this same range, a decrease to 0.5 ratio is represented by a change in DT fracture mode to flat, plane strain fracture.

These various observations confirm that the RAD may be indexed in relation to the ratio lines for all strength levels. Moreover, confirmation is also provided for the validity of the fracture mechanics procedures which are based on consideration of yield strength as a major element in the interpretations of fracture toughness test values. In conformance with these principles, the C_V shelf values and DT energy values are normalized by the slopes of the ratio lines. The importance of this contribution of fracture mechanics to the interpretations of relatively simple engineering fracture tests cannot be overestimated. It is in fact revolutionary and should affect all future engineering design and specification practices. The impact on alloy development is of similar major import.

Precautions – Metallurgical Considerations for Q&T Steels

Certain precautions should be noted in the use of the RAD for interpretations which apply to Q&T steels of 3 in. thickness. The primary purpose of this discussion is to emphasize that the extension of 1 in. DT analysis to 3 in. thickness is valid only if the 1 in. DT test is made for the 3 in. thickness. For example, it is not proper to use 1 in. plate data as representing 3 in. plate properties, unless it is known that there are no metallurgical changes resulting from increased thickness.

The metallurgical effects of increased thickness relate to the alloy content, and the Q&T steels are particularly sensitive in this respect. All of these steels are designed by controlled alloy content to provide through-hardening (required to produce proper metallurgical structures) to specific maximum thicknesses. This is a matter of "hardenability" and can be calculated with exactness by metallurgists. Because of alloy cost factors, commercial steels use the lowest alloy content commensurate with the maximum thickness in question. For example, the described low alloy Q&T steels are designed for a maximum of 1 to 2 in. thickness, depending on the specific type and the producer. As thickness is increased above the "designed" level, unfavorable metallurgical structures result which, in a low percentage of the total, catastrophically decrease fracture toughness to brittle levels. In effect, the transition temperature range is shifted from subzero to over the normal ambient. Thus, plane stress ductile fracture at room temperature for a 1 in. plate is changed to cleavage, brittle fracture for a 3 or 4 in. plate.

Another feature of the low alloy Q&T steels is that deviations from best welding practices may result in weld heat affected zone (HAZ) properties which fall below the 1.0 ratio line (C_V shelf values may be lowered to 14 to 18 ft-lb). Thus, it is possible to obtain plane strain fracture propagation at elastic loads in the HAZ (13). Unless appropriate welds are used for this strength level, it is also possible to obtain similar performance for the weld metal. The proper utilization of these steels in welded structures requires careful consideration of weld and HAZ fracture paths. While some producers supply extensive data and guidelines in these respects, this is by no means common practice. Moreover, there is unfortunate lack of respect for these guidelines by fabricators. Experience has shown that structural failures for these steels in thicknesses less than the "designed" thickness is always associated with weld or HAZ fracture paths. Failures of these steels, for thickness in excess of the "designed" thickness, have been associated with conventional brittle fracture of the base material.

The Navy HY-80 steel is now utilized extensively for industrial purposes. The high alloy composition of this steel is "designed" for maximum plate thickness of approximately 6 to 8 in. The 100 to 110 ksi yield strength grade (HY-110) is basically the same steel, heat treated to higher strength and features similar thickness limits. Unfortunate industrial applications of these steels (HY-80 and HY-100) have been made for much greater thickness, particularly as forgings. The results of greatly exceeding the design thickness (12 to 20 in.) are exactly the same as for the low alloy steels. The steels will then feature plane stress fracture toughness for a surface zone (of say 2 in. depth) and the remainder will entail a brittle core. DT test sampling through the thickness of such heavy section material discloses the presence of such conditions.

Energy Intensity Considerations

There are structural applications for which plane stress fracture of high energy "intensity" (fracture resistance) is required. These are applications which involve prevention of tearing propagation in the presence of a very long flaw or actual stoppage of tearing. These generally relate to pressure vessels; for example, nuclear containment vessels, gas pipe lines, compressed gas cylinders, etc. For a nuclear containment vessel the problem may be the arresting of fracture after a length of weld has broken. For gas pipe lines it may be desired to introduce a short section of fracture tough steel which arrests fracture or decreases the propagation velocity so that pressure is released. For a seamless pressure flask of large dimensions it may be the "control" of a large flaw created by the rupture of a lamination. For ships or similar large structures the need may be for welded "crack-arresters" to replace riveted items of this type.

The question of energy "intensity" for 1 in. thickness is answered directly by the DT energy scale for RAD positions relating to the plane stress fracture mode. For example, the energy intensity for the low alloy Q&T steels is approximately 1/3 to 1/4 that of the OMTL corridor material of the same strength level.

The question of "how much is enough" for these unusual conditions does not have a generalized answer, except the more the better. The reason is illustrated in the upper box of Fig. 35. If a flaw is many times the thickness (say 10X, 20X, etc.), bulging in the general flaw region will occur for a pressure vessel. This will result in gross plastic overload in the region of the crack tip. The nominal hoop stress then loses all significance. The longer the crack in relation to thickness, the lower is the hoop stress that will result in gross plastic overload at the region of the crack tip. In effect, by increasing crack-length-to-thickness ratio the required hoop stress falls to very low levels, such as one tenth of yield stress or less.

The RAD zoning of Fig. 35 was developed as a practical approach to providing some guidelines in these respects. The data presented relate to a 1 in. thick flat plate in pure tension. Critical flaw lengths for through thickness cracks and yield stress nominal load are presented in relation to the ratio lines. These data evolve from K_c calculations which are admittedly approximate; however, this is the best that can be done analytically. It is apparent that the critical flaw lengths for plane stress propagation increase rapidly with increasing DT energy.

The bold arrows of the diagram with the notation "fall back for plastic loads" indicate large decreases in critical flaw lengths due to bulging which develops for pressure vessels. Such large decreases have experimental verification in pressure vessel burst tests featuring large flaws (3,5). The approximate dimensions of the critical flaw lengths

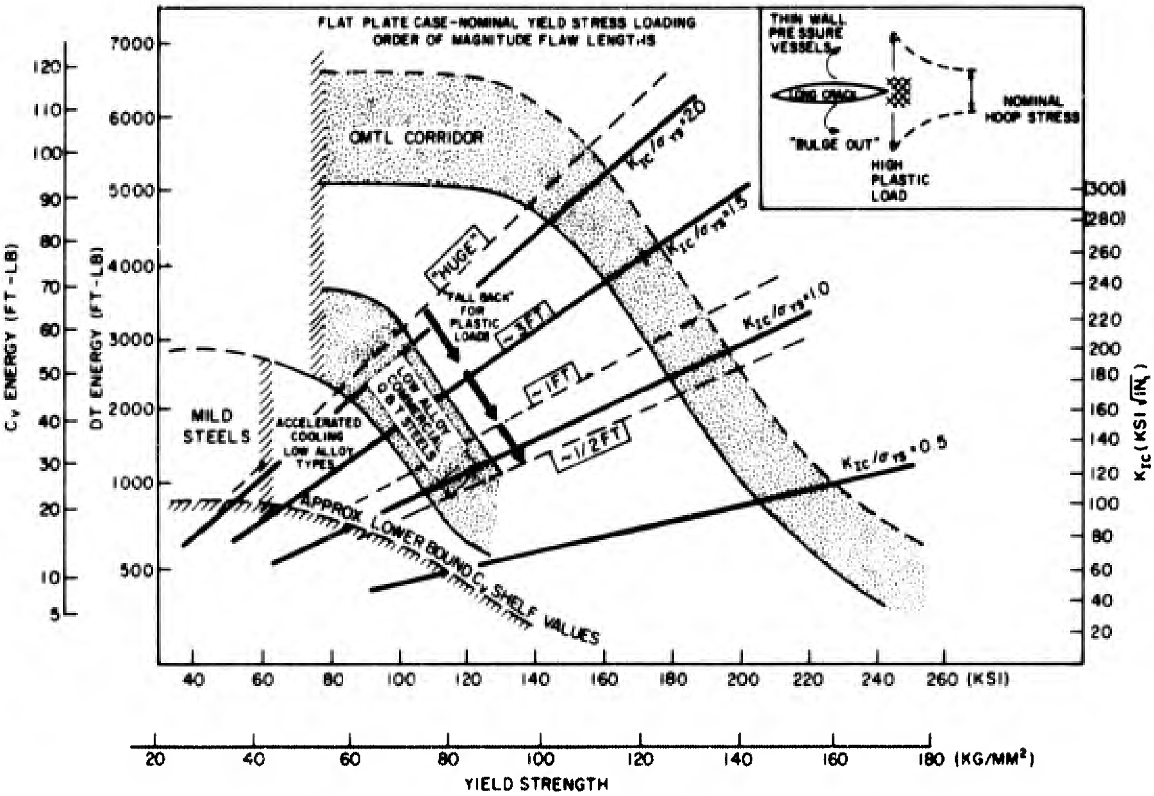

Fig. 35 - RAD analysis of approximate through-thickness flaw lengths for plane stress fracture propagation at nominal yield stress load, for 1 in. thick flat plates; also indicates large decrease in critical flaw lengths for pressure vessels, due to bulging developed in the flaw region

which relate to various steels of interest may be deduced by indexing to the diagram (for example, based on C_V shelf energy and yield strength). A generalized comparison may be made directly from the diagram for near-OMTL quality steels of 110 ksi yield strength in relation to the low-alloy, commercial Q&T steels of the same strength level. While large differences in critical flaw lengths will be indicated by this comparison, it should be emphasized that premium material with respect to plane stress energy "intensity" also involves necessary premium costs almost in direct ratio.

The above-described plane stress K_c condition would require $\mathcal{G}_c$ fracture mechanics testing for exact definition. The difficulty is that huge plate widths and huge flaw lengths are required for such tests. Moreover, these can only answer the flat plate question, because fracture mechanics cannot be applied presently to bending situations such as bulging. The only practical laboratory test assessment for energy "intensity" appears to be provided by the DT test fracture energy values.

Compendium RAD Indexing of Generic Classes of Steels

The foregoing charts have gradually evolved a panorama of the typical strength-fracture toughness characteristics of various classes of steels at ambient temperatures (above 0°F). Previous presentation of total coverage of the diagram for the various generic classes of steels was avoided for simplification. At this point it is appropriate to complete the entire spectrum; this is presented in Fig. 36. While some overlap obviously exists, the indicated zonal locations are inherently characteristic of the various

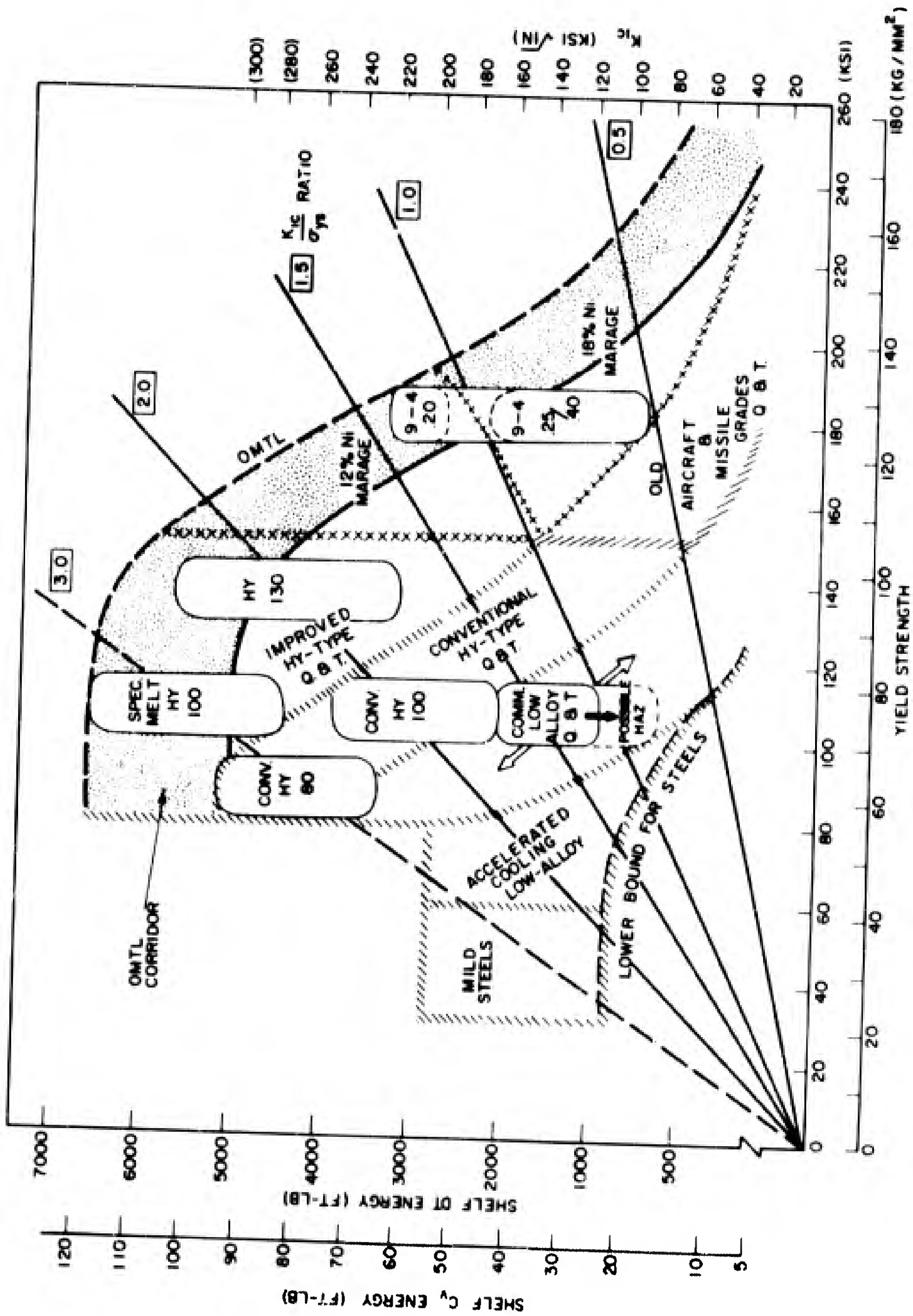

Fig. 36 - Compendium RAD indexing for generic classes of steels

classes and easily defined. The information derives from a compendium of C_v, DT, and K_{Ic} data derived from a wide variety of sources — all scales were utilized to complete the diagram. Obviously, the preponderance of data relating to the lower strength steels derive from C_v shelf values.

By superimposition of the RAD K_{Ic}/σ_{ys} ratio lines, a massive integration of data results. Many aspects, relating to processing variables, alloy composition features, thickness limitations, etc., described in the foregoing sections apply and will not be reenumerated here. Metallurgists who are familiar with specific families will readily recognize the characteristic features and specific data. For the engineer, the compendium provides useful orientation and guidance which serve a wide variety of practical purposes. It should be noted that there are sound metallurgical and economic reasons for the existence and the location of the various generic families — the complete filling of the diagram is not an accident.

ANALYTICAL PROCEDURES FOR THE TEMPERATURE TRANSITION

Applicability of Various Test Methods

The transition temperature range provides the major challenge in the evolution of practical fracture tests. The intense interest in the transition temperature range of the low strength steels derives from the fact that metallurgical factors result in shifts of the transition from below to above ambient temperatures. The temperature-induced transition from plane strain to mixed-mode has provided the basis for engineering test solutions which have been characterized as the "transition temperature approach." The unfortunate connotations of nonanalytical which have evolved in comparison to fracture mechanics tests should now be discarded. All tests which are concerned with the transition temperature range must necessarily involve transition temperature approaches.

Fracture mechanics testing and applications to date have been directed primarily to the temperature-insensitive metals of relatively low fracture toughness. The complications of the transition temperature range must be resolved if fracture mechanics tests are to be utilized in general engineering practice. The transition temperature region represents the area of primary applicability of any fracture test procedure. Unfortunately, attempts to define transition temperature features in K_{Ic} or K_c terms run into the previously described technical complications, plus prohibitive expense associated with the large number of tests required for definition of the full range. Presently, these procedures are not practical except for research investigations. Steels which feature transition temperature rise to high fracture toughness would require K_{Ic} test specimens of 1 in., 2 in., 4 in., and (theoretically) 10 in. or more size, to follow the transition curve from "toe" to "shelf."

Of the remaining tests, only the C_v and DT types provide practical solutions for defining the full course of the transition curve. The DWT-NDT test is restricted to defining the location of the toe region at which full plane strain fracture is attained. The Robertson test is prohibitively expensive for routine use. The C_v test interpretations for the transition range are subject to basic difficulties for which there does not appear to be a solution, except in specific calibrations for specific steels. This aspect will be discussed additionally in the final portion of this section.

The DT test appears to provide a significant definition of the transition temperature range with respect to both fracture toughness energy and fracture mode. The temperature range which applies to shelf analyses based on the RAD is readily defined. The toe region serves as an index of the NDT temperature; there is no need to repeat the NDT determination by use of the DWT.

The FAD may be indexed to the DT energy-transition curve within reasonable engineering limits by reference to the estimated NDT temperature. It may also be indexed to the CAT curve reference point for yield stress loading. In addition, the NDT related DT toe region may be analyzed in accordance with the interpretations of Fig. 6 (NAD), indexed to appropriate dynamic and static K_{Ic}/σ_{ys} ratios defined by the NAD scales.

DT Interpretations for Transition Temperature

The combined RAD, FAD, and NAD procedures serve to cover all primary aspects of analytical definition for DT test shelf, transition, and toe regions. These apply to steels in the range of 1 to 3 in. thickness, based on test data for 1 in. DT specimens. All of the required indexing data are obtained from the DT energy-transition curve determined by tests of eight to twelve specimens, spaced at appropriate temperature intervals. The procedures are illustrated in Fig. 37 for three typical DT curves representing high and low shelf, 110 ksi yield strength steels and a low strength mild steel. The notations relating to temperature indexing for the RAD (shelf), FAD (below DT midpoint), and NAD (toe) are self-evident.

The procedure for indexing the FAD to the midpoint of the DT energy curves is based on the correspondence of shear-lip fracture-mode transition features between the DT and Robertson tests. The rise of the DT transition from the toe region to the midpoint relates to the initial development and enlargement of shear lips. The rise of the Robertson CAT curve, from its toe region to high elastic stress levels, results from the same process of development and enlargements of shear lips. Above the DT curve midpoint, the shear lip condition is rapidly exaggerated to much larger regions of slant fracture, which ordinarily culminate to full-slant fracture at the shelf. Robertson tests cannot be conducted for stresses above yield level, hence direct comparison of fracture

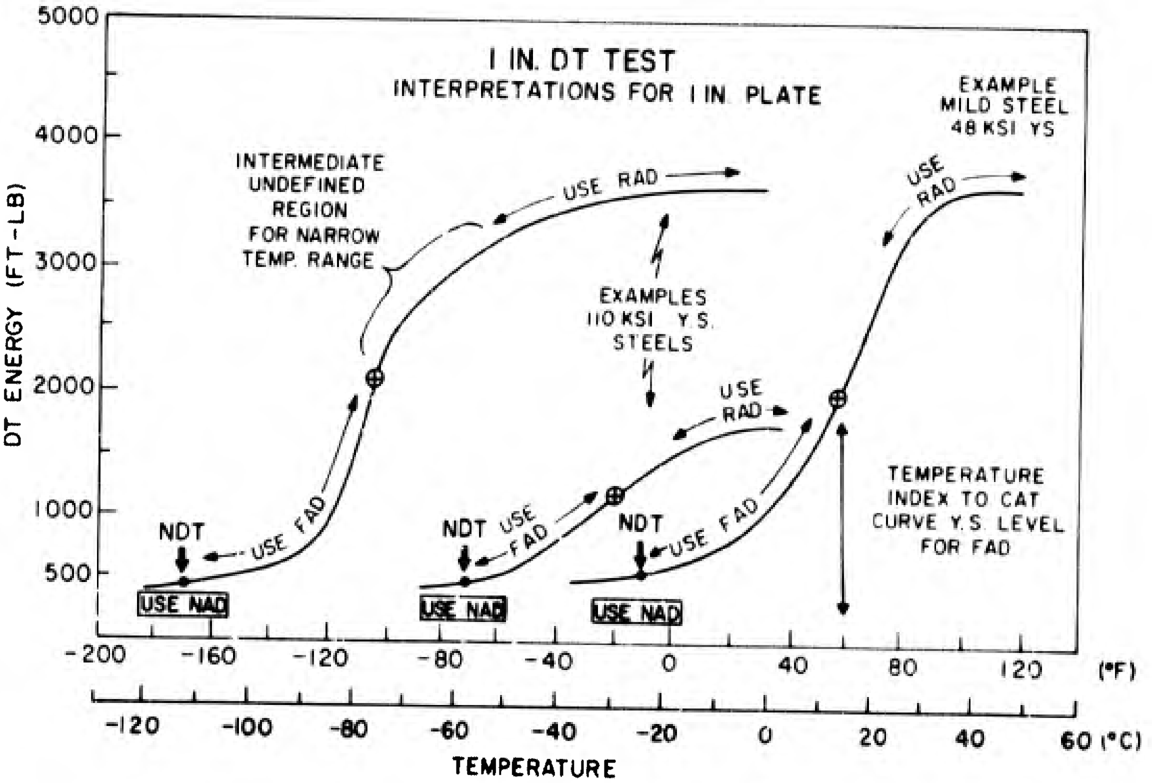

Fig. 37 - Indexing procedures for DT temperature transition curves of various forms. Regions commonly related to RAD, FAD, and NAD interpretations are indicated.

modes cannot be made. The FAD-CAT curve for the plastic strain region was derived from Explosion Crack Starter Test observations of increased resistance to fracture propagation and changes in fracture mode similar to those described for the DT test (4). Thus, the FAD representation for the plastic strain region of the CAT curve relates to the same change in fracture mode described for the upper half of the DT curve. The midpoint temperature of the DT energy transition thus may be indexed to the yield-stress reference point of the FAD Robertson CAT curve. The conventional FAD interpretations may then be applied by consideration of the temperature differences (FAD "Δt" scale) in relation to the indexed midpoint DT temperature.

The combined use of FAD and RAD analyses is illustrated in Fig. 38 for the three steels of Fig. 37. The shelf energy of the DT curve is indexed to proper location in the FAD by consideration of the yield strength. The DT curve defines the temperature range for which this indexing applies. The dashed line below each index point indicates that the "near shelf" portion of the DT energy curve is also analyzable by the FAD. This region is very close to the full plane stress condition. This observation is made to prevent undue concern as to exact temperature location of the point of full shelf attainment. The temperature ranges which apply to the shelf temperature locations of the FAD for the different steels are self-evident.

It is noted that the DT energy transition midpoint temperature, less 60°F, corresponds closely to the NDT temperature, obtained directly by the DWT or inferred by the toe region of the DT curve. This commonality is expected because the FAD is based on a NDT + 60°F as the determination of the CAT yield stress point for these steels.

The analyses leave an intermediate zone between the FAD and RAD interpretation portions of the DT energy curves undefined; however, this zone ordinarily covers only 20° to 40°F. Reasonable engineering deductions could be made by relating this zone to the FAD regions above the indexed CAT curve point for yield stress loading.

The DT toe region defines the temperatures for which the dynamic K_{Ic} values (K_{Id}) may be calculated from the DWT flaw size and yield stress conditions. As explained previously, Fig. 6 may then be used (NAD) to determine the flaw conditions related to appropriate dynamic or static K_{Ic}/σ_{ys} ratios. The choice of dynamic K_{Ic} (K_{Id}) or static K_{Ic} analyses is a matter of engineering judgment as to the applicable conditions. The NAD defined K_{Ic}/σ_{ys} ratios for dynamic and static conditions relate specifically to the NDT temperature region and should not be extended to temperatures far above or below this temperature. The limit of NDT + 20°F to NDT - 50°F was defined previously as a reasonable range for ordinary engineering use of the NAD. This limit corresponds to the nearly flat portion of the DT toe region.

Advantages of Energy Definition of Transition

The following comments relate to the importance of conducting DT tests based on energy determinations. These comments are particularly required to preclude extension of fracture-appearance definitions as a simple method of possibly attaining equivalent information. There are conditions for which this is true, but there also are others for which this procedure may be misleading. In general, the fracture appearance approach is unduly restrictive in its interpretive possibilities and should be reserved for special cases which are satisfied by such simplified procedures.

One of the added features provided by the DT energy curve is the assessment of relative plane stress energy "intensity" as related to Fig. 35 interpretations for unusual engineering conditions. There are other ramifications inherent to the interpretations of fracture appearance for low shelf-energy steels, and particularly to estimates of the transition temperature point relating to the attainment of plane stress conditions.

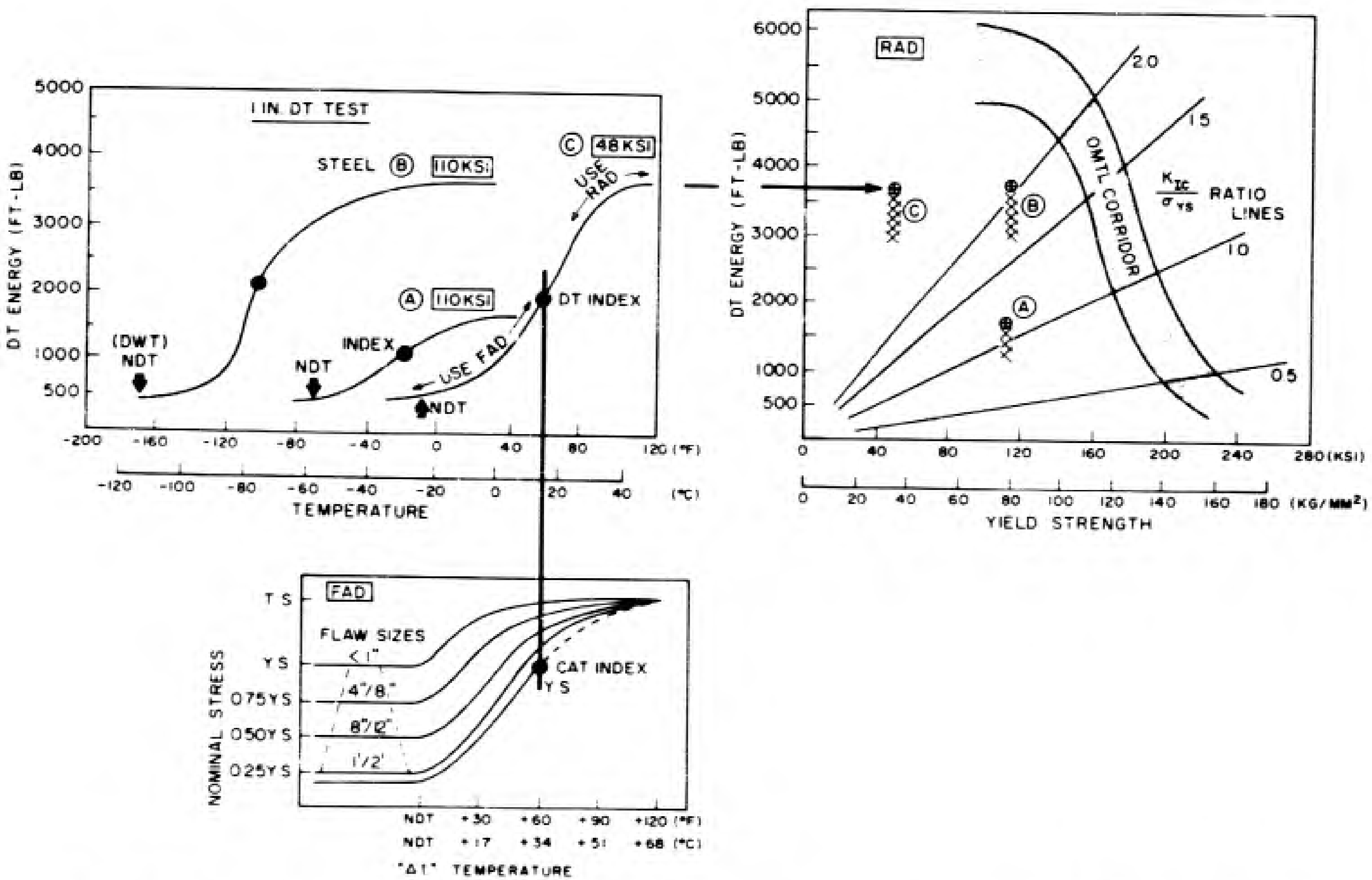

Fig. 38 - Example of the use of DT temperature transition curves for indexing of FAD and RAD

Discussion of this aspect was reserved to this late point so that it would be better understood, in context with the previous discussions.

Steels in excess of 100 ksi yield strength, featuring shelf energies which are significantly less than 3500 ft-lb for the 1 in. DT specimen may show incomplete shelf transition to slant fracture. That is, while the energy curve "shelfs out," the fracture appearance at the shelf retains a central region of flat fracture. This is easily mistaken for a mixed-mode (in transition range) fracture condition, whereas the energy curve correctly defines the attainment of shelf, plane stress conditions. The events which dictate this type of fracture may relate to a peculiar selection of the separation path through the middle of the large plastic enclave which provides the shelf-energy reading. It may be simply stated that the slant fracture paths, following the 45-degree shear planes of the highly plasticized region, are ordinarily restricted to metals of relatively high plane stress energy intensity. The higher the energy, the more dramatic is the appearance of the slant fracture.

Other evidence that such atypical fracture appearance relates to plane stress conditions is provided by observation of considerable lateral contraction consequent to the transition into the energy-defined, plane stress shelf. For the various reasons cited, it appears that the only unequivocal definition of plane stress shelf condition is provided by the energy transition curve. The visual method of "reading" the fracture appearance can be misleading for metals of low shelf-energy features. The inference may be that the temperature transition to shelf has not been reached. The energy reading always serves to properly designate that the plastic enclave in advance of the fracture increases rapidly with increasing temperature and saturates to "shelf," i.e., that plane stress fracture conditions are reached. The DT test thus serves to clarify possibly confusing aspects of the conventional definition of stress state from fracture appearance observations.

It is suggested that proper fracture mechanics terminology be evolved to define this condition so as to clearly separate it from that of true mixed-mode fracture. The danger is that the partially flat appearance of the center regions of such high energy fractures will be confused with low-toughness plane strain conditions ordinarily expected in the cleavage temperature region of the transition range.

It is proposed that this condition be recognized as "transition shelf, equi-plane stress fracture," or simply "equi-plane stress" fracture. It may be argued that the proper term should be "quasi-plane strain" fracture. This term is rejected for conditions which demonstrate significant increase in through-thickness lateral contraction consequent to entering the shelf region. Obviously, the lateral contraction provides firm evidence that plane strain constraint features are lost, i.e., plane stress controls. Irrespective of semantics, the only unambiguous fracture mechanics definition of plane strain is provided by experimental verification that maximum restraint (K_{Ic}) conditions are attained. There is no equivalently rigorous definition for plane stress because of the geometry dependence of this condition; in general, it is considered simply as a condition "other than plane strain." A clarification of this issue emerges by adopting the view that, since the DT toe region relates to plane strain then the DT energy shelf must clearly relate to plane stress.

Precautions for K_{Ic} Tests Related to Toe Region

The NAD interpretive procedures relating to the DT toe region were specially designated NAD to avoid confusion with shelf analyses. The importance of this separation derives from the need for considering dynamic (K_{Id}) conditions for the toe region which do not apply to the shelf condition. If the DT transition curve is available, there should be no reason for confusion as to temperatures relating to toe region, K_{Id} conditions. However, direct determinations of K_{Ic} values by fracture mechanics tests may not indicate per se if these are related to the shelf or to the toe of the transition range. To define this, it is necessary to completely fracture the specimen so that details of the fracture mode become evident. This caution derives from experience in K_{Ic} testing of high strength steels which provided lessons that data-book notations of the K_{Ic} value, in absence of a fracture-mode details may lead to erroneous conclusions of serious engineering consequences.

The shelf condition for high quality Q&T steels of intermediate and low strength ranges may extend considerably below ambient temperatures. Thus, it is ordinarily expected that room temperature tests will relate to shelf conditions. However, the toe region may shift back to the room temperature range for poorly heat treated, or otherwise embrittled, material. For these cases the shelf condition is then located at relatively high temperatures. Conventional K_{Ic} testing at room temperature obviously does not relate to shelf values for such steels. High "apparent" K_{Ic} values for static testing may be obtained at toe temperatures if the thickness is moderately inadequate. These are easily mistaken for the high values expected for the shelf condition. The reason is that the "first event" K_{Ic} determination of instability may involve ductile tearing at the crack tip for sections of inadequate thickness, for both the toe and the shelf conditions. For such tearing first event instabilities, the indicated K_{Ic}/σ_{ys} ratios may easily range from 1.0 to 1.5 for both toe and shelf conditions.

Failure to recognize high "apparent" K_{Ic} values which relate to toe conditions leads to the assumption that "iteration" correction calculations may be applied to deduce the approximate K_{Ic} value. While this procedure may be reasonably valid for shelf-related conditions it is misleading for toe conditions. Increase in the specimen thickness (B), or the application of dynamic loading, may then result in a major decrease of the measured fracture toughness value. These lower values of fracture toughness represent the true service-related fracture toughness potentials of the steel.

Caution should be exercised in interpretations of K_{Ic} values for specimens which show a cleavage fracture, preceded by a "crescent" of crack-tip ductile fracture. This combination of fracture modes serve to indicate that toe region considerations may apply in service.

Integration of Transition Features

The applicability of the DT test for conditions involving both the strength and temperature transitions provides for a unified, three-dimensional presentation of fracture toughness (Fig. 39). The figure is based on 1 in. DT tests, with sufficient sampling of 2 to 3 in. plates to represent metallurgical quality aspects for the 1 to 3 in. thickness range. The three-dimensional surface envelope relates to the best (OMTL) steels. Since these also provide the best transition temperature features, the envelope is defined as the Optimum Material Trend Envelope (OMTE). Material of lower fracture toughness quality will fall under the OMTE surface; see Fig. 15 as a schematic example.

The OMTL shelf transition is indicated by the curve which defines the intersection of the envelope by the 70°F temperature plane. The temperature limits of the shelf condition are indicated by the nearly flat, top portions of the diagram. The limit extends to approximately -60°F for the lower strength steels of OMTL quality and then gradually falls back toward room temperature for steels of higher strength levels. At about 160 ksi yield strength, the OMTL quality material undergoes transition (by strength effects) from plane stress to mixed-mode fracture appearance. Strength transition to full plane strain fracture occurs at approximately the 200 ksi level. The RAD interpretations apply to all of the described strength transition features. This is indicated by the "use RAD" notation.

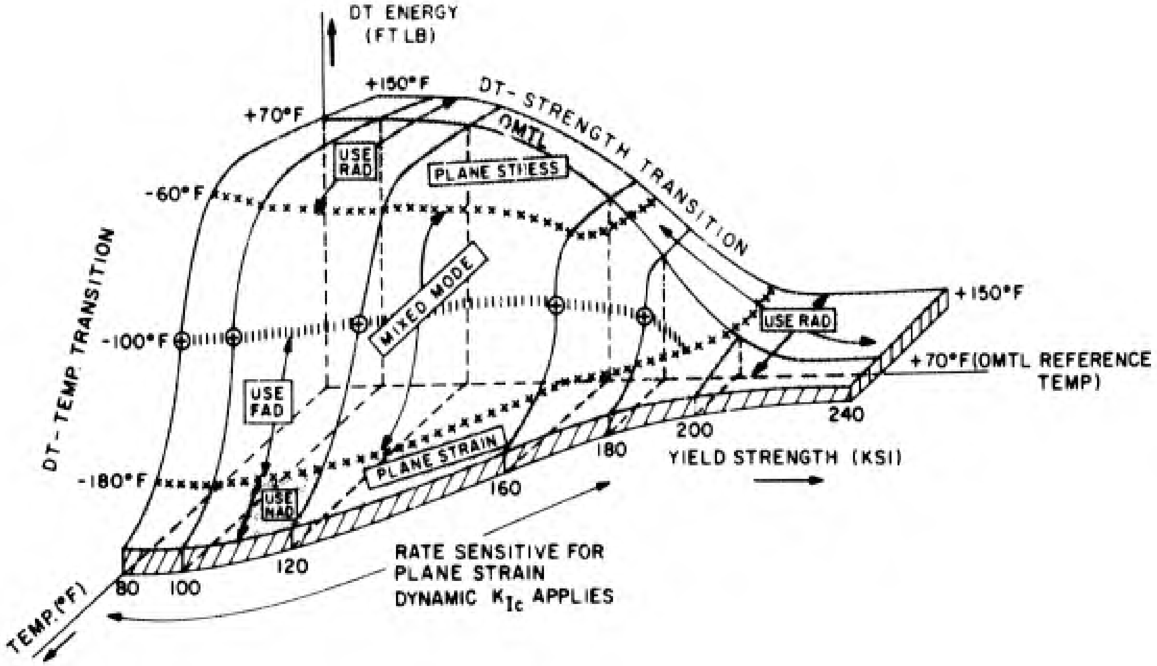

Fig. 39 - Optimum Material Trend Envelope, three-dimensional illustration of temperature and strength transition features for OMTL quality, high strength steels. The OMTL quality steels define the envelope surface; all other steels fall within the described volume. The regions of applicable RAD, FAD, and NAD interpretations are indicated.

The temperature transition features are evident from the illustration. Full plane strain, toe region conditions are attained at approximately -180°F for the OMTL quality steels of the 80 to 100 ksi yield strength levels. It is indicated that the toe region temperature range also falls back rapidly with increasing strength level. The intersection of the temperature-induced and strength-induced plane strain conditions is attained at approximately the 190 to 200 ksi yield strength level. Above this strength level the plane strain condition extends to relatively high temperatures. The dynamic NAD interpretations apply to approximately the 180 ksi yield strength. Above this strength level the static K_{Ic} condition may be analyzed by the RAD or NAD diagrams.

The mixed-mode fracture range of the temperature transition is evident from the labeling. For the OMTL quality steels of the 80 to 100 ksi yield strength level, the mixed-mode condition covers the temperature range of -60° to -180°F. The midpoint DT energy which serves to index the FAD is at approximately -100°F. The temperature "fall back" with increasing strength for the DT midpoint is evident. The extreme limit for FAD interpretations is at approximately 180 ksi yield strength — the temperature transition features essentially disappear above this level.

The approximate relative position of the corresponding surface envelope for the very best quality to be expected for the commercial, low-alloy Q&T steels is illustrated in Fig. 15. The course of the strength transition for these steels is evident from the respective corridor of Fig. 36. The temperature transition features for an average quality steel of this grade are represented by the low shelf steel of Fig. 37. In general, the shelf levels are depressed to approximately one third of the OMTL value. The strength transition culminates to plane strain conditions at approximately 150 ksi yield strength. The temperature transition shifts back to the -20 to 0°F range.

These effects result from microstructural conditions and also from "cleanliness" aspects which decrease the d_T process zone size compared to the premium quality OMTL steels of equivalent strength levels. Because of these metallurgical features, the fracture transition at the energy shelf may involve "equi-plane stress" fracture, as illustrated in Fig. 40. The example represents the low shelf 110 ksi steel of Fig. 37. These features may be compared with those shown in Fig. 16 for the temperature transition of high shelf energy, OMTL-quality steels.

Difficulties of C_V Test Interpretations for the Transition Temperature Range

The problem of the variable indexing of the C_V transition curve for different steels has been debated since 1952. The original demonstration of such variable indexing in relation to the DWT-NDT was confirmed by Robertson Tests, Explosion Crack-Starter Tests, and service failures (2,3). This fact is now accepted, and all attempts to circumvent these basic difficulties by use of notch root lateral contraction or shear-fraction curves have failed. The basic reason is that these features generally parallel the energy curve.

Figure 41 illustrates the wide variations of C_V transition temperature features in relation to DT transition curves. The variable location of the C_V curve with respect to the DT curve and the NDT temperature is in sharp contrast to the fixed relationships between the NDT temperature and the toe region of the DT temperature curve. Despite this variability, the C_V shelf energy is always in invariant correlation with the DT shelf

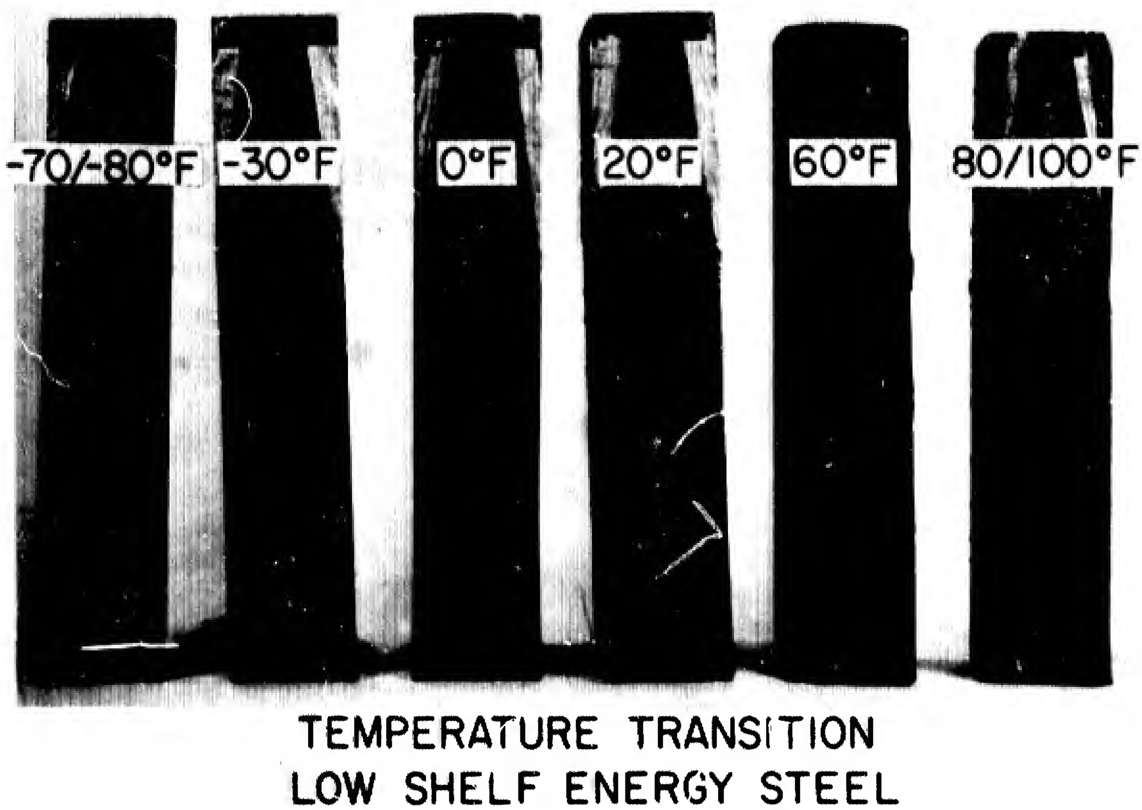

Fig. 40 - Example of "equi-plane stress" transition to DT energy shelf temperatures for a steel of low shelf energy; represents the commercial, low alloy Q&T steel of Fig. 37 which features 1600 ft-lb DT shelf energy

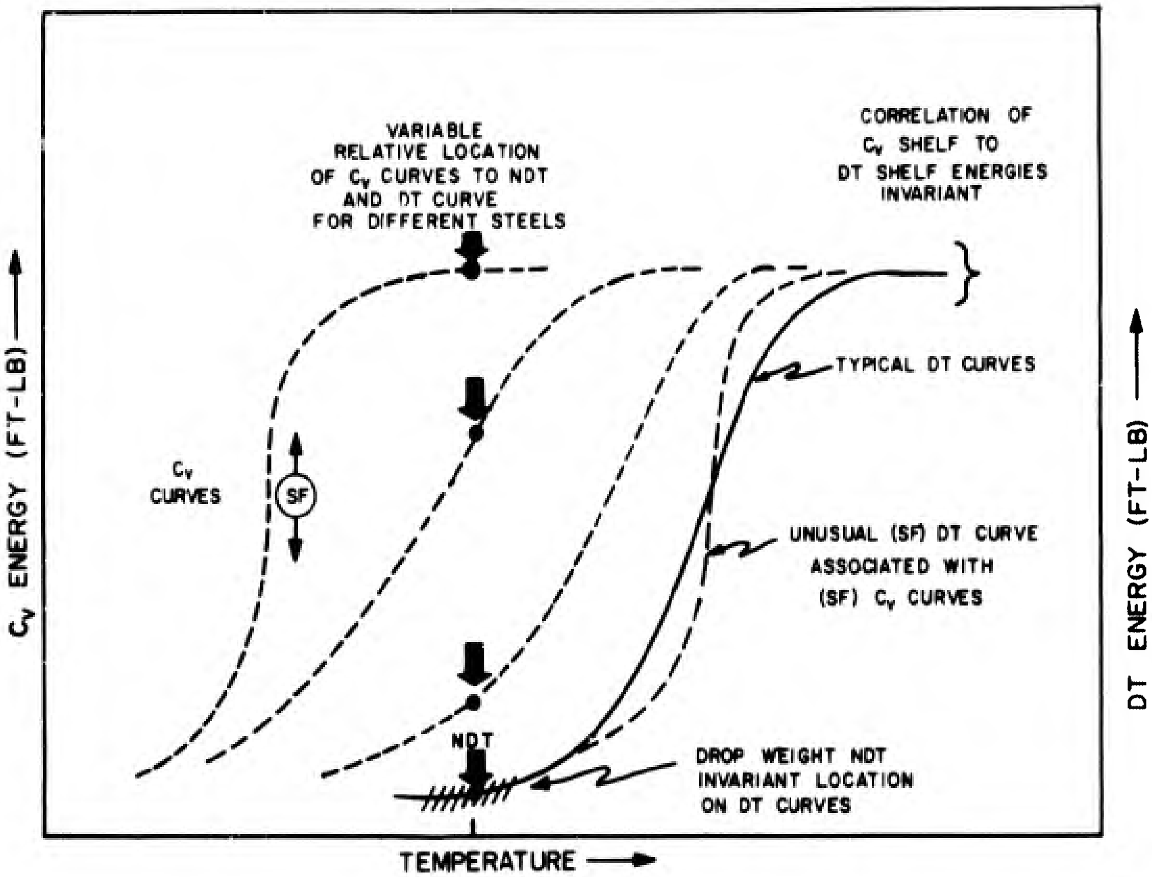

Fig. 41 - Problems of variable relative location of C_V curves with respect to DT curves and NDT temperatures. Shelf-to-shelf correlations hold, despite wide differences of the C_V and DT shelf temperatures. NDT location with respect to the DT toe region is invariant.

energy, even for C_V and DT tests which indicate widely different temperatures at which the shelf is reached. This feature provides for common treatment with respect to the RAD interpretations. However, it should be emphasized that the C_V data may be misleading as to the temperatures which relate to shelf conditions. Thus, even with respect to shelf values, the C_V test cannot be interpreted with confidence, unless the specific C_V features of the steel in question are established in advance by calibration with NDT, DT, or Robertson tests.

Figure 41 illustrates an extreme case of sharply falling (SF) C_V curves which are nonindexable to the NDT temperature, because of its location relating to the C_V shelf. In the examples of this type that have been encountered in NRL studies, other atypical features have included extremely high C_V shelf values (150 to 180 ft-lb) and temperature separations from the DT transition curve in the order of 100° to 150° F. Such extreme situations have involved steels in commercial use, as will be described. At this stage of experience it is not clear if the described peculiar features of the Charpy curve provide reliable warning of possible wide deviation from conventionality. For the few cases of this type which have been investigated, even the DT curve assumes a sharp fall (SF) configuration, as illustrated in the figure. However, all of the index procedures described for the DT curves still apply.

Extensive data exist to illustrate such an extreme case of unreliability of C_V transition temperature curves in contrast to DT interpretations to service conditions. Other aspects of this case were reported previously (5), in relation to analyses of pneumatic burst tests of two 1 in. thick, seamless pressure vessels, which were conducted in 1962. Figure 42 illustrates the previously reported C_V curves and NDT determinations for the 2-1/4% Cr - 1% Mo Q&T steels of the two flasks. The pneumatic burst tests were conducted using a 2 ft long, 0.8 in. deep slit flaw for initiation. Despite almost exactly similar chemical composition and supposed controlled Q&T treatment, the bursts resulted in completely different fractures. Flask E71, which was tested at 48°F, fragmented and exhibited fractures with 1/8 in. shear lips. Flask E75, which was tested at 55°F, burst with a single tear and exhibited fully ductile, slant fracture. The difference in yield strength (84 and 96 ksi respectively) provided the clue that heat treatment variables were involved.

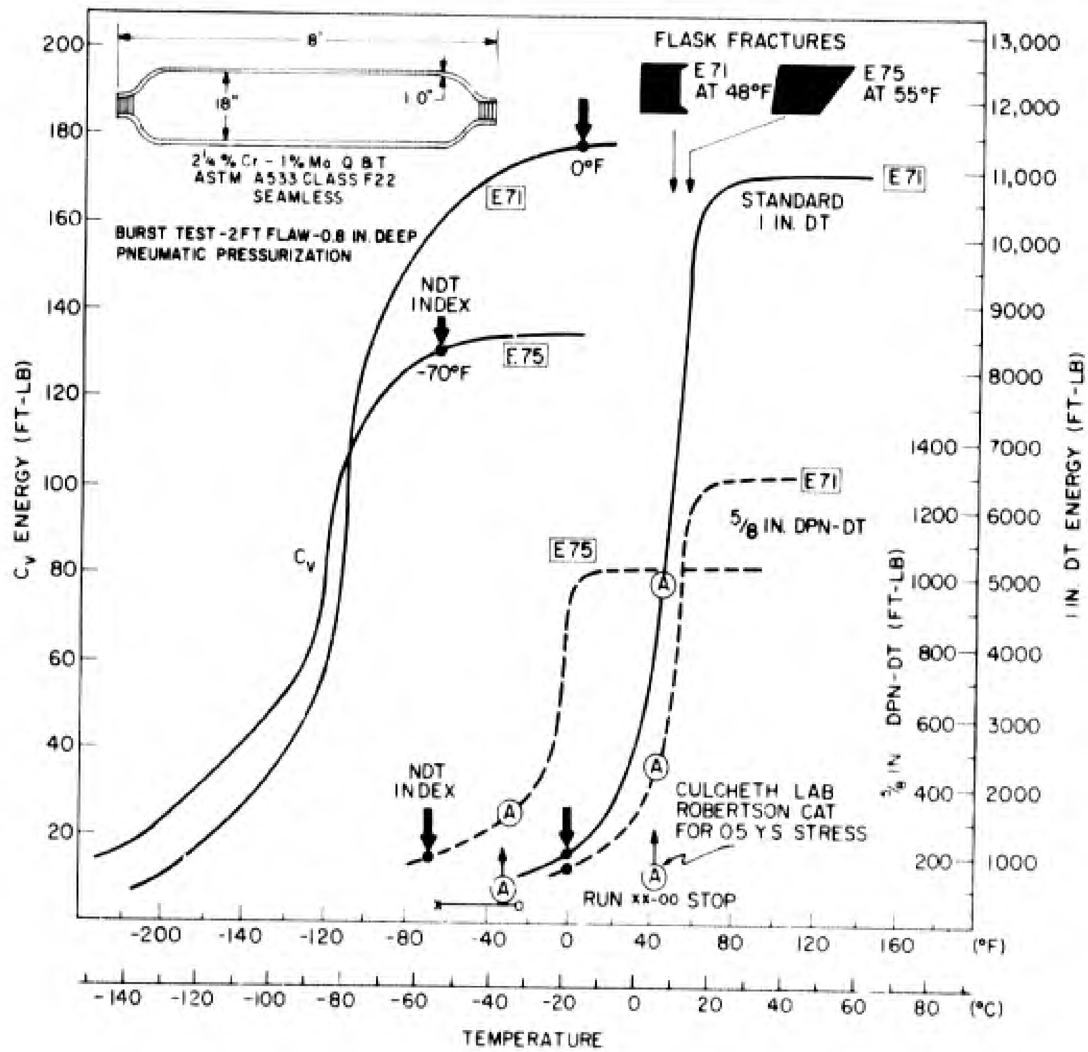

Fig. 42 - Example of the extreme lack of correspondence of C_V transition curves to service performance for a 2.25% Cr - 1% Mo, Q&T steel. The DT transition curve and the FAD (as indexed by the NDT) correctly predicted the failure modes of the subject flasks. Proper characterization was also provided by the Robertson test.

The unbelievable aspects at the time included the close similarity of the two sharply falling C_V transition curves located at -120°F, and the development of very high value C_V shelf conditions at approximately -60°F. By any standard assessment of these data, it would have been concluded that both flasks should fracture in a very tough, ductile slant mode at ambient temperatures. Because of the brittle fracture of E71 at 48°F, a determination was made of the NDT temperatures; these were found to be at -70°F and 0°F for the E75 and E71 flasks respectively. As may be noted from the figure, the NDT positions are indexed to temperatures relating to the C_V shelf. Analyses of the expected fracture modes by the NDT indexed FAD correctly predicted the fracture modes of the flasks. The flask burst temperatures were related to NDT + 125°F for E75 (slant fracture predicted), while for flask E71 the burst temperature related to NDT + 48°F (brittle fracture with approximately 1/8 in. shear lips predicted).

Because of the adverse implications to conventional C_V test interpretation practices, the U.K. Reactor Materials Laboratory at Culcheth, England offered to conduct Robertson tests. The CAT data, obtained for one-half of yield stress, fully confirmed the FAD predictions of the arrest temperatures for the two steels. Two Robertson tests served to define approximately the CAT curve for E75 as below -25°F, and four tests sharply defined its position for E71 at +45°F. Thus, the Robertson tests corroborated the failure conditions of the two flasks and also provided additional validation of the CAT curve location procedures of the FAD.

A small amount of the subject steels remained available, and we have now conducted 5/8 in. DT tests featuring a Deep Pressed Notch (DPN-DT) and also standard 1 in. DT tests. Unfortunately, sufficient material for the 1 in. DT tests was available only for the E71 flask. The DT tests were conducted by welding stub extensions to square sections of the flask material. The fractures were developed in the square inserts sufficiently removed from the welds to preclude effects due to welding. The DT data are also presented in Fig. 42.

The 5/8 in. DPN-DT test was used as part of an ongoing investigation for the development of 5/8 in. DT specimens. It is interesting to note that the 5/8 in. DPN-DT temperature transition curves for the E71 steel is closely related to the 1 in. DT curve and to the quoted Robertson arrest temperatures. The position of the sharply defined, 45°F CAT point is indexed to the two DT curves by the (A) designation. The DT tests demonstrated 1/8 in. shear lip fracture conditions for E71 at the burst temperature, thus reproducing the failure conditions exactly. The E75 fracture of the 5/8 in. DPN-DT test properly indicated slant, plane stress fracture in correspondence to the flask failure condition at 55°F. It is also noted that the temperature separation of the two 5/8 in. DPN-DT curves are in the same relation as the NDT separation. For all three DT tests, the NDT temperature is appropriately indexable to the DT toe region.

The very sharp "snap-over" to plane stress fracture in a narrow temperature region is accompanied by extreme dimpling (lateral contraction) associated with the fractures. For the 1 in. test piece the lateral contraction consequent to fracture reduced the thickness to approximately 0.8 in. This extreme behavior has not been observed for any other steel, including those of highest plane stress fracture toughness associated with high positions in the OMTL corridor. The DT shelf energy values are very high and correspond to the very high C_V shelf values. Both of these values exceed the correlation range but appear to be in proper relation, as indicated by extrapolation of the DT-C_V shelf correlation.

In addition to documenting the 1 in. standard DT test interpretations and FAD indexing techniques, these data serve to explain other "C_V unexplainable" ambient-temperature brittle failures which have been cited for 2-1/4% Cr - 1% Mo and steels of similar composition. Conventional, but incorrect, interpretations of C_V transition curves have led engineers to conclusions that these steels are conservatively fracture safe far below ambient temperatures. For the E71 flask steel, the C_V transition temperature range would have been deduced to be 150°F lower than the true transition. For E75 a more modest error of 100°F would be indicated. An interesting question is posed — how many such unusual steels are in service on similar assumptions?

SUMMARY

This is a particularly appropriate period to review the course of evolution of applied engineering fracture mechanics. It has now become clear that the unfortunate dichotomy which has separated investigators of this field is coming to an end. The merits of linear elastic fracture mechanics are becoming appreciated by the engineering oriented fracture specialists. At the same time the limitations of the linear elastic aspects are becoming recognized by the fracture mechanics experts. In fact, the preferred term seems to have become simply "fracture mechanics," or "engineering fracture mechanics." The emphasis of this report is placed on promoting the extension of these trends toward the goal of applied-engineering fracture mechanics.

The general practicing engineer, as represented by the membership of ASTM and ASME Committees and Code Bodies, faces difficult issues in deciding how to advance from present practices, which in large measure antedate the pre-WWII period. Despite all the inducements offered in the fracture literature, the primary specification tool still remains the obsolete Charpy Keyhole. The status quo does not result simply by default of decision on how to proceed. For practical reasons the first objective has been a change to more extensive utilization of the Charpy V test. Since this has been the aim for a decade, there obviously must be serious problems in effecting this change. The time has come to face up to the issue of the limitations of the Charpy V test.

The vexing problem of transfer of specification procedures from Charpy Keyhole to C_V test values cannot be resolved in any practical way except by resort to the use of a great variety of energy index values, for either the temperature or strength transitions. It should now be obvious that the desired, generalized C_V specification values, that do not consider the type of steel and its yield strength, are not feasible for fundamental reasons that cannot be violated. There is no escape from these facts by consideration of lateral contraction, or shear fraction. These features generally parallel the course of the C_V energy curves. Fatigue-cracked Charpy tests may possibly provide interesting research explanations for the peculiarities of the C_V transition curve. However, fatigue cracking is an expensive procedure and is not promising for routine use — it is difficult to convert to "batch" operations, such as the machining of notches.

Similarly, there is no escape to the use of fracture mechanics K_{Ic} or $\mathcal{G}_{Ic}$ tests for general specification purposes. These tests are essentially research tools. General engineering use requires highly simplified test procedures which are not in sight for conventional fracture mechanics tests. It is not implied that the tests being evolved by the ASTM E24 Committee are not useful for the solution of real problems. Indeed they are, but only in the hands of expert laboratory groups, and even then, not without some honest differences of opinion as to procedures and limits for the reasonably fracture tough metals. Emphasis on exactness of definition of fracture mechanics values restricts the practicality of tests for engineering use — one or the other aspect must become subordinate in judicious balance.

These considerations suggest that the required integration of aims (analytical and practical) may best evolve via the route of new tests and test procedures which may be classed as engineering fracture mechanics tests. Since fracture mechanics theory must provide the underlying base for analytical interpretations to structures, the new tests must provide for interpretability to fracture mechanics. This "two-step" interpretability approach (test specimen indexing to fracture mechanics parameters, and the utilization of fracture mechanics to define flaw size-stress conditions) emerges as the only apparent practical, near-term solution. It may also be the only practical long-term solution.

The Drop Weight-NDT and the Dynamic Tear tests, coupled with the related Analysis Diagram procedures, provide for this two-step approach. By the use of specialized indexing procedures, the C_V test may also be used in this fashion. It is possible that modified versions of the C_V test (small brittle weld, change of geometry, etc.) may provide future solutions to its present limitations. Simplified procedures for conducting fracture mechanics tests are a subject of continuing research, and such developments should be expected. Meanwhile it is necessary to proceed to meet present needs with the best available tools.

The discussions in this report have emphasized that it is not sufficient simply to invent a new test. There must be a rationale for the test, such as features of natural cracks and limit-severity testing procedures. There must be sufficient use of the test across a spectrum of metals to provide a coherent framework of characterization guidelines. There must be analyses of interpretation possibilities, by matching with, and then against, the values derived by fracture mechanics tests. At fracture toughness levels such that the reliability of the K_{Ic} value is degraded or lost, there must be independent or extrapolated rationales for engineering translation of the test procedures.

In addition to all of these conditions there must be demonstration of test reproducibility and of practicality for routine engineering use. The procedural guidelines must be simple and unequivocal. The translations to engineering interpretations of flaw size-stress conditions should be reducible to simple graphical form. The various analysis diagrams, presented in this report, evolve from this consideration. Such diagrams provide evidence of the practicality of both the test procedure and test interpretation methods. At the same time, the inherent simplicity of the diagrams serves for continuing engineering evaluation of their validity. Acceptance by the engineer-user may be expected only after a period of use and documentation of reliability in practice.

The original Fracture Analysis Diagram (FAD) has withstood the test of engineering usage successfully for over six years. With extensive use, there has been no evidence that it does not work, as defined. Moreover, evidence is now presented that it corresponds to fracture mechanics predictions, as well as to service experience. The FAD requires the use of the Drop Weight Test (DWT) for determination of the NDT temperature. The DWT-NDT has itself withstood the test of time and engineering usage. Additionally, it has now evolved as a practical method for definition of dynamic K_{Ic} (K_{Id}) values. Extensions to definition of K_{Ic}/σ_{ys} ratios for the slow-load (static) case provide further amplification of its potentialities.

The new NDT Analysis Diagram (NAD) has now been evolved to provide finer definition of flaw size-stress conditions than are given by the FAD. The NAD procedures do not replace the FAD procedures—the two may be used in concert, one amplifying the other. For most engineering problems relating to steels of low and intermediate strength levels, the FAD suffices. For more complex situations involving higher strength steels in particular, the NAD provides added sophistication of treatment. The use of the NAD also provides a means for understanding the implications of fracture mechanics. It deserves careful study for educational reasons alone.

The strength transition for the high and ultrahigh strength range has been an item of considerable engineering confusion. Fracture mechanics tests have covered adequately the ultrahigh strength range which relates to relatively brittle metals. The intermediate strength range, which may feature high fracture toughness, has been left to the C_V, without much direction as to interpretability. This area has now been brought to order by extensive explorations based on the Dynamic Tear (DT) test. At the same time, correlative procedures have evolved interpretations of the significance of C_V shelf energy values in terms of K_{Ic} values. These include calculation-corrected type K_{Ic} values which are not generally accepted because they represent approximate values of K_{Ic}. It should be recognized that past some point of increasing fracture toughness, there is no need for exactness of definition; the approximate K_{Ic} values relating to high fracture toughness serve perfectly well for engineering purposes and should be accepted for practical reasons.

All of the preceding aspects have been brought into reasonable coherency for high strength steels by the K_{Ic}/σ_{ys} Ratio Analysis Diagram (RAD), coupled with the Optimum Material Trend Line (OMTL) diagrams, which include definitions of zonal location for generic classes of steels. The same simplicity of treatment which is provided by the FAD and NAD is inherent to RAD procedures.

The FAD, NAD, RAD mix provides for essentially total coverage of the spectrum of engineering problems, related to either the temperature or to the strength transitions. All of these aspects may be analyzed by the use of the DT test to define the DT energy temperature transition curve. The DT test thus emerges as a simple and readily interpretable method for metals characterization and for interpretations to fracture-safe design. Its applicability also includes direct assessment of size effects, i.e., the effects of increased section size on mechanical constraint in fracture processes.

It is suggested that the DT test has many of the desired features which make it a simple and inexpensive K_{Ic}, K_c, or $\mathcal{G}_c$ engineering fracture mechanics test. While it may seem rudimentary and a wide departure from classical fracture mechanics tests, it faces no difficulty in separating K_{Ic} plane strain from K_c mixed-mode or plane stress conditions. It serves to define K_{Ic} and K_c ($\mathcal{G}_c$) values by correlation, for both the temperature and strength transitions. The DT temperature transition curve provides all the necessary information. Because of its reproducibility, few tests (say eight to twelve) should suffice for most purposes. There is no need for machining the specimens; simple sawing suffices. For plate material even flame cutting may be used. For 5/8 in. and 1 in. specimens the brittle weld is easily applied in batches, as for "gang" cutting of C_V specimens. Electron beam welders are now generally available for preparation of the brittle crack-starting weld.

The FAD-NAD-RAD procedures may be adjusted readily for interpretations to very thick sections, as information becomes available. For the RAD this simply involves the use of different K_{Ic}/σ_{ys} ratio lines, as the index relationships for thick steels, based on 1 in. DT test data. For the FAD, adjustments to the slope of the CAT curve may be made, if required. The NAD system presently incorporates thickness-adjustment procedures derived from fracture mechanics principles.

Exploratory research studies for very thick steels in the range of 6 to 12 in. sections are being conducted with full-thickness DT tests, and the results are being correlated with the 1 in. DT test. Techniques for introducing brittle electron beam welds for these huge specimens have been evolved, and successful tests have been made to date. Additional studies are being conducted for "sub size" 5/8 in. and Charpy-dimension DT tests; also for alternate methods of introducing a brittle crack-starting element. The total interpretive system is sufficiently flexible to accommodate such improvements as these are investigated and validated. When these are added, the coverage should approach practical attainable limits of long-term interest.

The plane strain K_{Ic} condition poses fracture-safe design problems for the engineer. The use of such materials should be avoided, if alternate materials of K_c mixed-mode or plane stress fracture toughness are metallurgically feasible and economically defensible. The full plane stress K_c condition is not generally required for most fracture-safe design solutions. Information that the mixed-mode K_c condition is attained generally suffices. Full-plane stress fracture toughness of high energy intensity is required only for special design problems. The DT test provides direct assessment of this aspect also.

The argument that "we must learn to use brittle, plane strain material safely" certainly holds for the ultrahigh-strength region. For the low and intermediate strength region this argument bears some cost effectiveness analyses, long overdue. The cost of structures is not decided by base metal costs alone — fabrication quality, quality control strictness, nondestructive testing requirements, operational inspection, maintenance, etc., bear on value analyses.

The question of what tests to use is a matter for decision by informed engineers. The input of fracture specialists is only a part of the required engineering equation. Moreover, this input must be provided with a reasonable interpretive framework, preferably presented in easily understood graphical form. Many engineering successes or fiascos are decided in the predesign stage, when options relating to materials are resolved. For such purposes it is not sufficient to have fracture toughness diagrams alone. Reasonably integrated data that relates to expected properties for various classes of steels are required.

For this purpose, reference diagrams which also relate to materials characteristics have been evolved. An example is represented by the Optimum Materials Trend Line (OMTL) diagrams, which feature zoning of the expected location of steels of primary interest. By overlay of these diagrams, with the RAD flaw size-stress indexing charts, integrated analyses of metallurgical and fracture mechanics aspects emerge. This coupling procedure is analogous to the process of characterizing specific classes of commercial steels by the expected NDT temperature frequency distribution range. It provides a basis for selection of metals without specific requirements for testing.

The process of continual evolution of new steels and new information on the effects of metals processing requires general use of relatively simple and yet interpretable tests, so that a data bank can be evolved from many sources. It also requires a scheme for indexing the generalized charts which provide ready reference of relative fracture toughness quality. The new "point" must fit in a framework of previous data, so that its quality index vis a vis other steels of equivalent strength and price range can be established. It is only by such procedures that we can avoid "drowning in a sea of data." Questions of practical tests and their interpretations have many ramifications indeed.

REFERENCES

1. "Tentative Method for Conducting Drop-Weight Test to Determine Nil-Ductility Transition Temperature of Ferritic Steels," ASTM E208-66T

2. Puzak, P.P., Schuster, M.E., and Pellini, W.S., "Crack Starter Tests of Ship Fracture and Project Steels," Welding J. Research Supplement, 33(10):481s (Oct. 1954)

3. Irwin, G.R., Krafft, J.M., Paris, P.C., and Wells, A.A., "Basic Aspects of Crack Growth and Fracture," NRL Report 6598, Nov. 1967; also in Whitman, G.D., Robinson, G.C., Jr. and Savolainen, A.W., "Technology of Steel Pressure Vessels for Water-Cooled Nuclear Reactors," Nuclear Safety Information Center, Oak Ridge National Laboratory, Dec. 1967

4. Pellini, W.S., and Puzak, P.P., "Fracture Analysis Diagram Procedures for the Fracture-Safe Engineering Design of Steel Structures," NRL Report 5920, Mar. 15, 1963; also Welding Research Council Bulletin Series No. 88, May 1963

5. Pellini, W.S., and Puzak, P.P., "Practical Considerations in Applying Laboratory Fracture Test Criteria to the Fracture-Safe Design of Pressure Vessels," NRL Report 6030, Nov. 5, 1963; also, Trans. ASME, Series A, J. Engineering for Power, 86:429-443 (Oct. 1964)

6. Brubaker, E.H., and Dennison, J.R., "Use of the Battelle Drop-Weight Tear Test for Determining the Notch Toughness of Line Pipe Steel," J. Metals 17:985-989 (Sept. 1965)

7. Pellini, W.S., Goode, R.J., Puzak, P.P., Lange, E.A., and Huber, R.W., "Review of Concepts and Status of Procedures for Fracture-Safe Design of Complex Welded Structures Involving Metals of Low to Ultra-High Strength Levels," NRL Report 6300, June 1965

8. Goode, R.J., Huber, R.W., Howe, D.G., Judy, R.W., Crooker, T.W., Lange, E.A., Freed, C.N., and Puzak, P.P., "Metallurgical and Mechanical Characteristics of Ultra-High Strength Metals, Twelfth Progress Report," NRL Report 6607, Sept. 1967

9. Freed, C.N., "A Comparison of Fracture Toughness Parameters for Titanium Alloys," Engineering Fracture Mechanics, Vol. 1, No. 1, Jan. 1968 (publication pending)

10. Brown, W.F., and Srawley, J.E., "Plane Strain Crack Toughness Testing of High Strength Metallic Materials," ASTM Special Technical Publication (ASTM-STP 410) p. 126, American Society for Testing and Materials, Philadelphia, 1966

11. Pellini, W.S., Sandoz, G., and Bishop, H.F., "Notch Ductility of Nodular Iron," ASM Trans. 26:418-445 (1954)

12. Sandoz, G.A., Howells, N.C., Bishop, H.F., and Pellini, W.S., "Notch Ductility of Malleable Irons," ASM Trans. 49:204-231 (1957)

13. Lange, E.A., Pickett, A.G., and Wylie, R.D., "A Study of Materials Properties and Fracture Development," Welding Research Council Bulletin 98, Aug. 1964

BIBLIOGRAPHY

Irwin, G.R., "Fracture Mechanics," in Goodier, J.N., and Hoff, N.J., eds., "Structural Mechanics," Pergamon Press, New York, 1960

Irwin, G.R., "Crack-Extension Force for a Part-Through Crack in a Plate," Trans. ASME 29 (Series E):651-654 (1962)

Irwin, G.R., "Fracture," in Encyclopedia of Physics, Vol. VI, 551-590, Springer, Berlin, 1958

Irwin, G.R., Kies, J.A., and Smith, H.L., "Fracture Strengths Relative to Onset and Arrest of Crack Propagation," Proc. ASTM 58:640-660 (1958)

Bluhm, J.L., "A Model for the Effect of Thickness on Fracture Toughness," Proc. ASTM 61:1324-1331 (1961)

Srawley, J.E., and Brown, W.F., "Fracture Toughness Testing," NASA Technical Note NASA TN-D-2599, Jan. 1965

"Fracture Toughness Testing and Its Applications," ASTM STP 381, 1965

"Plane Strain Crack Toughness Testing of High Strength Metallic Materials," ASTM STP 410, 1966

Irwin, G.R., "Relation of Crack Toughness Measurements to Practical Applications," Welding J. Research Supplement, 41(11):519s-528s (Nov. 1962)

Krafft, J.M., "Correlation of Plane Strain Crack Toughness with Strain Hardening Characteristics of a Low, a Medium and a High Strength Steel," Appl. Materials Research 3:88-101 (Apr. 1964)

Eftis, J., and Krafft, J.M., "A Comparison of the Initiation with the Rapid Propagation of a Crack in a Mild Steel Plate," ASME Paper 64-Met-16, May 1964

NOMENCLATURE

a	Depth, half length, or half diameter of crack (in.)
$2c$	Crack width (in.)
B	Thickness of plate or specimen (in.)
E	Young's modulus (psi)
$\mathcal{G}_{Ic}$	Critical strain energy release rate with crack extension per unit length of crack front (in.-lb/in^2)
K, K_I	Stress intensity factor; subscript I denotes opening mode of crack extension (ksi $\sqrt{\text{in.}}$)
K_{Ic}	Slow load (static) plane strain fracture toughness (ksi $\sqrt{\text{in.}}$)
K_{Id}	Dynamic load plane strain fracture toughness (ksi $\sqrt{\text{in.}}$)
K_c	Plane stress condition at crack tip for initiation - also crack conditions in propagation as related to this fracture mode (ksi $\sqrt{\text{in.}}$)
K_c (mixed mode)	Plane stress (surface) and plane strain (center) condition for crack tip initiation - also crack conditions in propagation as related to this fracture mode (ksi $\sqrt{\text{in.}}$)
β_{Ic}	Parameter which defines the degree of constraint in relation to the section thickness
r	Plastic zone radius (in.)
ν	Poisson's ratio
σ or σ_N	Applied stress (psi or ksi)
σ_{ys}	Yield strength (psi or ksi)
Q	Crack shape parameter for semielliptical surface cracks

d_T	Process zone of high strain intensity within the plastic zone
ϵ	Tensile strain
ϵ_c	Critical instability value of ϵ
NDT	Nil Ductility Transition Temperature obtained by Drop Weight Test
DWT	Drop Weight Test
DWTT	Drop Weight Tear Test (now DT)
DT	Dynamic Tear Test - all sizes
CAT	Robertson Crack Arrest Temperature
C_V	Charpy-V Test
ETT	Explosion Tear Test
FAD	Fracture Analysis Diagram
RAD	K_{Ic}/σ_{ys} Ratio Analysis Diagram
NAD	NDT Analysis Diagram
OMTL	Optimum Material Trend Line
OMTE	Optimum Material Trend Envelope

Appendix

COMPENDIUM OF FRACTURE MECHANICS TERMS AND EQUATIONS

1. Strain Energy Release Rate, $\mathcal{G}$

Elastic energy released, per unit crack surface area, as the crack extends. The strain energy, $\mathcal{G}$, is a measure of the force driving the crack.

$$\mathcal{G} = \frac{\pi\sigma^2 a}{E}$$

where

a = one-half crack length for a through-thickness crack in a semi-infinite tension plate

σ = nominal applied prefracture stress

E = modulus.

2. Plastic Work Energy, $\mathcal{G}_c$

Index of resistance of the material to crack extension; related to elastic energy absorbed, per unit area of new crack surface, in crack extension. Plastic work energy at the crack tip opposes the elastic energy release, $\mathcal{G}$. At the point of instability the elastic energy and the plastic work energy (resistance) are in balance.

$$\mathcal{G}_c = \frac{\pi\sigma_f^2 a}{E}$$

where

σ_f = nominal stress at crack extension

$\mathcal{G}_c$ = critical $\mathcal{G}$.

3. Stress Intensity Factor, K

Elevation of stress in advance of the crack tip plastic zone, related to plastic work energy term $\mathcal{G}$.

$$K = (E\mathcal{G})^{1/2} \text{ (for plane stress)}$$

$$K = \left(\frac{E\mathcal{G}}{1-\nu^2}\right)^{1/2} \text{ (for plane strain)}$$

where ν = Poisson's ratio.

4. Stress Intensity Factor at Instability, K_c

In the preceding equation, replace K with K_c and replace $\mathcal{G}$ with $\mathcal{G}_c$ (and therefore use σ_f as nominal stress at crack instability). Subscript c means K is critical or at the point of instability.

5. Plastic Zone Correction

To correct for presence of plastic zone, apply an apparent increase in initial crack depth a_o by adding r_p (plastic zone radius). The crack length then becomes $a = a_o + r_p$,

$$r_p = \frac{1}{2\pi}\left(\frac{K_c}{\sigma_{ys}}\right)^2 \text{ (plane stress)}$$

$$r_p = \frac{1}{6\pi}\left(\frac{K_{Ic}}{\sigma_{ys}}\right)^2 \text{ (plane strain).}$$

6. Increase of Plastic Zone Size with Increase in K

The plastic zone is related to the plastic work energy described earlier. From above equations note that the plastic zone size increases as K^2 for a fixed level of yield stress. The increase is approximately three times larger for plane stress. For different yield strengths the plastic zone size is a function of $(K_{Ic}/\sigma_{ys})^2$ for both plane stress and plane strain.

7. K_{Ic} Calculations for Plane Strain Condition Cracks

Generalized form

$$K_{Ic} = \alpha\beta\sigma\sqrt{\pi a}$$

where

σ = nominal static stress applied under slow loading

a = crack depth or length

α = flaw geometry factor ranging from 1 to 3 (approximately)

β = function of crack tip sharpness, loading rate, crack tip metallurgical damage, etc. Ranges from 1/2 to 2 (approximately).

Thus the critical flaw size for surface cracks may be influenced by combined α and β factors which on the low side reduce the critical crack depth by a combined factor of 1/2, and on the high side increase the flaw depth by a factor of 6.

8. K_{Ic} Calculations for Plane Strain Surface Cracks

Formal equation for a surface crack in a tension-loaded plate

$$K_{Ic} = \alpha\sigma\sqrt{\pi a} = \frac{1.1\sigma\sqrt{\pi a}}{\sqrt{Q}}$$

where

a = crack depth

σ = applied stress

$1.1\sqrt{Q}$ = specimen geometry and flaw-shape factor obtained from charts.

This equation assumes that K_{Ic} relates to either dynamic or static load-rate conditions. The calculated flaw depths are based on the same assumption.

9. K_{Ic} Calculations for Internal Cracks Which Become Unstable Under Plane Strain Conditions

Roughly generalized, for the same geometry, the internal crack depth (short dimension) requires a slightly higher stress for instability (a 1 $\sqrt{Q}$) when the preceding equation is applied.

10. Calculation of Surface Crack Involving K_c (plane stress) Conditions

When the constraint necessary for plane strain is not present, an approximation may be made of the stress-intensity factor under plane stress conditions, K_c. This approximation is based on a definition of K_{Ic}, σ_{ys}, and B for the material. The following equation may be used to estimate K_c.

$$K_c = K_{Ic}\left[1 + \frac{1.4}{B^2}\left(\frac{K_{Ic}}{\sigma_{ys}}\right)^4\right]^{1/2}.$$

From K_c, the critical flaw size for instability under plane stress conditions for the same level of nominal stress may be calculated:

$$\frac{K_c^2}{K_{Ic}^2} = \frac{a_{K_c}}{a_{K_{Ic}}}$$

where

a_{K_c} = critical flaw size under plane stress

$a_{K_{Ic}}$ = critical flaw size under plane strain.

11. Definition of β_c and β_{Ic}

The type of stress state which exists ahead of the crack will depend on the degree to which the crack tip plastic zone is constrained. A measure of constraint in the plate thickness direction is provided by the parameter β which is a function of the plastic zone size relationship to the thickness. For a plane strain state of stress,

$$\beta_{Ic} = 1/B\,(K_{Ic}/\sigma_{ys})^2$$

where

β_{Ic} = β under plane-strain conditions

B = plate thickness (in.)

K_{Ic} = plane-strain stress intensity factor

σ_{ys} = yield strength.

For plane stress state of stress

$$\beta_c = \frac{1}{B}\,(K_c/\sigma_{ys})^2$$

where β_c [illegible] under plane stress conditions.

12. Typical Formula for K_{Ic} Calculation of Notched-Bend Specimen

$$K_I = \frac{3}{2}\,\frac{PS\sqrt{a}}{BW^2}\left[1.93 - 3.07\left(\frac{a}{W}\right) + 14.53\left(\frac{a}{W}\right)^2 - 25.11\left(\frac{a}{W}\right)^3 + 25.80\left(\frac{a}{W}\right)^4\right]$$

where

P = load

B = thickness

S = total span

W = depth

a = notch depth plus fatigue crack.

NOTE: The above equation is for three-point bending and $S/W = 4$ only.

13. Typical Formula for K_{Ic} Calculation for Single Edge Notch Tension Specimen

$$K_I = \frac{P\sqrt{a}}{BW}\left[1.99 - 0.41\left(\frac{a}{W}\right) + 18.70\left(\frac{a}{W}\right)^2 - 38.48\left(\frac{a}{W}\right)^3 + 53.85\left(\frac{a}{W}\right)^4\right].$$

Security Classification

DOCUMENT CONTROL DATA - R & D

(Security classification of title, body of abstract and indexing annotation must be entered when the overall report is classified)

1. ORIGINATING ACTIVITY (Corporate author) Naval Research Laboratory Washington, D.C. 20390	2a. REPORT SECURITY CLASSIFICATION Unclassified 2b. GROUP --

3. REPORT TITLE

ADVANCES IN FRACTURE TOUGHNESS CHARACTERIZATION PROCEDURES AND IN QUANTITATIVE INTERPRETATIONS TO FRACTURE-SAFE DESIGN FOR STRUCTURAL STEELS

4. DESCRIPTIVE NOTES (Type of report and inclusive dates)

Special summary and interpretative report.

5. AUTHOR(S) (First name, middle initial, last name)

William S. Pellini

6. REPORT DATE	7a. TOTAL NO. OF PAGES	7b. NO. OF REFS
April 3, 1968	86	13

8a. CONTRACT OR GRANT NO. NRL Problems M01-18; M03-01; F01-17 b. PROJECT NO. RR 007-01-46-5420, SF 020-01-05-0731, MIPR ENG-NAV-67-1; c. RR 007-01-46-5414, SF 020-01-01-0850; DSSP P07-001-11894 d.	9a. ORIGINATOR'S REPORT NUMBER(S) NRL Report 6713 9b. OTHER REPORT NO(S) (Any other numbers that may be assigned this report)

10. DISTRIBUTION STATEMENT

This document has been approved for public release and sale; its distribution is unlimited.

11. SUPPLEMENTARY NOTES	12. SPONSORING MILITARY ACTIVITY
	NAVSHIPSYSCOM and DSSP, Dept. of Navy, Washington, D. C.

13. ABSTRACT

The state of knowledge of fracture-safe design for steels is examined in relation to the requirements for achieving practical solutions to general engineering problems. Analytical procedures evolved from fracture mechanics theory are demonstrated to provide for quantitative interpretations of engineering fracture toughness tests. It is thus possible to couple the procedural simplicity which is inherent to engineering tests with the analytical advantages of fracture mechanics theory. The coupling of these two approaches provides for practical advances in fracture-safe design which cover the totality of general engineering problems and requirements.

The Charpy V test is shown to have applicability for use in the described fashion primarily in relation to the strength transition for high strength steels. Serious limitations exist for reliable quantitative interpretations involving the temperature transition. The Drop Weight Test (DWT) and the related Fracture Analysis Diagram (FAD) are demonstrated to be interpretable in terms of fracture mechanics parameters. Additional applications of the DWT which provide for separate definition of static and dynamic fracture initiation conditions have been evolved for the Nil Ductility Transition (NDT) temperature region. The resulting new reference diagram is defined as the NDT Analysis Diagram (NAD).

(over)

DD FORM 1 NOV 65 1473 (PAGE 1)

S/N 0101-807-6801

Security Classification

Security Classification

14 KEY WORDS	LINK A		LINK B		LINK C	
	ROLE	WT	ROLE	WT	ROLE	WT
Engineering fracture mechanics						
Fracture toughness test						
Fracture mechanics test						
Fracture-safe design						
Structural steels						
High strength steels						
Engineering fracture tests						
Interpretations of fracture tests						
Thick section steels						
Design applications of fracture tests						
Interpretations of fracture mechanics theory to engineering design						

Combined coverage of temperature and strength transition aspects are provided by the Dynamic Tear (DT) test. The DT test temperature transition curve provides for indexing to the FAD and NAD interpretive procedures. In addition, the DT shelf energy level is analyzable, in terms of flaw size-stress conditions for fracture, by the K_{Ic}/σ_{ys} Ratio Analysis Diagram (RAD). By zoning of the expected position in this diagram for generic classes of steels, coherent matrices are evolved which combine metallurgical and mechanics aspects. The combined diagrams should serve the needs of both the materials and design fields.

DD FORM 1 NOV 65 1473 (BACK)
(PAGE 2)

Security Classification